UNIVERSITÀ DEGLI STUDI DEL PIEMONTE ORIENTALE

Dipartimento di Medicina Traslazionale

Corso di Dottorato di Ricerca in Biotecnologie e Scienze mediche

Ciclo XXXIII

Titolo tesi:

Role of lymphocyte co-stimulation pathways and extracellular vesicles in cardiovascular damage of chronic uremic patients and new therapeutic strategies

SSD (Settore Scientifico Disciplinare) della tesi MED/14

Coordinatore

Prof.ssa Marisa Gariglio

Tutor

Prof. Vincenzo Cantaluppi

Dottorando

Guido Merlotti, MD

A.A. 2019/2020

TABLE OF CONTENTS

1. Summary

Introduction: Chronic kidney disease (CKD) is characterized by high cardiovascular (CV) risk and the RISCAVID study identified a correlation between CV risk and blood levels of sCD40L in uremia. Moreover, sCD40L correlates with osteoblastic differentiation of vascular smooth muscle cells (VSMC) and endothelial cells (EC) inflammation. In addition, CKD-related extracellular vesicles (EVs) express CD40L and polymethylmethacrylate (PMMA) dialyzer could reduce not only uremic toxins as indoxyl sulfate (IS), but also sCD40L and EVs by adsorption.

Aim of the study: 1) identify a sCD40L predictive value for major cardiovascular events (MACE) in uremia, 2) assess the sCD40L role, 3) compare the efficacy of PMMA vs polysulfone (PS) in sCD40L and other molecule removal, and 4) perform CKD-EV characterization and analysis of their role CKD vascular damage.

Patients and methods: In 201 dialysis patients from 6 Italian dialysis Centers, we assessed sCD40L and MACE during the follow-up. 48 high CV risk patients started 9 months randomized double-crossover study (treatment with PMMA or PS). We assessed SCD40L and biochemical parameters every 3 months. We evaluated sCD40L/IS mass removal and sCD40L effects on EC and VSMC in vitro. We characterized CKD-EVs and evaluate their role incubating EC and VSMC in vitro.

Results: sCD40L cut-off of 7,8 ng/mL was the best predictor of MACE and PMMA was more efficient in reducing hepcidin, sCD40L and IS. PMMA decreased ROS production, monocyte adhesion and osteoblastic differentiation. CKD-EVs expressed CD40L and other inflammation markers, were internalized by EC and VSMC and modulated osteoblastic differentiation.

Conclusions: sCD40L predicts MACE in CKD patients and PMMA is able to remove this molecule. sCD40L is not only a marker of CKD-CV damage, but also a mediator of progression. sCD40L and IS reduction could therefore have an impact on CKD-CV risk and CKD-EVs could also be considered true uremic toxins and effective mediators of damage.

Introduzione: La malattia renale cronica (CKD) è caratterizzata da un alto rischio cardiovascolare (CV) e lo studio RISCAVID ha identificato una correlazione tra il rischio CV e i livelli ematici di sCD40L nell'uremia. Inoltre, sCD40L correla con la differenziazione osteoblastica delle cellule muscolari lisce vascolari (VSMC) e delle cellule endoteliali (EC) infiammate. Le vescicole extracellulari (EV) plasmatiche nell'uremia esprimono CD40L e i filtri in polimetilmetacrilato (PMMA) potrebbero ridurre non solo le tossine uremiche come l'indoxil solfato (IS), ma anche sCD40L e EV tramite adsorbimento.

Obiettivi: 1) identificare un valore predittivo sCD40L per eventi cardiovascolari maggiori (MACE) nell'uremia, 2) valutare il ruolo di sCD40L, 3) confrontare l'efficacia del PMMA vs polisulfone (PS) nella rimozione di sCD40L e altre molecole, e 4) eseguire una analisi delle CKD-EVs e del loro ruolo nella CKD.

Pazienti e metodi: In 201 pazienti in dialisi da 6 Centri italiani, abbiamo valutato sCD40L e MACE nel follow-up. 48 pz ad alto rischio CV hanno iniziato uno studio randomizzato doppio-crossover di 9 mesi (trattamento con PMMA o PS). Abbiamo valutato SCD40L e parametri biochimici ogni 3 mesi, la rimozione di massa di sCD40L/IS e gli effetti di sCD40L su EC e VSMC in vitro. Abbiamo inoltre caratterizzato le CKD-EV valutandone il ruolo incubando EC e VSMC in vitro.

Risultati: il cut-off di 7,8 ng/mL è risultato essere predittore di MACE. Il PMMA era più efficiente nel ridurre epcidina, sCD40L e IS e la produzione di ROS, adesione monocitaria e differenziazione osteoblastica in vitro. Le CKD-EV esprimono CD40L e altri marcatori di infiammazione, vengono internalizzate da EC e VSMC e modulano la differenziazione osteoblastica.

Conclusioni: sCD40L predice MACE nei pazienti affetti da CKD e il PMMA è in grado di rimuovere efficacemente sCD40L e IS. sCD40L non è solo un indicatore di danno CV, ma anche di progressione. La riduzione di sCD40L e IS potrebbe avere un impatto sul rischio CV e le CKD-EV potrebbero anche essere considerate come tossine uremiche e mediatori di danno.

2. Introduction

2.1. Definition and staging of chronic kidney disease (CKD)

CKD is defined by the presence of kidney damage or decreased kidney function for three or more months, irrespective of the cause[1]. The persistence of the damage or decreased function for at least three months is necessary to distinguish CKD from acute kidney disease. Kidney damage refers to pathologic abnormalities, whether established via kidney biopsy or imaging studies, or inferred from markers such as urinary sediment abnormalities or increased rates of urinary albumin excretion. Decreased kidney function refers to a decreased glomerular filtration rate (GFR), which is usually estimated (eGFR) using serum creatinine and one of several available equations. Based on GFR threshold, cause of disease and categories of albuminuria, CKD is classified and staged to guide management, including stratification of risk for progression and complications of CKD (Figure 1)[1].

GFR stages	GFR (mL/min/1.73 m^2)	Terms
G1	≥90	Normal or high
G2	60 to 89	Mildly decreased
G3a	45 to 59	Mildly to moderately decreased
G3b	30 to 44	Moderately to severely decreased
G4	15 to 29	Severely decreased
G5	<15	Kidney failure (add D if treated by dialysis)
Albuminuria stages	**AER (mg/day)**	**Terms**
A1	<30	Normal to mildly increased (may be subdivided for risk prediction)
A2	30 to 300	Moderately increased
A3	>300	Severely increased (may be subdivided into nephrotic and nonnephrotic for differential diagnosis, management, and risk prediction)

The cause of CKD is also included in the KDIGO revised classification but is not included in this table.

GFR: glomerular filtration rate; AER: albumin excretion rate; CKD: chronic kidney disease; KDIGO: Kidney Disease Improving Global Outcomes.

Fig. 1 CKD classification based upon glomerular filtration rate and albuminuria

2.2. Chronic kidney disease and cardiovascular disease

CKD has been showing an increased prevalence over the last 20 years and represents nowadays one of the main causes of death due to several comorbidities including cardiovascular diseases (CVD)[2]. CKD is characterized by frequent hospitalizations and consequent increase of healthcare costs. Early diagnosis and treatment of CKD using appropriate and low-cost therapies may prevent or at least slow the progression of renal disease, reducing the need of replacement therapy, clinical complications and associated high mortality rates[3]. Basing on the previous considerations, CKD is currently considered a major public health problem and the interest in CKD from the scientific community and health authorities particularly aroused by epidemiological data[4]. The last survey available showed that about 13% of the general adult population in the US has evidence of CKD and enter one of the five CKD stages identified according to K/DOQI classification[5]. In addition, the prevalence of CKD increases to 15-30% in the elderly and exceed 50% in patients with CVD and/or metabolic diseases, which are related to the steadily aging of population[6]. Moreover, in the next few years, a doubling of CKD patients due to the increasing incidence of hypertension, diabetes and metabolic syndrome is expected. The italian study CARHES (CArdiovascular Risk in Renal patients of the Health Examination Survey) has shown a prevalence of CKD of about 7%: this discrepancy compared to US data could be due to protective effects of genetic factors or to a different environment (i.e., Mediterranean diet)[7]. Other epidemiological studies have shown that, even in patients in stage III-IV CKD, mortality is mainly associated with CVD and it exponentially increases with the progression of renal damage[8]. The high risk of CVD in these patients implies that the incidence of death may even exceed (2 to 50 times greater) the incidence of end-stage renal disease (ESRD), which is the culmination of CKD (need for replacement treatment with dialysis or kidney transplantation)[9]. In ESRD patients, the risk of major adverse cardiovascular events (MACE) and consequently of cardiovascular mortality is approximately 10 to 20- fold higher than in people not affected by CKD (Figure 2)[10].

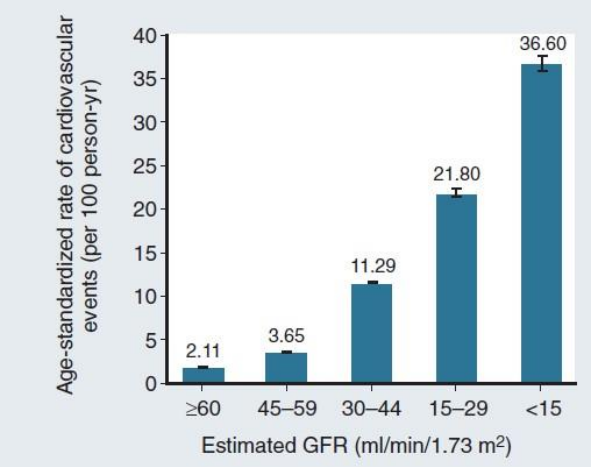

Fig.2: age-standardized rate of MACE in patients with CKD

2.3. CKD-related premature atherosclerotic disease

Chronic inflammation plays a key role and seems to be closely related to accelerated atherogenesis processes. Inflammatory cytokines, adipokines and uremic toxins that are responsible for endothelial dysfunction and vascular calcification. Endothelial dysfunction represents the first clinical element to stimulate the atherosclerotic disease. This is important for subintimal accumulation of LDL, and their following modifications (aggregation, oxidation, and glycosylation) mediated by oxygen free radicals and hydrolytic enzymes secreted by macrophages and smooth muscle cells. Then, endothelial cells, as well as smooth muscle cells, express adhesion molecules on their surface and produce chemokines able to activate an inflammatory reaction with migration and adhesion of monocytes and T-cells in subintimal space[11] . Modified LDLs are perceived as antigens, therefore they activate the immune response and are phagocytized by macrophages, once recognized by their scavenger receptors. Due to the impossibility of metabolizing the cholesterol, they transform into foam cells characteristic of the lipid striae (Fatty streaks). At this point the lesion progresses to enlarge evolving until the constitution of a complicated plaque, so defined as characterized by the high risk of rupture. Typically, in course of evolution from lipid stria to complicated plate, areas of calcification are formed also intimal. The adhesion of platelets and the formation of intramural clots, resulting from erosion/ulceration of atheroma, contribute to the growth of lesions (Figure 3)[12].

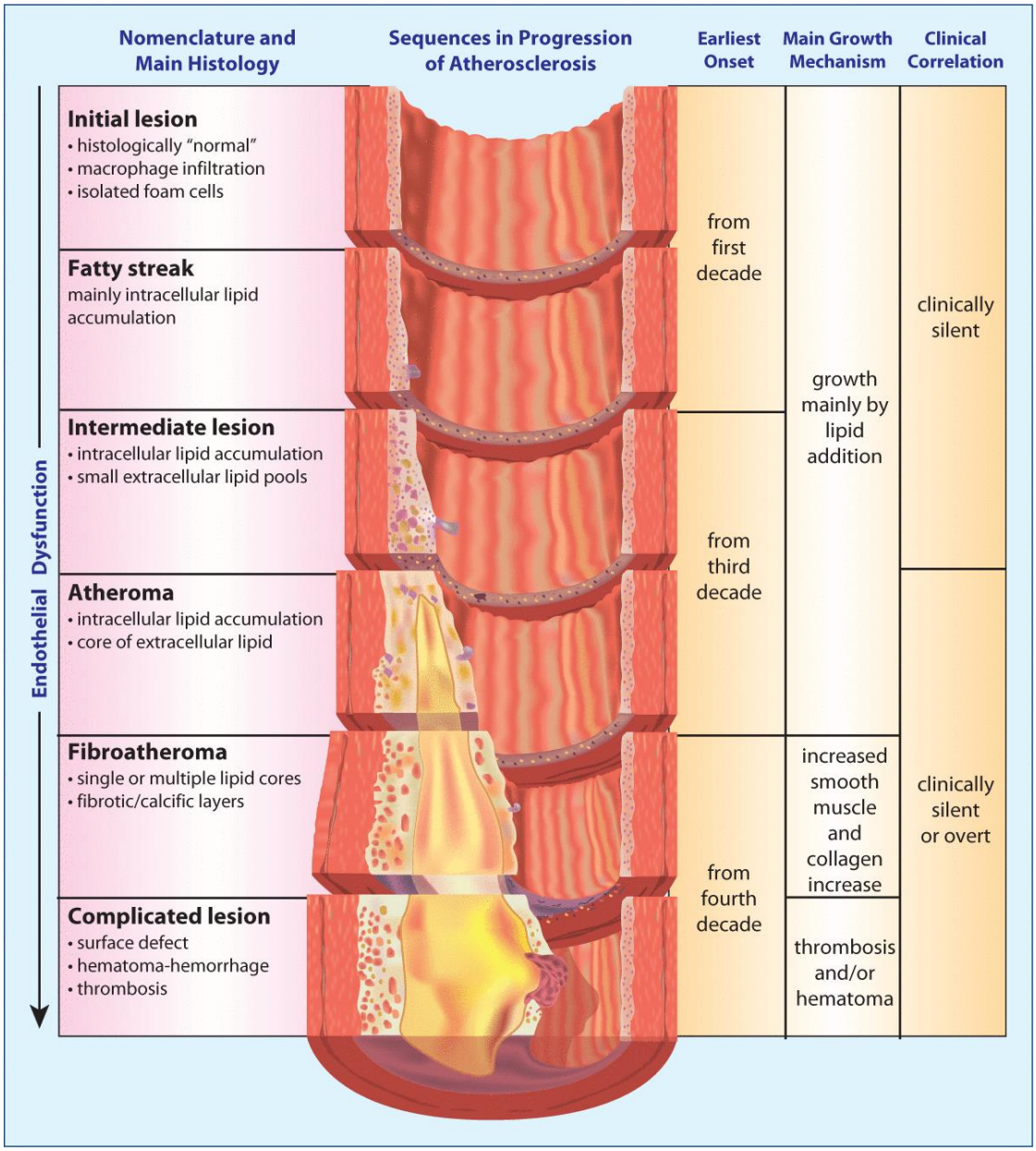

Fig. 3: Progression of atherosclerosis

2.4. Senescence and non-traditional CKD-related risk factors

The high prevalence of CVD in CKD patients is explained by accelerated senescence and pro-aging effects due to non-traditional CKD-related risk factors, combined with traditional risk factors (age, hypertension, diabetes mellitus, dyslipidemia, cigarette smoke, etc.)

2.4.1. Senescence

Senescence is the progressive deterioration of functional characteristics over time, due to the loss of the efficiency of physiological functions, and is strongly associated with a chronic inflammatory state, increased oxidative stress, mitochondrial dysfunction, necro-apoptosis. From a cellular and molecular point of view, CKD is currently considered a model of premature aging and frailty: indeed, several studies demonstrated that CKD patients are biologically older than their unaffected peers with marked effects on vascular, immunologic and cognitive senescence[13]. Of interest, all these biological processes are similar to those observed during aging. Vascular senescence is represented by the degeneration of the vascular structures (smooth muscle cells and endothelium), determining the alteration of the functional and mechanical properties with widespread media stiffening and alterations of the intima, associated with a state of chronic inflammation[11,14]. In this setting, selected molecules such as Klotho and Sirtuin1 (Sirt1) that are known to be involved in the aging process are also significantly reduced in CKD patients. Klotho is able to increase resistance to oxidative stress through suppression of ROS generation: the deficit of Klotho gene expression in mice accelerates cellular senescence and death with an enhancement of vascular calcification and CKD incidence. Moreover, Klotho prevents endothelial senescence induced by uremia preventing NF-kB translocation, thus limiting systemic inflammation. Several water soluble and protein bound uremic toxins typical of CKD patients can induce methyltransferase protein expression leading to Klotho silencing through hypermethylation with a synergy in the induction of endothelial dysfunction and smooth muscle cell osteogenic differentiation responsible for calcification[15–18]. Silent information regulators Sirtuin proteins are deeply involved in cellular senescence processes through regulation of DNA repair, chromosomal stability and gene transcription. In particular, Sirt1 upregulation suppresses age-related cardiac hypertrophy, apoptosis and senescence[19]. Sirt1 is increased after ROS generation as a protective mechanism and activation of sirtuins is known to increase resistance to metabolic, oxidative and hypoxic stress in different tissues including the kidney[20,21]. Of interest, some diet-associated antioxidant agents such as phenols are able to modulate Sirt1 expression[22]: our research group previously reported that resveratrol and other

compounds such as tyrosol and caffeic acid are able to increase Sirt1 expression in human kidney cells interfering with senescence processes.

2.4.2. Non-traditional CKD-related risk factors

The identification of a group of non-traditional risk factors associated with CKD (albuminuria, anemia, disorders of mineral-bone metabolism, malnutrition, hyperhomocysteinemia, inflammation, endothelial dysfunction, oxidative stress, uremic toxins, volume overload), allowed to understand mainly the increased risk of CVD development in CKD patients:

- OXIDATIVE STRESS: the increase of reactive oxygen species (ROS) is a typical feature of atherosclerotic disease and CKD, therefore persistent oxidative stress may be implicated in the pathogenesis of MACE in CKD[23]
- ENDOTHELIAL DYSFUNCTION: Endothelial dysfunction, an alteration of normal endothelial function, which leads to the loss of structural and/or functional properties, is an important feature of CKD and is defined by the finding of impaired endothelial-dependent vasodilation due to inflammation, oxidative stress, dyslipidemia, hyperglycemia and hypertension[23]
- INFLAMMATION: In CKD patients, especially dialysis patients, the inflammatory status represents a triggering factor for cardiovascular events, for example, many inflammatory biomarkers, such as IL-6, are found to have direct and indirect pro-atherogenic properties such as the ability to modulate bone remodeling
- DISORDES OF MINERAL-BONE METABOLISM: Disorders of calcium and phosphate metabolism play an important role in the development of cardiovascular calcification. A serum phosphate level of 5.0 mg/dl or higher is associated with an increased risk of heart valve surgery. Vascular calcification is a highly regulated active process in which other factors, such as numerous mediators and cytokines also play a role, for example, hyperphosphatemia and altered level of FGF-23 have pro-inflammatory and pro-atherogenic effects.6
- AGEs AND UREMIC TOXIN ACCUMULATION: Uremic toxins and the end products of intensive glycation (AGEs), which are collected because of non-

enzymatic glycation and oxidative stress. They are metabolic, inflammatory, and oxidative stress biomarkers

- ANAEMIA: Anemia is one of the main causes of left ventricular hypertrophy and consequently congestive heart failure in CKD[6]. The pathogenesis of anemia in CKD is complex, but a central feature is an inadequate availability of both erythropoietin and iron (Figure 4). The deficiency of iron available for erythropoiesis in CKD is linked to a relative block in iron absorption from the intestines and in reduced iron release from storage in macrophages and the liver. This iron blockade phenomenon is mediated by the master regulator of iron homeostasis, the liver-produced circulating protein hepcidin that is increased in presence of inflammation such as in CKD. Elevated hepcidin levels cause the internalization into cells of cellular iron transporter ferroportin, and consequently this maladaptive response blocks iron available for erythropoiesis. In addition, Iron deficiency is common in patients with CKD, occurring in ≥50% of patients with non–dialysis-dependent CKD and a greater percentage of patients receiving dialysis[24].

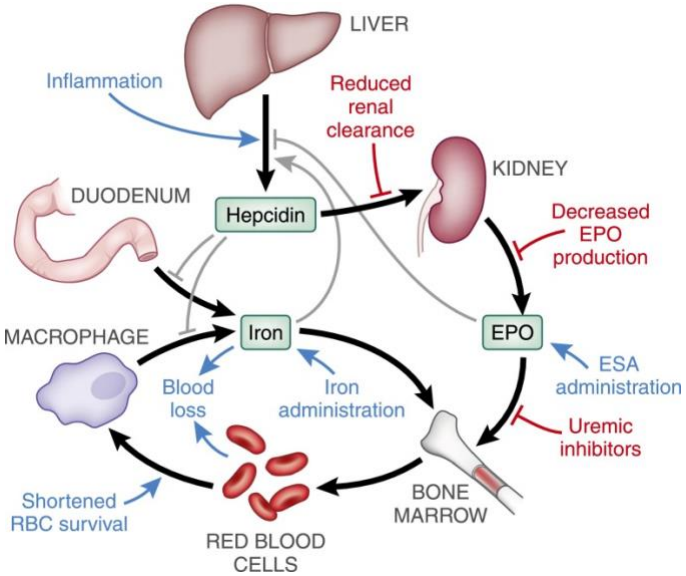

Fig. 4 Representation of the mechanisms underlying anemia of CKD

- TYPE OF HEMODIALYTIC TREATMENT: Hemodialysis (HD) existed for more than 50 years and has extended the lives of millions of patients with renal failure worldwide. The aim of the HD system is to deliver blood in a fail-safe manner from the patient to the dialyzer, enable the efficient removal of uremic toxins and excess fluid, and deliver the cleared blood back to the patient. The dialyzer provides countercurrent transfer of solutes and

fluid across a semipermeable membrane due to (1) the concentration gradient (diffusive transport) and (2) the hydrostatic pressure gradient across the membrane (convective transport) and depends on membrane pore size. Although the basic principles of HD are still being applied today, dialysis technology has improved markedly. Hemofiltration (HF) and hemodiafiltration (HDF) involve the removal of large fluid volumes from the patient, with the removed fluid replaced by substitution fluid. It is the use of substitution fluid that sets these techniques apart from simple ultrafiltration. HF is a convective elimination technique by which water and solutes from the blood compartment are driven solely by positive hydrostatic pressure across the dialyzer membrane into the filtrate compartment without the use of dialysate. As a result of solvent drag effects, small and larger solutes are eliminated at a rate depending on membrane features. HDF combines diffusive (HD) and convective (HF) solute transport using a high-flux membrane. Fluid is removed by ultrafiltration, and the volume of filtered fluid exceeding the volume to achieve target weight loss is replaced by ultrapure, non-pyrogenic infusion solution. Online HDF refers to the online production by the dialysis machine of nearly unlimited amounts of ultrapure, nonpyrogenic dialysate, which is also used as infusion solution. High-volume HDF refers to an effective convection volume of at least 20% of the total blood volume processed[25]. In addition to the type of technique used, an extremely important role is related to the type of filter used. Considerable progress has been made in recent years, leading to the improvement of dialysis replacement therapy where the physical principles governing dialysis did not appear sufficient to optimize the process itself[26]. The membranes used during replacement treatment have evolved significantly: the initial membranes were formed from natural materials, such as cellulose, or simple synthetic compositions, like polysulfone, characterized by a symmetrical structure and good performance relative to the elimination of small molecules[27]. However, these membranes determined significant interactions with the complement pathway and immune response. The subsequent modification of hydroxyl groups on

cellulose membranes gave the same similar performance levels, but less bioactivity (diacetate cellulose membrane and hemophan).

2.5. Inflammation and uremic toxins

About 30% of pre-dialysis patients and 50% of ESRD patients demonstrate an increased inflammatory response, characterized by high levels of C-reactive protein (CRP) proportionally related to uremic toxin levels[28]. Inflammation plays a key role among the risk factors for MACE and the prognosis of CKD patients. In patients with CKD, it is frequent to find circulating high levels of mediators of inflammation, such as IL-1, IL-6, TNF-α, C-reactive protein (CRP), fibrinogen, while albumin levels are low[29]. Not only there is an inverse correlation between levels of inflammatory mediators and GFR, but also CKD patients with a higher level of inflammatory cytokines, in particular IL-1, IL-6, TNF-α, are those with lower chance of survival[29]. In addition, the accumulation of uremic toxins can interfere with biological functions.

The *European Uremic Toxin Work Group* (EUTox) classifies the uremic toxins in three different groups[30]:

- **Water-soluble compounds with molecular weight < 500 Dalton**: in this group we can find creatinine, urea, uric acid, which could be easily removed through the most common types of hemodialysis
- **Compounds with higher molecular weight (>500 Da), so-called middle molecules**: ANP, β2-microglobulin, endothelin, FGF-23, ghrelin, light chains, IL-6,-8,-18, PTH, TNFα, neuropeptide Y, lipids, and lipoproteins. The most representative is β2-microglobulin, removed by high cut-off dialyzer in diffusive, convective, or mixed modalities.
- **Liposoluble compounds and/or protein-bound toxins (PBUT):** AGEs, homocysteine, indoxyl-sulfate, indolacetate, kynurenine, p-cresyl-sulfate, phenylacetate. Most solutes in this group have a low molecular weight, but some have features from medium molecules, such as leptin and retinol binding protein. Typical prototypes of PBUT are phenols and indoles. These compounds are difficult to remove from most of the dialysis techniques currently available. Their removal largely depends on the

balance between free and bound fractions; hemodiafiltration and adsorbent techniques appear to be more effective.

Therefore, the association between traditional and non-traditional risk factors significantly influences cardiovascular mortality in uremic patients and the development of premature atherosclerotic disease.

2.6. Endothelial dysfunction and vascular calcifications

Inflammation is the main cause of the high cardiovascular risk in CKD patients. Inflammatory status is mediated by circulating uremic toxins which can directly or indirectly modulate vascular function and physiology. Furthermore, dysregulation of calcium-phosphorus metabolism contributes to diffuse vascular calcifications[31].

2.6.1. Endothelial dysfunction

Uremic toxins stimulate oxidative stress through the production of reactive oxygen species (ROS). This process brings to altered availability nitric oxide (NO) and consequent endothelium dependent vasodilation of blood vessels. Nitric oxide is important for maintenance vascular homeostasis, muscle tone, platelet adhesion, migration, and proliferation of vascular smooth muscle cells. Therefore, altered NO metabolism and increased oxygen free radicals cause endothelial dysfunction[14]. The loss of vascular compliance is mediated by uremic toxins which influence intracellular and intercellular signaling in endothelium and smooth muscle cells (Figure 5)[32].

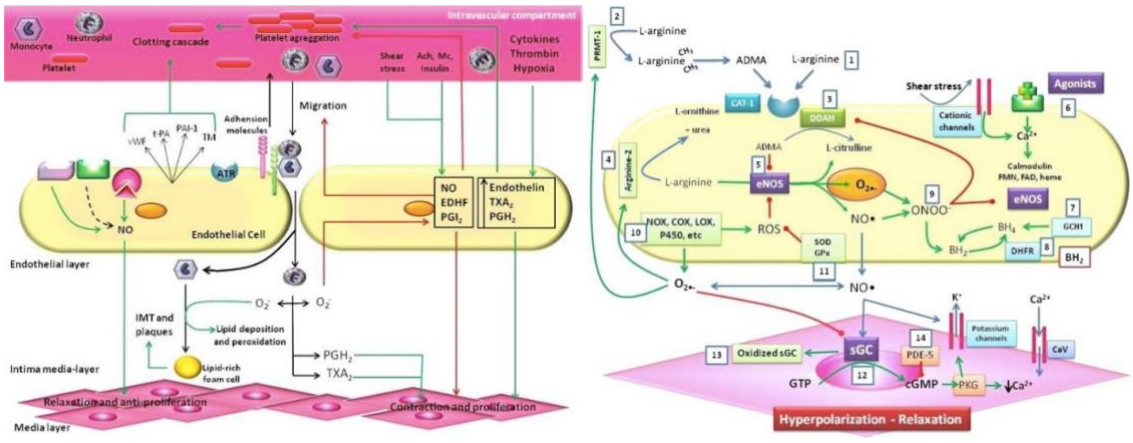

Fig. 5 intracellular and intercellular signaling in endothelium and smooth muscle cells

Then, endothelial dysfunction is associated with an inadequate NO bioavailability, due to high level of circulating uremic toxins: this makes blood vessels less compliant and more prone to inflammatory injury.

2.6.2. Vascular calcifications

Endothelial dysfunction leads to the development of vascular calcifications. In addition, patients with CKD progressively lose the ability to adjust serum levels of calcium and phosphate. Altered calcium-phosphate metabolism stimulates transition of smooth muscle cells into osteoblast-like cells (Figure 6)[33].

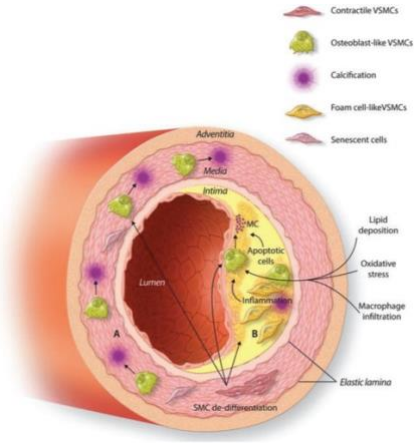

Fig. 6: mechanism of vascular calcification

Two genes are known to be strongly involved into vascular senescence and calcification: FGF23 and KLOTHO, respectively encoding for fibroblastic growth factor and its receptor. KLOTHO seems to have protective effects on vascular calcification, left ventricular hypertrophy and cellular senescence, while high levels of FGF23 stimulate hepatic production of inflammatory cytokines. Hyperphosphatemia, a specific feature of patient with end--stage renal disease (ESRD), both increases FGF23 and inhibits KLOTHO expression. The modulation of FGF23/KLOTHO levels leads to severe endothelial dysfunction, increased susceptibility to vascular calcifications and, more generally, increased risk of MACE. (Figure 7)[34].

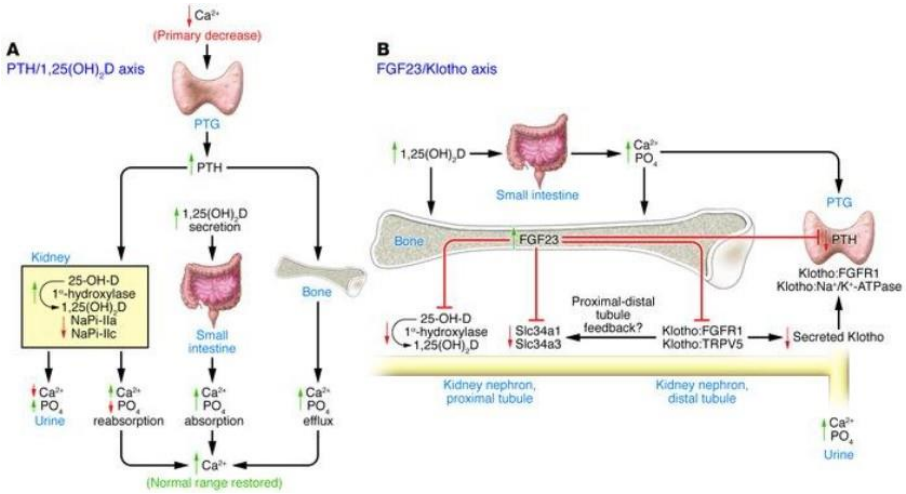

Fig. 7: KLOTHO and FGF23 in calcium-phosphate metabolism

In addition, circulating uremic toxins have inhibitory effect on KLOTHO expression: this means a decreased inhibition of vascular calcifications and increased oxidative stress[35].

Therefore, uremic toxins and inflammatory cytokines removal through high--flux hemodialysis is nowadays considered the better therapeutic strategy to reduce the mortality rate for cardiovascular disease in patients with ESRD[36]. However, the relationship between uremic toxins and inflammation, endothelial dysfunction, reactive oxygen species and altered calcium--phosphate metabolism can only partially explain the development mechanism of cardiovascular injury in ESRD patients. Other biological factors seem to be deeply involved: uremic toxins, T-cell co-stimulatory molecules, extracellular vesicles, and activation of the complement cascade.

2.7. T-cell co-stimulatory molecules

T-cell co-stimulatory molecules are expressed on the surface of leukocytes and modulate T cell activation. Lymphocyte's stimulation is mediated by binding of T cell receptor (TCR) to specific HLA--antigens present on the membrane of antigen--presenting cells (APC). Moreover, lymphocyte co-stimulation is due to the interaction between different molecules expressed on APC and T-Cells. This causes T cell proliferation and differentiation and, consequently, the activation of the immune response. The lack of co-stimulation leads to T cell apoptosis and anergy. CD40/CD40L, B7/CD28, PD-1/PDL1 and ICOS/ICOSL are considered the most

relevant costimulatory pathways (Figure 8)[37]. These molecules are expressed not only on the surface of immune cell, but also on different epithelial and endothelial cells of different organs. Several studies reported the expression of CD40 and ICOSL on endothelial cells and vascular smooth muscle cells in the vessels, in the presence of inflammation and calcification.

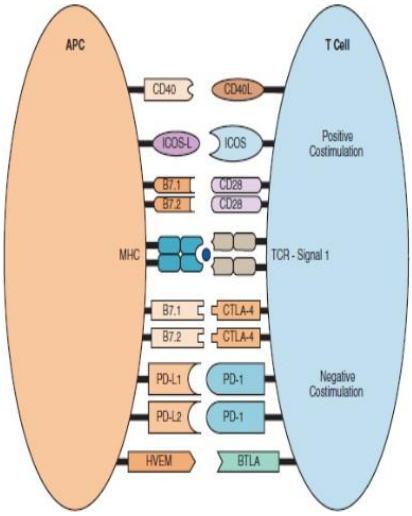

Fig. 8: T-cell co-stimulatory molecules

2.7.1. ICOS and ICOSL

ICOS is an inducible T-cell co-stimulatory molecule which needs the cooperation of other surface antigens (CD28 or CTLA-4) to activate T-lymphocytes. These three antigens are expressed on activated CD4+ and CD8+ T-cells. ICOS has a specific ligand, named ICOSL, expressed on B-cells, macrophages and dendritic cells. Its selective binding to ICOS stimulates T-cell proliferation and the production of different inflammatory cytokines such as IFNγ, IL-4, IL-10. ICOS seems also to be involved in atherosclerotic disease, then research on ICOS/ICOSL system could be useful to improve prevention and treatment of cardiovascular injury (Figure 9)[38].

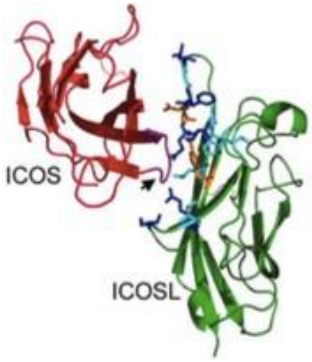

Fig. 9: tertiary structure of ICOS-ICOSL

2.7.2. CD40 and CD40L

CD40/CD40L pathway seems to be related to atherosclerosis and vascular injury. CD40 is a T-cell co-stimulator belonging to the TNF receptor superfamily. It is constitutively expressed not only on immune cell surface (B-lymphocytes, macrophages and dendritic cells), but also on endothelial cells, smooth muscle cells, platelets, and fibroblasts. The interaction between CD40 and its ligand CD154 (CD40 ”Ligand” or CD40L) on these different cells causes the production of interleukins (IL-1, IL-6, IL-8) and metallo-proteases, stimulating inflammatory response (Figure 10)[37].

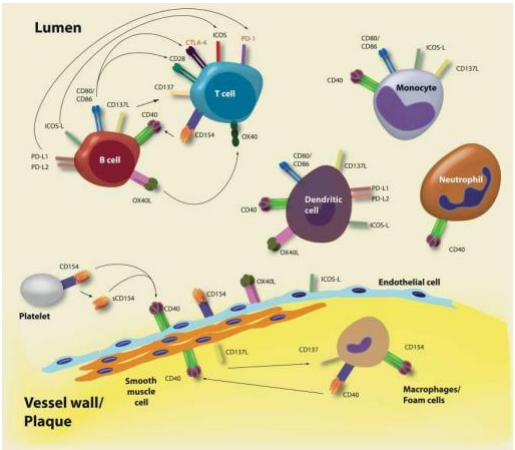

Fig. 10: CD40/CD40-L co-stimulation pathway

CD40 and CD40L are available in two different forms: plasma protein--bound type and soluble type. Soluble CD40L (sCD40L) is mainly produced by platelets: indeed, after platelet activation, CD40L is expressed on their surface and is cut by metallo-proteases to form the soluble fragment sCD40L. This molecule can bind

CD40 and activate the CD40/CD40L intracellular pathway. This leads to activation of inflammatory response, cytokine release and endothelial expression of adhesion molecules[37].

High levels of sCD40L can be found in patients with hypercholesterolemia, angina, and ischemic heart disease, and, locally, in unstable atheromatous plaques. Silencing of CD40/CD40L signaling can blunt atheromatous plaque progression, suggesting a key role of this pathway in the development of atherosclerotic complications[39(p40)].

One of the largest clinical trial about cardiovascular risk in end-stage uremic patients (RISCAVID study) demonstrated that a concentration of sCD40L >7.6 ng/ml is associated with an increased incidence of cardiovascular and cerebrovascular events and mortality rate in hemodialysis patients. Therefore, chronic activation of the CD40/CD40L system can facilitate premature and accelerated atherosclerosis[40].

2.8. Extracellular vesicles

Extracellular vesicles (EVs) are small lipid bilayer-delimited particles naturally released from a different cell in different ways. They have a fundamental role in intercellular communication, thanks to their ability to transfer proteins, lipids and nucleic acids to target cells[41]. We can distinguish three different subgroups, as reported in Figure 11 and 12.

Type and Size	Biogenesis	Markers	Contents
Exosomes (40–130 nm)	Endolysosomal pathway. Release by exocytosis of multivesicular bodies	Tetraspanins (CD63, CD9, CD81), Alix, TSG101, Hsp60, Hsp70, Hsp90	miRNA and mRNA; lipids (cholesterol, ceramide, sphingomyelin), cytokines receptors, MHC molecules
Microvesicles (100–1000 nm)	Cell surface. Outward budding of plasma membrane	Integrins, selectins, metalloproteinases, Phosphatidyl-serine	mRNA, non-coding RNAs, membrane receptors, cytoplasmic proteins (cytokines)
Apoptotic bodies (50–5000 nm)	Cell surface. Release from cellular blebs during apoptosis	Phosphatidyl-serine	Nuclear fractions, cell organelles, DNA, rRNA, mRNA

Fig. 11: EVs classification

- Exosomes (40-130 nm), which arise from the endo-lysosomal compartment through the formation of multiple endoluminal vesicles, are released by exocytosis into the extracellular compartment. Exosomes are rich in

tetraspanine (CD9, CD63, CD81) and other molecules involved in signal transduction (TSG 101, RAB);

- Microvesicles (or microparticles) differ from exosomes by their larger size (100-1000 nm) and formation mechanism, as they are released directly from the plasma cell membrane by gemmation, typically via a calcium-process-dependent, which modifies the distribution of membrane phospholipids;
- Apoptotic bodies, larger extracellular vesicles (50-5000 nm), are released into the extracellular environment during the apoptosis process.

Vesicle contents may include nucleic acids (DNA, mRNA, rRNA, miRNA), cytokine receptors, cytoplasmic proteins, MHC molecules and lipids

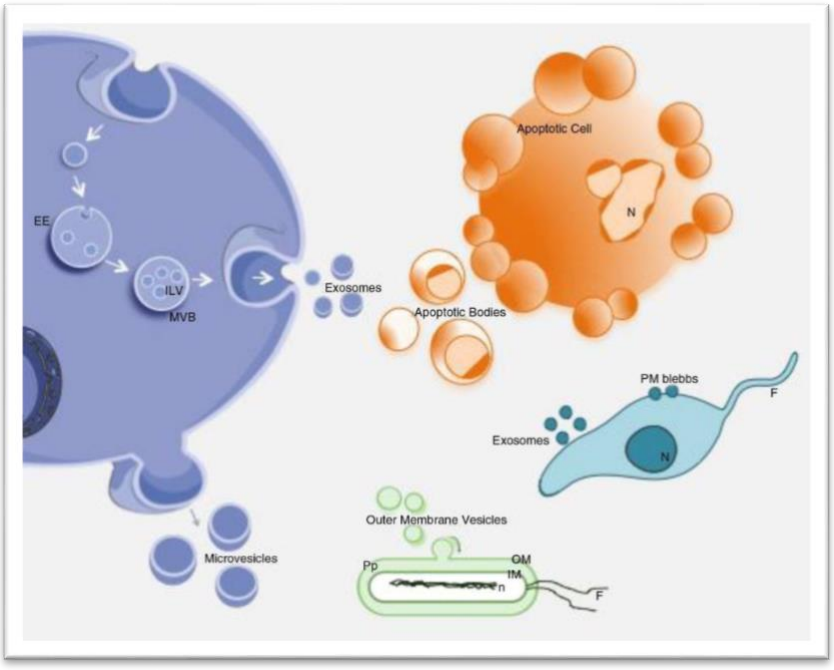

Fig. 12: Genesis and release of EVs from source cell

EVs were found about 1950, when these mediators were initially called "platelet dust". In the following decades, several studies have allowed a better characterization of circulating EVs isolated by plasma and serum. Released EVs may remain in the extracellular space in proximity of the place of origin or may enter the biological fluids reaching distant sites. This may explain the presence of MVs in the plasma, urine, milk, and cerebrospinal fluid[41]. The bulk of MVs present in the circulation is derived from platelets (specific markers CD41a, CD6 and

GPIb), and in less extent from other blood cells and endothelial cells[41]. The release of EVs may be constitutive or consequent to cell activation by soluble agonists, by physical or chemical stress such as the oxidative stress and hypoxia, and by shear stress in different inflammatory diseases (i.e diabetes, hypertension, infections, neoplasm, chronic heart failure).

Only in recent years has been recognized the role played by the EVs as mediators of intercellular communication, opening new scenarios regarding the mechanisms of cell-cell interaction, activation, and growth: this event can be induced by several stimuli coming from extracellular (hypoxia, oxidative stress) and intracellular space (cytoplasmic calcium concentration and alterations of cytoskeleton). Once released, they can interact with specific target cells through various mechanisms (Figure 13)[42]:

- direct fusion of EVs with the cell cytoplasmic membrane and release of vesicular content into the cytoplasm;
- endocytosis-mediated internalization and subsequent release of EVs content into the cell cytoplasm;
- ligand/receptor interaction expressed on the cell surface and vesicular;
- transfer of membrane receptors expressed by EVs to the surface of the target cell;
- interaction with the extracellular matrix and release of their contents

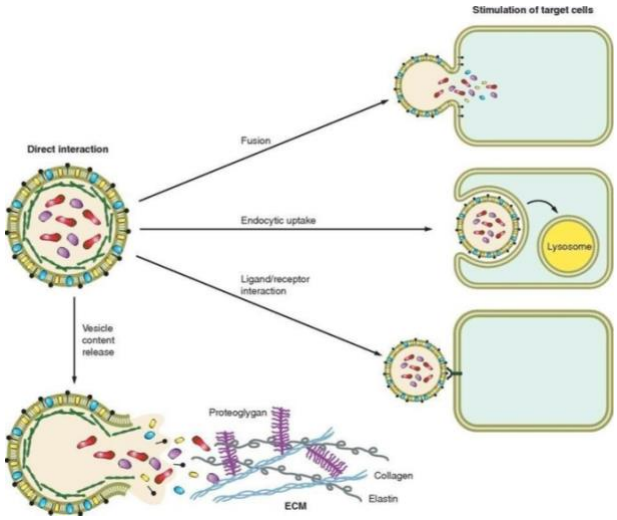

Fig. 13: Interaction between EVs and cellular targets

Most EVs effects seem to be mediated by:

- the presence of different types of microRNA (miRNA) within the EVs, potentially transferable to target cells. MicroRNAs are small non-coding RNA sequences of about 22 nucleotides, already identified in different species (animal, plant, virus)[43]. It is now known that they have an important role in the progression of different diseases, especially in cancer diseases, but numerous evidences associate the action of microRNA also to the pathophysiology of myocardial infarction, cardiac hypertrophy, cardiomyopathy, arrhythmias, as well as in the regulation CVD-related epigenetic cell damage processes in CKD[43,44]
- the effects of EVs, however, are also determined by the structures present on their surface. Indeed, EVs can express peculiar surface markers involved in inflammation, coagulative cascade activation and apoptosis, e.g., CD40L, TF, C5b9, ICOS[42]. Due to the presence of these same surface markers, plasma EVs seem to be effectively internalized, with different effects depending on the target cell: for example, in a study of Boulanger et al., in patient CKD, when affected endothelial cells, an increase in ROS was detected, when smooth vascular muscle cells, a faster osteoblastic transition was determined[45].

2.9. EVs in cardiovascular damage of CKD patients

Plasma Endothelial-EV levels are higher in CVD patients than in healthy subjects[46]. The release of EVs seems to be mediated by numerous pro-inflammatory elements such as cytokines, activated platelets or oxidized LDL; Moreover, the EVs themselves, appear to be involved in the modulation of inflammation by acting on several targets, both as pro-inflammatory and anti-inflammatory factors such as cytokines, activated platelets or oxidized LDL[45]. EVs are involved in thrombus formation, presenting on their surface multiple platelet activation mediators, such as tissue factor (TF)[47]. In particular, EVs cause an increase in the intra-plaque TF concentration, resulting in activation of the coagulation cascade[46]. In addition, the EVs release pro-inflammatory cytokines (IL-1, IL-6, IL-8, TGFβ)[42], induce an increase in the exposure of adhesion molecules and are involved in the activation of Platelet Activating Factor Receptors. The consequent endothelial activation induces the adhesion and

diapedesis of leukocytes and neutrophils, a crucial point in the atherosclerotic plaque formation process (Figure 14)[48]. In addition, the EVs are involved in inhibiting the release of nitric oxide by endothelial cells, without alterations in the expression of NO synthetase[43,48]. In patients with heart disease, the quantitative analysis of the circulating levels of endothelial-derived EVs after stimuli with acetylcholine showed that higher quantities of these EVs correspond to greater stiffness of the arterial wall, a lower capacity for vasodilation in response to the increase of blood flow and/or stimulation with acetylcholine[42,45].

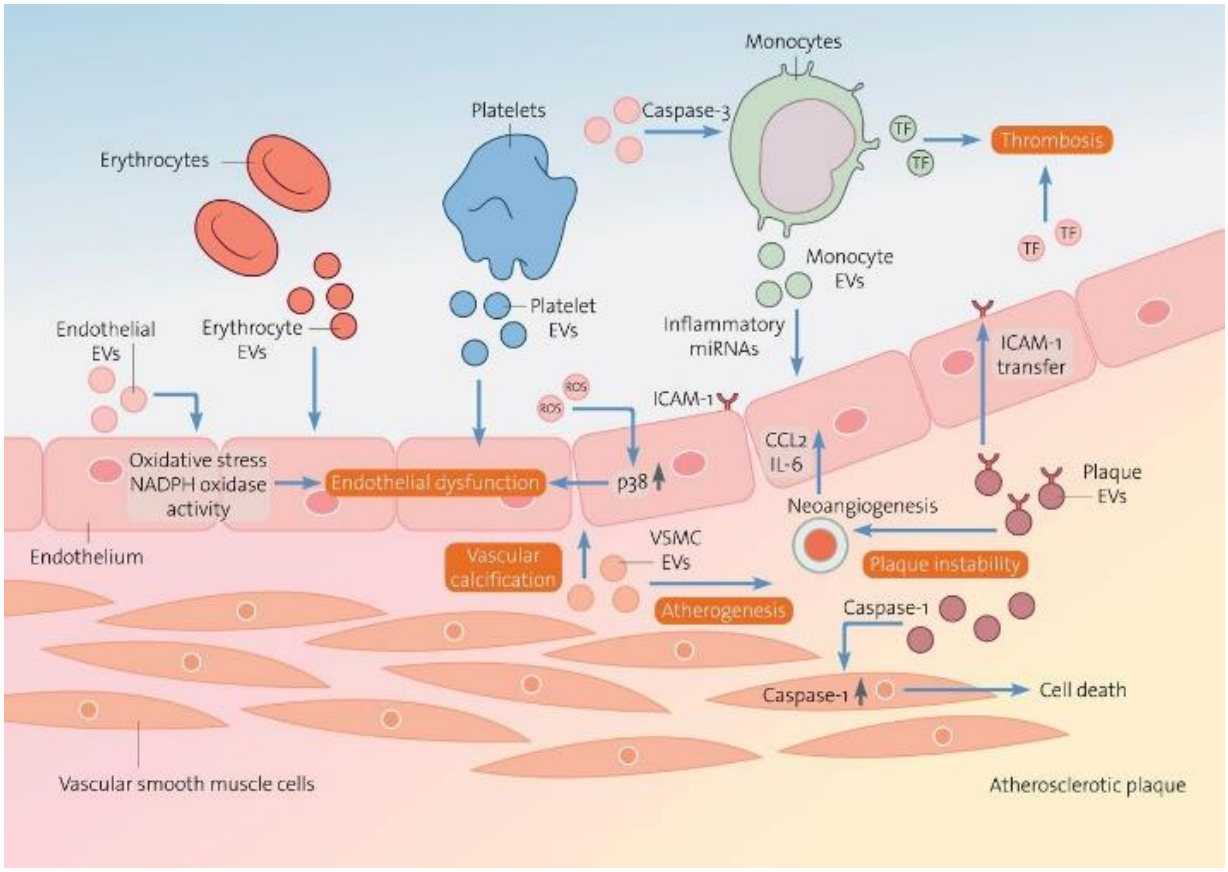

Fig. 14: Representation of EVs in endothelial dysfunction and vascular calcification

Similarly, in chronic kidney disease, high endothelial EVs levels correlate with the development of atherosclerosis and an increase in CVD. The high levels of EVs would be a consequence of the persistent inflammatory environment induced by uremia (uremic toxins, hyperphosphatemia, hypercalcemia, elevated levels of FGF23, decreased levels of KLOTHO)[49]. For example, it is precisely the high levels of phosphate, together with hypercalcemia and the presence of cytokines such as

TNFα, that stimulate the secretion of EVs that release miRNAs favoring the formation of calcium deposit (miRNA133b, -155, -204, -211, -223)[50] (Figure 15).

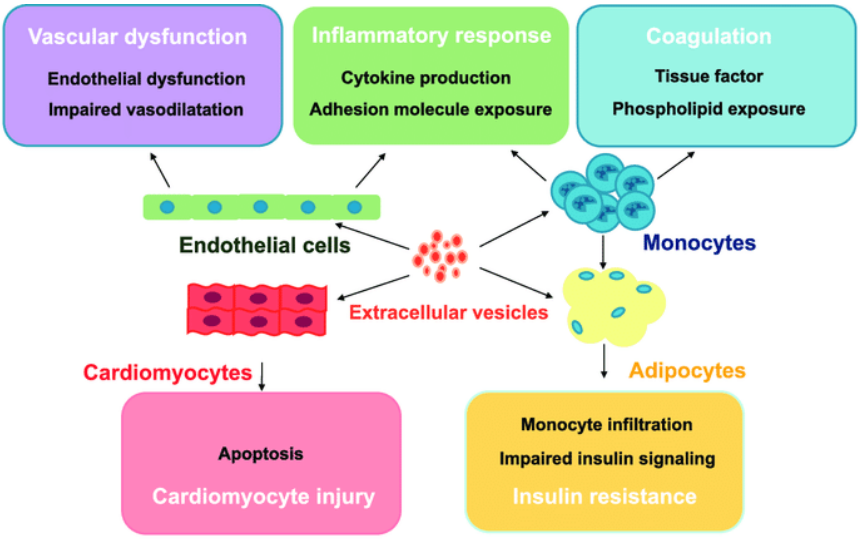

Fig. 15: Simplification of EV role in vascular injury

2.10. Complement system

For decades, hemodialysis has been known to activate the complement system. In dialysis, complement activation is mainly caused by the interaction of blood with the membrane. Regardless of the efforts to improve biocompatibility, complement activation still occurs in HD, even with modern membranes. It has been hypothesized that complement activation leads to HD-induced inflammation and thereby increases the subsequent cardiovascular risk. However, the link between complement activation products and CV-events remains poorly characterized. Furthermore, previous experimental studies proposed a link between HD-induced complement activation, pro-inflammatory cytokines, and the coagulation system. Recently, complement activation prior to a HD session was associated with the occurrence of CV-events in HD patients and it has been shown that activation of the alternative pathway of the complement cascade (indicated as C3d/C3 ratio) during dialysis is linked to the development of CV-events. Daha et al. were the first to assess the relationship between intradialytic complement activation and subsequent outcome (Figure 16)[51].

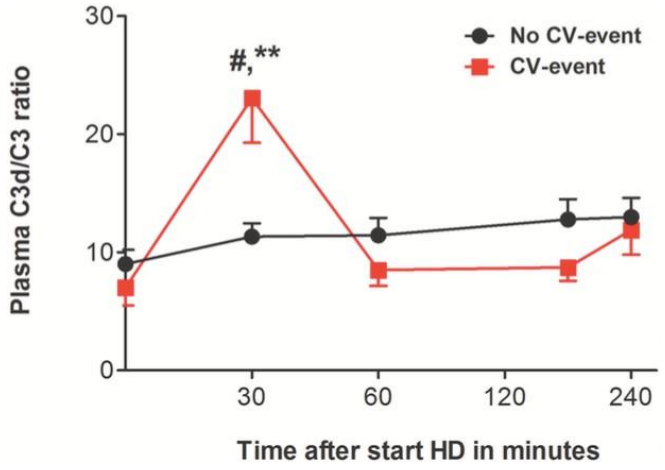

Fig. 16: Correlation between C3 level and CV-events

The same group also found that MBL was consumed in the event-free group, implying that this decrease is actually beneficial. In accordance, MBL has been proposed to be involved in the removal of atherogenic particles, thereby decreasing atherosclerosis. Higher MBL levels in HD patients were associated with protection against cardiovascular disease[52]. In addition, it has been found a rise in properdin levels in patients without CV events. Properdin, unlike other complement factors, is produced by leukocytes, predominately neutrophils. Therefore, the increase in properdin is presumably the result of leukocyte activation by the HD membrane leading to degranulation. Since, this rise was not observed in the CV-event group, it was speculated that this effect was due to properdin consumption by alternative pathway activation (Figure 17)[51].

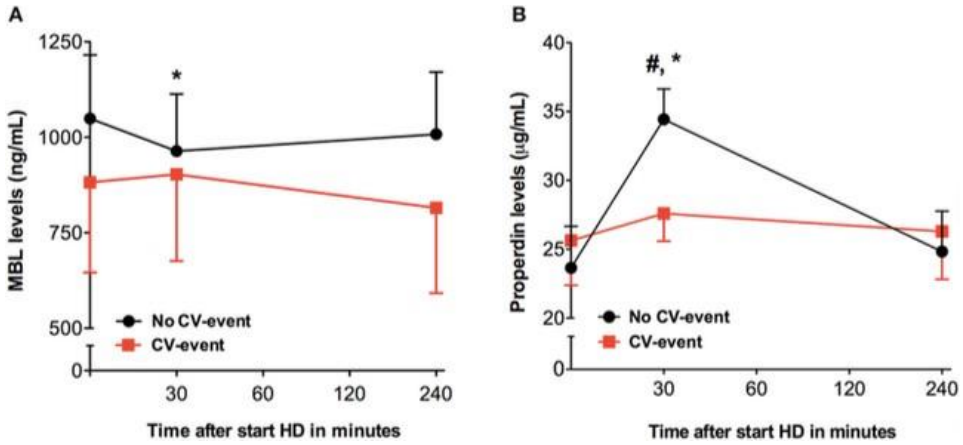

Fig. 17: Correlation between MBL/Properdin levels and CV-events

The conclusions of Daha et al. were that intradialytic differences in complement activation may allow the identification of uremic patients at high risk to develop MACE.

2.11. Renal replacement therapy and cardiovascular risk

Because of the strong relationship between ESRD and cardiovascular risk, the different strategies of dialysis could be used not only for blood purification, but also to remove the above-mentioned molecules involved in inflammation, endothelial dysfunction, and oxidative stress. This would significantly improve the prevention of cardiovascular and cerebrovascular events in ESRD patients.

Even though HDF seems to be the best strategy for blood purification due to an increased clearance of middle molecules and to reduce inflammatory parameters, the most recent randomized clinical trials did not prove HDF superiority over standard high flux HD in terms of incidence of MACE. A recent Japanese observational study registry demonstrated a considerable reduction of cardiovascular mortality in dialysis dependent people using a membrane with enhanced capacity of adsorption[53], a process that helps to remove medium- and high molecular weight molecules, having a crucial role in the reduction of inflammatory mediators and consequently in the modulation of the development of cardiovascular damage. Among dialyzers with adsorption characteristics, polymethylmethacrylate (**PMMA**) membranes have the following features: better biocompatibility and high performance in removing uremic toxins. By lowering the uremic environment, PMMA membranes also improve the immune response of the CKD patient, reduce comorbidities, determine a superior ability to maintain muscle mass and protein, and reduce uremic itching.

There are different PMMA dialyzer, in order to adapt to the different dialysis methods:

- B3 PMMA series for low-flux hemodialysis
- B1 PMMA series for high flow or low flow hemodiafiltration
- PMMA series BKF, specific for the removal of high weight molecules (sCD40L)[54]
- PMMA BGU series for removing medium-small molecules and uremic itching

- PMMA EAD series, for the removal of free light chains; this filter maximizes the absorption performance of light chains using a specific blood line set and a second BKF dialyzer; the result is a significant increase in the removal of light chains, working in bicarbonate dialysis standard mode.

Moreover, these membranes have a very great biocompatibility (evaluated by WBC count, PLTS, C3 fraction).

Other innovative filters have just been put on the market, such as the Theranova filter, a membrane optimized to remove medium and high weight molecules. The dialysis technique in which these filters are used does not change compared to the HD, however It cannot be used in HDF or HF.

In addition, while convective and diffusive procedures clear and filter out low and medium molecular weight metabolites from the blood, adsorption can also remove high water-soluble molecular weight molecules as well as *protein-bound uremic toxins* (***PBUT***) independently from their molecular weight[55]. Basing on these considerations, PMMA dialyzers may remove metabolites involved in cardiovascular disease in people with ESRD, thus reducing the incidence of cardiovascular and cerebrovascular accidents[53].

In conclusion, recent clinical trials about cardiovascular risk in uremic patients underline the important role of sCD40L in atherosclerosis. In the same way, endothelial EVs can influence inflammatory status and nitric oxide concentration: they represent a reliable marker of endothelial dysfunction. The use of dialyzers with high adsorptive capabilities (e.g., PMMA) may improve uremic toxin removal efficiency, thus reducing cardiovascular mortality in dialysis patients.

3. Preliminary data and research activities during PhD program

On this background, in the first and second years of PhD program we performed preliminary ELISA assay of sCD40L's plasma levels in a group of hemodialysis patients (n=310), of which 175 (56.45%) patients had sCD40L values higher than 7.6 ng/ml (Figure 18).

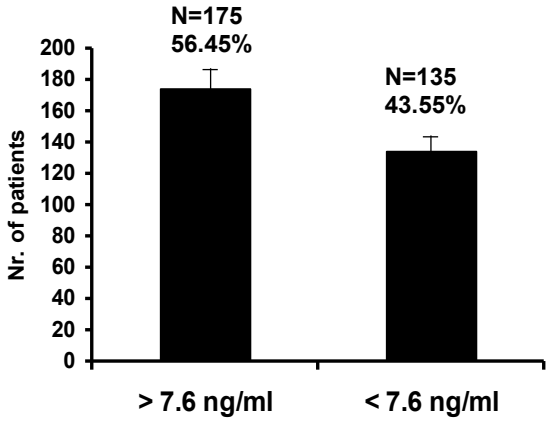

Fig. 18: Distribution of patients with sCD40L values higher than 7.6 ng/ml in a cohort of hemodialysis patients (n=310)

Subsequently, in a subgroup of these patients (n=10) and in a group of healthy subjects (n=10), we performed quantification and characterization of the plasma EVs, in vitro studies on human endothelial cells and smooth muscle cells to evaluate the biological role of EVs isolated from CKD plasma and analysis of microRNA content of plasma EVs. Preliminary data generated in UPO labs and external collaborators using Nanotrack particle analysis showed higher levels of circulating EVs in stage V CKD patients in chronic hemodialysis treatment in respect to healthy subjects (Figure 19).

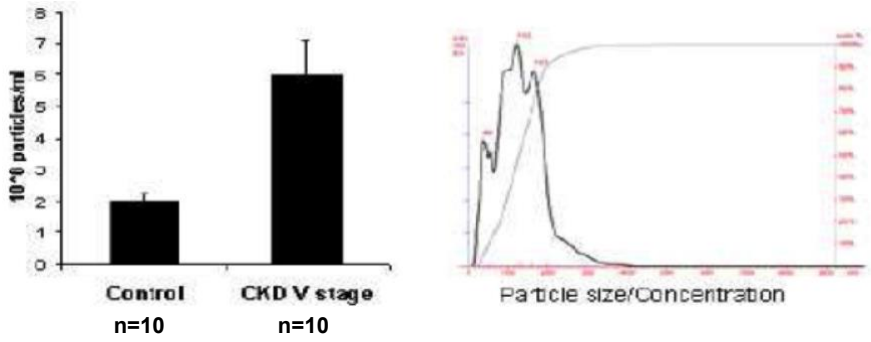

Fig. 19: higher levels of circulating EV in hemodialysis patients than healthy subjects

FACS analysis of EVs isolated from plasma of patients with stage V CKD revealed the presence of surface antigens typical of platelets, mononuclear cells, and endothelial cells. Of interest, endothelial-derived EVs are not present in control healthy subjects. In addition, CKD plasma EVs express low levels of T and B cell antigens and exosomal markers, whereas they express high levels of class I HLA and molecules involved in inflammation, activation of the coagulation cascade and apoptosis such as CD40L, Tissue Factor (TF) and the terminal component of the complement cascade C5b9 or MAC (Figure 20).

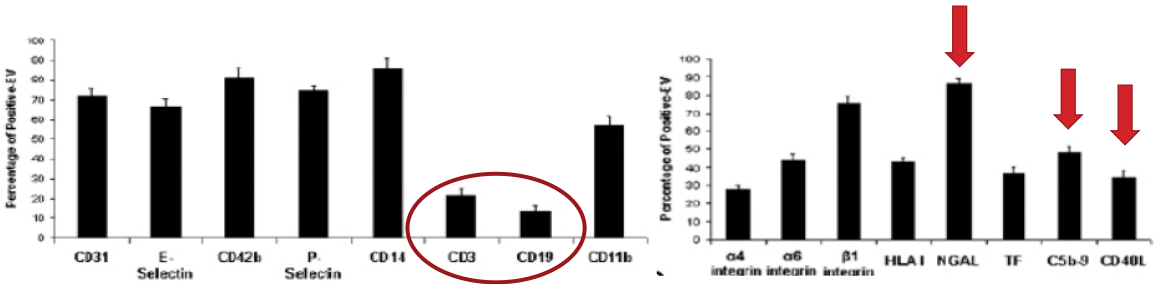

Fig. 20: Surface antigen expression of CKD plasma EVs

After internalization, CKD plasma EVs exerted different biological effects within target cells. In endothelial cells, in respect to vehicle alone or EVs isolated from control healthy subjects, CKD EVs increased ROS production. In smooth muscle cells, in respect to vehicle alone or EVs isolated from control healthy subjects, CKD EVs increased osteoblast differentiation of SMC, a known marker of calcification (Figure 21).

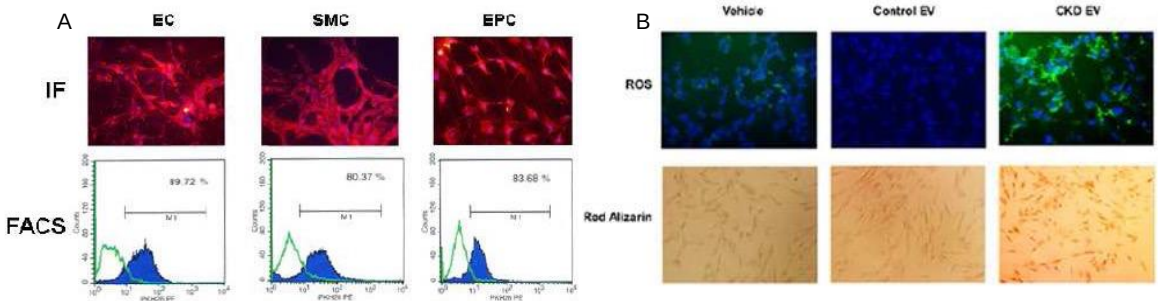

Fig. 21: (A) CKD plasma EV internalization in vitro within human endothelial cells (EC), artery smooth muscle cells (SMC) and (B) In EC, CKD EV increased ROS production and in SMC, CKD EV increased osteoblast differentiation, a known marker of calcification

The preliminary analysis of microRNA content of CKD plasma EVs (using the web platform Protein Quest to design the pathways potentially involved in CKD plasma EV-induced endothelial dysfunction and SMC calcification) identified 5 microRNAs

(miR-17-5p, miR-92a, miR-423-5p, miR-451a and in particular miR-223) that showed an increased expression in CKD plasma EV in comparison to EVs isolated from control healthy plasma.

We also evaluated in this group of patients whether citrate-buffered dialysis improves HD efficiency, inflammatory parameters and chemerin-mediated microvascular injury. Patients were treated in sequence with acetate, citrate and, again, acetate-buffered dialysis solution (3 months per interval). At study admission and after each treatment switch, we evaluated dialysis efficacy and circulating levels of chemerin and different inflammatory biomarkers. In vitro, we stimulated EC and VSMC with patients' plasma and we investigated the role of chemerin as uremic toxin.

Our investigation showed that citrate dialysis increased HD efficacy and reduced plasma levels of CRP, fibrinogen, IL6 and chemerin (Figure 22).

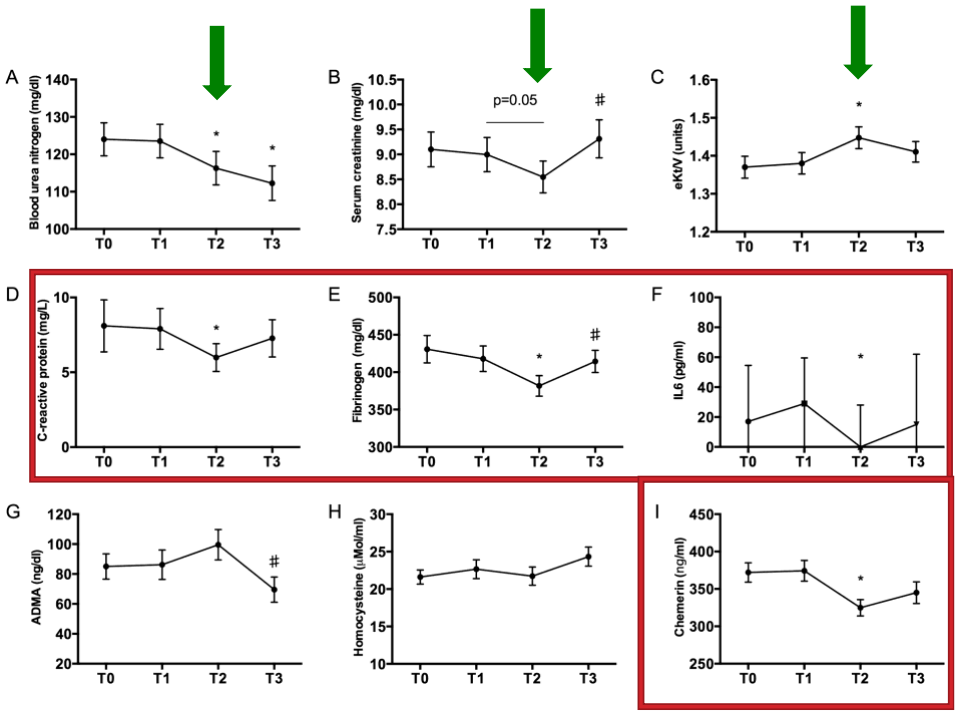

Fig. 22: Citrate dialysis increased HD efficacy (A-B-C) and reduced plasma levels of CRP, fibrinogen, IL6 and chemerin (D-E-F-I)

In vitro, patients' plasma induced EC and VSMC dysfunction. These effects were reduced by citrate-buffered solutions and paralleled by the decrease of chemerin levels. Consistently, chemerin receptor knockdown reduced EC and VSMC dysfunction. In conclusion, switching from acetate to citrate improved dialysis

efficacy and inflammatory parameters; in vitro, chemerin-induced EC and VSMC injury were decreased by using citrate as dialysis buffer.

4. Aims of the study

We think that lymphocyte co-stimulation pathways and EVs may at least in part fill the gap of knowledge in the pathogenic mechanisms of CKD-related CVD that may be only in part explained by the presence of middle/large molecular weight water soluble, and protein bound uremic toxins. Basing on previous literature and our preliminary results, we carried out an experimental study with the aim of analyzing the effect of the removal of the sCD40L by different dialysis treatments to identify the most effective and with a greater cardio-effect and vascular protection in the chronic uremic patient. In addition, in the second part of the study we evaluated the role of EVs in the modulation of cardiovascular damage of the chronic uremic patient.

This study has three different purposes:

- To identify a predictive value of sCD40L serum levels for incidence of cardiovascular events in a cohort of dialysis patients;;
- To assess the role of sCD40L and its pathway, and compare the efficacy of two different types of dialyzers (PMMA BKF vs PS) in the removal of sCD40L and other molecules (double-crossover study);
- To evaluate the effect of PS and PMMA-BKF on pro-inflammatory, pro-atherosclerotic and pro-calcific uremic sera on endothelial cells and smooth human muscle cells in vitro, in particular by analyzing the role of the CD40/CD40L pathway;
- To perform a characterization of CKD-EVs and an analysis of their role in conditioning endothelial dysfunction and vascular calcifications.

5. Patients and methods

5.1. Clinical trial design

5.1.1. Study population

In this multicentric, prospective, double-cross-over study, we enrolled patients with end stage renal disease in hemodialytic treatment from 6 dialysis centers (A.O.U. Città della Salute e della Scienza di Torino, ASL Versilia, ASL CN1, ASL Asti, ASL Biella, ASL VCO).

The inclusion criteria were the following:

- Age from 18 to 75 years old
- Patients in bicarbonate HD thrice weekly for at least 6 months
- Patients with vascular access for hemodialysis allowing Qb > 250 ml/min

Patients with neoplastic, acute, or chronic inflammatory disease (including HIV, HBV or HCV infection) and allergic to polysulfone/PMMA were excluded due to possible nonspecific increase of sCD40L serum levels.
A written informed consent was obtained, and the study protocol reviewed and approved by local ethic committees.

At the time of enrollment, demographic (age and gender) and clinical (start date of dialysis, diabetes, hypertension, dyslipidemia, nephropathy cause of ESRD and previous cardiovascular events) data of the whole population were entered into a centralized database.

Serum sCD40L level were assessed at the time of the enrollment and during a median follow-up of 29 months. Cardiovascular and cerebrovascular events (acute myocardial infarction, congestive heart failure, severe peripheral vascular disease, and stroke) were registered.

5.1.2. Patients with high cardiovascular risk

In order to select patients with high cardiovascular risk, firstly we identified the sCD40L value with the best statistical performance to assess patients with highest cardiovascular risk of events – similarly to RISCAVID study – and secondly, we excluded people with sCD40L concentration lower than the cut-off value found.
This selected cohort was randomized into two different groups to receive two

different type of hemodialysis treatment for an observational period of 9 months (Figure 23). Moreover, both groups were divided into two different hemodialysis programs, with two different dialyzers (RRT = Renal Replacement Therapy; PS = polysulfone; PMMA BKF = polymethylmethacrylate):

- GROUP 1:
  - T0 – T6 (months): RRT with PMMA BKF dialyzer
  - T3 – T6 (months): RRT with PS dialyzer
  - T6 – T9 (months): RRT with PMMA BKF dialyzer
- GROUP 2:
  - T0 – T3 (months): RRT with PS dialyzer
  - T3 – T6 (months): RRT with PMMA BKF dialyzer
  - T6 – T9 (months): RRT with PS dialyzer

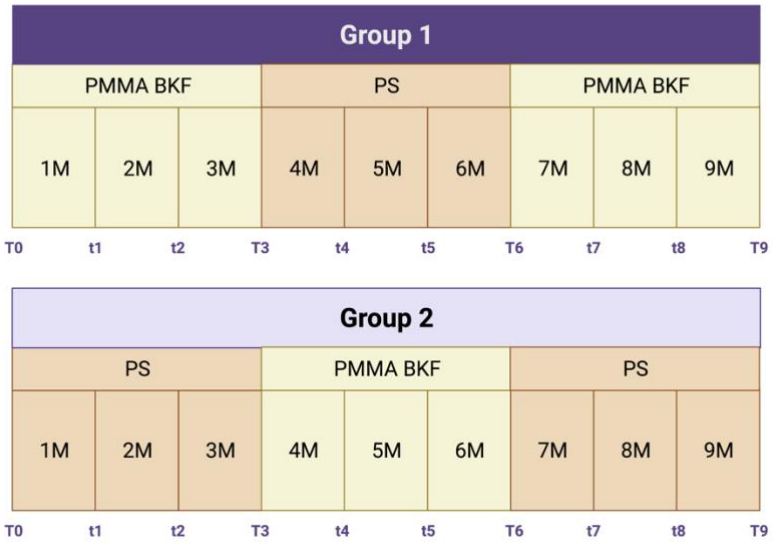

Fig. 23: study protocol of the main project

As a control group for clinical-laboratory evaluations, the selected cohort represents the control of itself, being a double cross-over study. As a control group for the comparison of in vitro analyses were enrolled n = 15 healthy subjects, corresponding by sex and age.

Furthermore, during this study, using serum or plasma from the test population, further clinical or in vitro studies were carried out, such as: study of the effects of membranes on mass removal of sCD40L and PBUT, modulation of inflammation

following RRT with PMMA BKF or PS, expression of CD40L on the surface of EVs and sCD40L concentration after platelet stimulation with PBUT.

5.2. Collection and storage of biological samples

Blood samples have been collected through peripheral venous sampling: to separate the serum, whole blood samples have been centrifuged at 3500 g for 15 minutes at room temperature; To separate the plasma, whole blood samples into EDTA anticoagulant were centrifuged at 1500 g for 15 minutes at room temperature. The plasma and serum samples thus obtained were stored at -80° C until their use.

5.3. Laboratory measurements

Peripheral blood samples from patients at the different time points in the study were used to:

- Biochemical tests such as: PCR reactive C protein (mg/l), fribrinogen (mg/dl), ß2microglobulin (mg/l), ferritin (ng/ml), leukocyte count WBC (/microl), hemoglobin Hb (g/dl), platelets PLTs (/microl), hepcidin (ng/ml), parathormone PTH (pg/ml), albumin (g/dl), indoxil sulphate (ng/ml)
- Quali-quantitative analysis of circulating EVs (concentration, content in miRNA, molecules expressed in membrane)

In both groups, serum sCD40L levels, PCR, ß2microglobulin, Hb and Kt/V were assessed at the time of enrollment and every 3 months (T0 – T3 – T6 – T9), while every month the biochemical tests mentioned above were carried out. The Kt/V ratio is the parameter used to assess the adequacy of dialysis treatment, or the efficiency of the elimination of uremic toxins that accumulate in the body (usually the clearance of urea is considered); the ratio is calculated according to the formula of Gotch and Sargent. Hemoglobin (Hb) values are corrected by the erythropoietin resistance index because all patients enrolled were in erythropoietin therapy and this drug could alter the levels of hemoglobin.

5.4. Mass removal of sCD40L and indoxyl sulphate

We evaluate the sCD40L and indoxyl sulphate mass removal to obtain a quantitative measurement of solute removed from plasma using different membranes (PS vs. PMMA). This evaluation will be performed in group 2 patients

at the time T3 (at the switch from RRT with PS to PMMA BKF), according to the following scheme:

- During the last week of RRT with filter in PS: degree of removal of sCD40L evaluated on Mondays and Fridays, at the first, second and fourth hours from the start of treatment.
- During the first week of RRT with PMMA filter: degree of removal of sCD40L assessed on Mondays and Fridays, at the first, second and fourth hours from the start of treatment

The mass removal amount has been calculated through this mathematical formula:

$$\text{Removal amount} = \left[\text{Body Volume before dialysis (ml)} \times \text{sCD40L before dialysis (ng/ml)}\right] - \left[\text{Body Volume after 1 / 2 or 4 h of dialysis (ml)} \times \text{sCD40L after 1 / 2 or 4 h of dialysis (ng/ml)}\right]$$

Body Volume before dialysis (ml) = 1000 x Body Weight before dialysis (Kg) x (1/13)

Body Volume after 1/2 or 4h = Body Weight before dialysis (ml) x HcT before dialysis (%)/HcT after 1/2 or 4h (%)

To assess sCD40L concentration was used the following technique: dialysate was collected and then the concentration of the molecule was evaluated by ELISA test. To obtain a quantitative measurement of indoxyl sulphate removed in the different dialysis sessions with PMMA BKF or PS, also in this case the mass removal parameter has been calculated in patients, similarly to sCD40L, but the concentration of the molecule has been evaluated by mass spectrometers.

5.5. Cell cultures

- Human endothelial cells derived from the umbilical vein (HUVEC) were obtained from ATCC (PCS-100-010-ATCC USA). HUVEC were stored in EBM medium supplemented with 10% fetal calf serum and various endothelial growth factors. The experiments were carried out without FCS and after incubation with plasma of the patient diluted 1:10. They have subsequently been used in selected experiments, such as the evaluation of ROS production and the degree of activation of ROS (evaluated by the degree of adhesion of monocyte cells).

- Vascular smooth muscle cells (VSMC) were incubated at 37°C in 5% CO2 with MEM integrated with 1 mm of l-glutamine, 100 IU/ml of penicillin, 100 µg/ml of streptomycin and 10% of FBS. They were later used in selected experiments, such as the evaluation of osteoblastic differentiation and RUNX2 expression.

- Monocyte cells were obtained from sound controls after isolation with Ficoll-Hypaque density gradient (GE Health Care) and added to cell cultures in selected experiments. The monocytes were marked, to be evaluated in immunofluorescence, with green fluorescent marker.

- Platelets: Platelet preparations (obtained from the Blood Bank) and laboratory PBUT have also been used to perform in vitro experiments assessing the correlation between sCD40L and PBUT concentrations.

5.6. In vitro assessments using uremic sera

- Endothelial activation: endothelial cells, after being incubated with the sera of uremic patients, were incubated with monocyte cells. The endothelial nuclei were highlighted with Propidium iodide dye (red), the monocytes were highlighted with membrane dye type PKH16 (green). The areas of fluorescence corresponding to monocytes were then counted.
- Cellular calcification: intracellular calcium deposits were quantified by means of Alizarin red colouring. The muscle cells were cultured in 24-well plates and fixed with 4% paraformaldehyde in PBS for 45 minutes to 4°C. The cells were then washed in distilled water, exposed to Alizarin red (2% aqueous, Sigma Aldrich, St. Louis, MO) for 5 minutes, washed again and analyzed by inverted light microscopy. The cell lysates were analyzed in an automated spectrophotometer at a wavelength of 570 nm (Perkin Elmer), with detection of the relative degree of absorbance.
- RUNX2: Positivity to RUNX2 was evaluated in immunofluorescence. An antibody was used that specifically detects RUNX2 produced by Covance (Princeton, NJ, USA). Positivity was also evaluated in FACS. The activation feedback of RUNX-2 was also investigated by amplification of the same in qRT-PCR, although the results were not presented in this study.

- ROS: ROS production rate was measured using CM-H2DCFDA (Invitrogen™ Molecular Probes™, Thermo Fisher Scientific, Canada), a fluorescent probe. The endothelial cells grown in multi-well plates were washed twice with PBS to remove the medium. Then 0,5 ml of buffer containing 2 mM CM-H2DCFDA were added. Immediately after addition, fluorescence was measured in kinetic mode with excitation at 485 nm. This probe was used both for immunofluorescence reaction and in FACS for quantitative evaluation.
- Immunofluorescence studies were conducted as follows: the cells were fixed with 4% formaldehyde for 10 minutes at room temperature and then incubated overnight at 4°C with specific primary antibodies (and with the appropriate dilution). After incubation, fluorescence was detected using an Olympus Fluoview 500 confocal laser scanning microscopy system with a 100x oil immersion objective at room temperature.

5.7. sCD40L/CD40L ELISA

The concentration of sCD40L/CD40L was determined using the following kit: HUMAN CD40L QUANTIKINE ELISA KIT (Red Systems, Miminneapolis, MN). The specific primary antibodies were already adhered to the plates provided in the kits.

The protocol used was as follows: each well was filled with 100 ul of sample and the plate was incubated for 2 hours at 37°C. Then the sample was removed from each well and 100 ul of Detection Reagent A was added (prepared according to the indications in the kit with Detection A and Assay Diluent A with concentration 1:100); after an incubation of 1 hour at 37°C, the Detection Reagent A was aspirated, and 3 washes were carried out with Wash Solution 1x (prepared according to the instructions in the kit). Then 100 ul of Detection Reagent B were added (prepared according to the indications contained in the kit with Detection B and Assay Diluent B with concentration 1:100) and left in incubation for 30 minutes at 37' C. 5 washes were performed with Wash Solution 1x. Finally, 90 ul of 3,3',5'-Tetramethylbenzidine (TMB) Substrate Solution were added in each well, leaving it in incubation for 20 minutes, then the reaction was stopped by adding 50 ul of Stop Solution in each well. The absorbance of each sample was then measured at the spectrometer (Perkin Elmer) at a wavelength of 450 nm.

5.8. Cytometric analysis (FACS Analysis)

Cytofluorimetric analysis was carried out using the GUAVA system (GUAVA Easy-Cyte, Millipore). Endothelial cells were treated with sera taken from patients enrolled in the study at different times, and the production of ROS was evaluated in both immunofluorescence method to produce representative microphotographs, either by FACS analysis to quantify their production on a cellular level or to obtain a more precise quantitative analysis.

Specifically, the production of reactive oxygen species (ROS) was evaluated by Image-iT® Detection Kit (Life Technologies, Carlsbad, CA, USA). The test is based on 5- (e-6) -carbase-2 ', 7'-dichlorodyfluorinated diacetate (carboxyH2 DCFDA), a compound that releases fluorescence after the association of ROS, as previously reported. The experiments were conducted according to the manufacturers' instructions; after incubation with selected stimuli, the cells were resourced with EDTA and analyzed by FACS.

Muscle cells were treated with serums taken from patients enrolled in the study at different times, and the positivity for RUNX2 was evaluated in both immunofluorescence method to produce representative microphotographs, either by FACS analysis to quantify their positivity or to obtain a precise quantitative analysis. The method is like that for the evaluation of the production of reactive oxygen species.

Isotype IgG antibodies, of murine derivation, associated with fluorescine (FITC) or phytooserin (PE) have been used as controls. The sera were incubated with each antibody or control isotype for 1 hour at 4°C and, after the necessary preparations (washing and centrifuging), were analyzed with FACS. The results obtained were expressed in % positivity for each marker analyzed.

5.9. PBUT mass spectrometry (MS) analysis

A mass spectrometry analysis has been performed for the PBUT concentration assessment; indoxyl sulphate has been selected as an example toxin and all assessments have been carried out on this. A mass spectrometer LTT Orbitrap (Thermo Scientific, Milan, Italy) with an electrospray ionization source (ESI) was used. LCcolumn effluent was fed into the ESI source using nitrogen sheath and

auxiliary gas. The capillary voltage and the optical voltage of the tube in the ESI source were maintained at 28 V and 70 V respectively. The source voltage was set to 3.5 kV (in both positive and negative ion mode). The capillary temperature was maintained at 270°C. The acquisition method used was previously optimized in tuningsections for the parent compound (capillary, magnetic lenses and variable octapolar voltages) to obtain maximum sensitivity. The analyses were performed using the full MS (range 50-1000 m/z) scan, MS2acquisition in positive ion mode, with a resolution of 30,000 (500 m/z FWHM) in FTMS mode (full transmission). The collision energy was set to 30% for all MS2acquisition methods. The acquisition range MS2 was between the cut-off values of the ion cage and the m / z value of the ion [M + H] +. The software X calibur (Thermo Scientif, Milan, Italy) is used both for the acquisition and for the analysis of data.

5.10. Identification and characterization of microRNA content of plasma EV in CKD patients and evaluation of their pathogenic role

5.10.1. Isolation and characterization of EVs

For the isolation of EVs, peripheral blood samples stored in tubes with EDTA were centrifuged at 1300 g for 10 min at ambient temperature to obtain plasma. To isolate EVs, the plasma was subjected to additional 3 successive centrifuges at 3300 g for 5 min at 4°C to remove debris. The samples thus obtained were then diluted 1:200 with 0.9% saline solution, sterile, and analyzed through the instrument Nanosight LM10 equipped with Nanoparticles Analysis System and NTA 1.4 Analytical Software, to evaluate concentration and size. The total number of EVs for each patient was obtained by multiplying the data provided by the instrument (EV/ml) by the dilution performed for the analysis. The part of the serum not used for the analyses, has been frozen at -80°C for any subsequent deepening.

5.10.2. EVs cytometric analysis (Guava FACS Analysis)

Cytometric analysis was carried out using the GUAVA system (GUAVA Easy-Cyte, Millipore). EVs from hemodialysis patients were incubated with antibodies directed against exosomes markers (CD9, CD81, CD63, CD86), platelets (Cd42b, CD62P, CD41), monocytes/macrophages (CD14, CD15), hematopoietic cells (CD34),

leukocytes (CD45), B cells (CD19, CD5, CD40), endothelial cells (CD144, CD31, CD105, CD146) and T cells (CD3) and antibodies against FAS-L, C5b-9, TF, ICOS and CD40L. Isotype IgG antibodies, of murine derivation, associated with fluorescine (FITC) or phytooserin (PE) have been used as controls. The EVs were incubated with each antibody or with the control isotype for 1 hour at 4 weeks C and, after the necessary preparations (washing and centrifuge), were analyzed with FACS. The internalization of EVs by endothelial and smooth muscle cells was evaluated qualitatively by indirect immunofluorescence and quantitatively by FACS analysis.

5.10.3. Protein Quest

To identify the most relevant microRNAs for cardiovascular disease in our patients, the literature has been analyzed with the appropriate web platform "Protein Quest" (PQ - Biodigital Valley, Aosta, Italy), which manages to automatically isolate what is required, screening all the information contained in the titles or abstracts of Pubmed, in the articles available as full text, in US patents and clinical trials. In addition, it classifies terminology through biomedical dictionaries and elaborates correlations between terms according to a hierarchical criterion. Using a proper search string it was then possible to select all the literature available on the web concerning vascular dysfunction and the problem of vascular calcifications in uremic patients. PQ then selected all microRNAs and related protein products described in the pathological processes of endothelial dysfunction and vascular calcification typical of advanced CKD.

5.10.4. EVs RNA extraction and quantitative microRNA analysis (qRT-PCR)

All the RNA contained in the EVs was extracted using the "All in one" method (Norgne, Thorold, ON, Canada). The RNA concentration and its purity were detected by the Nanodrop1000 spectrophotometer. Absorbance ratios of 260/280 nm were considered with values between 1.8 and 2.0. The microRNAs detected by the protein quest were studied using the miScript Reverse Transcription Kit and the miScript SYBR Green PCR Kit (both of Qiagen). MicroRNA-specific Primers were used: hsa-mir-17-5p, -92-a, -223, -423-5p, -451a. RNU48 was used as a

reference control to normalize the data. RNA expression changes were calculated using 2-ΔΔCt method.

5.10.5. CKD-EV internalization assay

The cells were fixed with 4% formaldehyde for 10 minutes at room temperature and then counterstained with Hoechst (dilution 1:100) to identify the nuclei. By marking the Evs of CKD patients with a red fluorescent dye (PKH26 Sigma Aldrich), it was possible to observe the possible internalization within endothelial cells and smooth vascular muscle cells. After incubation, fluorescence was detected using an Olympus Fluoview 500 confocal laser scanning microscopy system with a 100-oil immersion objective at room temperature.

5.10.6. Evaluation of CKD-EV effects in VSMC calcification

To assess CKD-EV effects in VSMC calcification, intracellular calcium deposits were quantified by red-alizarin staining. The smooth muscle cells were cultured in 24-well plates and fixed with 4% paraformaldehyde in PBS for 45 minutes at 4°C. The cells were then washed in distilled water, exposed to Alizarin red (2% aqueous, Sigma Aldrich, St. Louis, MO) for 5 minutes, wash again and analyzed by inverted light microscopy. Cell lysates were analyzed in an automated spectrophotometer at a wavelength of 570 nm, which delivered an absorbance parameter.

5.11. Statistical analysis of patient data in the study

The statistical processing of the data was carried out with PRISM system for MAC. Normality distribution was assessed preliminarily by q-q plot, Kolmogorov–Smirnov and Shapiro–Wilk tests. In the case of normal distribution, the quantitative variables were expressed by mean and standard deviation, if not by median, interquartile range (IQR). Categorical variables were expressed by absolute and relative frequencies. Differences between independent groups for continuous and categorical variables were estimated respectively by non-parametric Mann–Whitney U-test and Fisher's Exact test (or Chi-Square test). Differences between time points were evaluated by non-parametric Friedman test and, if statistically significant ($p<0.05$), differences between paired group (T0 vs T3, T3 vs T6, T6 vs

T9) were evaluated by non-parametric Wilcoxon signed-rank test with Bonferroni's correction. Difference in cardiovascular events between groups positive or negative for sCD40L in the follow up period was evaluated by Kaplan-Meier analysis, Log-rank or Breslow test. Predictors for time to first cardiovascular event were evaluated by univariate and multivariate Cox regression. Predictors for cardiovascular events within 2 years were evaluated by logistic regression.

5.12. Statistical analysis of in vitro studies

The statistical processing of the data was carried out with PRISM system for MAC. The categorical variables were expressed as percentages, the continuous variables were expressed as means and standard deviation in the case of parametric variables, or median and interquartile ranges in the case of non-parametric variables. Variance analysis (ANOVA) and Student-Newman-Keuls analysis were used when appropriate. For the experiments at the FACS was used the analysis of Kolmogorov Smirnov. Significant values of $p<0,05$ (set at 0,05) were considered.

6. Results

6.1. Enrolled population and clinical-demographic features

We initially selected 201 patients corresponding to the inclusion criteria from 6 different hemodialysis centers (A.O.U. Città della Salute e della Scienza di Torino, ASL Versilia, ASL CN1, ASL Asti, ASL Biella, ASL VCO) and have been analyzed for different demographic and clinical features, as described in Table 1.

Tab. 1: Baseline characteristics of initial population of 201 patients. Data are presented as median (interquartile range – IQR) and percentage.

Variables	median (IQR) and percentage
Age at enrollment (years)	68 (57 – 74)
Age at dialysis initiation (years)	64 (53 – 71)
Dialytic vintage (months)	28 (14 – 56.5)
Male	54%
Diabetes	42%
Hypertension	83%
Dyslipidemia	39%
Smoke history	37%
Previous cardiovascular events	40%

At the time of enrollment, the median serum concentration of sCD40L was 8.4 (IQR 2.9 – 12.7) ng/ml. We registered cardiovascular and cerebrovascular events for a median follow-up of 29 (IQR 22 – 53) months. The minimum follow-up period was of 24 months. A total of 51 (25.4%) patients experienced a CV event during the whole follow-up: 44 events (21.9%) occurred within 24 months from enrollment. Moreover, 33 (16.4%) participants died, 9 of them because of a recognized cardiovascular cause.

6.2. Identification of sCD40L predictive value for cardiovascular events

Our first aim was to detect the best sCD40L cut-off value to identify patients with higher risk for MACE. We used 2 different ROC curves (Figures 24 and 25).

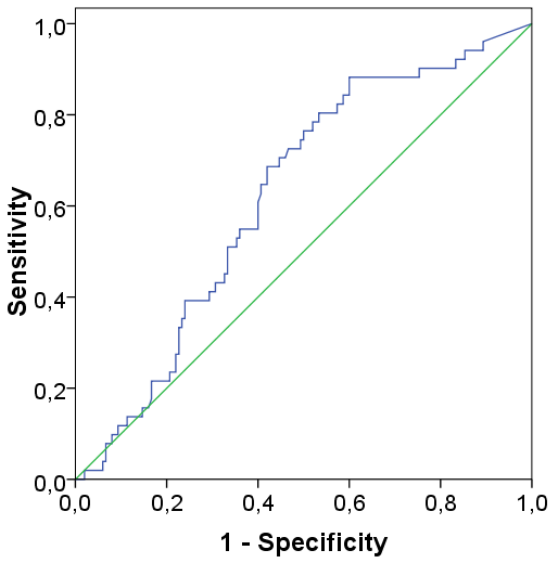

Fig. 24: ROC curve for global CV events

A sCD40L plasma concentration equal to 7.7 ng/ml was determined to be the value with the best statistical performance to identify patients with shortest time to MACE (i.e with shortest event-free survival).

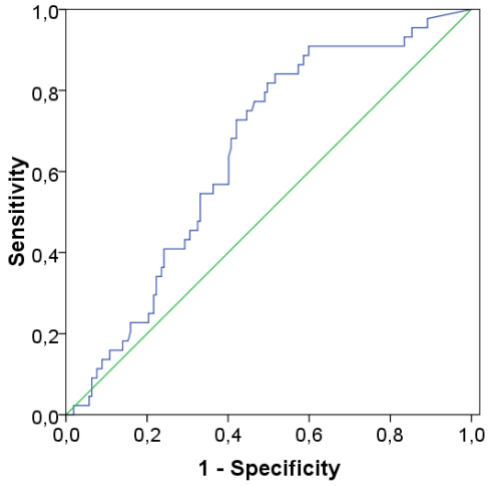

Fig. 25: ROC curve for CV events within 2 years of follow-up

Similarly, sCD40L plasma concentration equal to 7.8 ng/ml turned out to be the value with the best statistical performance to identify patients with highest risk of events within two years of follow-up. Using the cut-off value of 7.8 ng/ml, which was very closed to the RISCAVID study value, we divided our cohort into two different groups: people with sCD40L concentration higher or lower than 7.8 ng/ml.

We compared these 2 groups for the principal demographic and clinical features (Table 2).

Tab. 2 Comparison between patients with sCD40L < or > 7.8 ng/ml. Data are presented as median (IQR). Percentages are calculated on column totals.

Variables	Patients with sCD40L < 7.8 ng/ml	Patients with sCD40L > 7.8 ng/ml	p-value
Age (years)	69 (57 - 75)	67 (56 - 74)	0.573
HD vintage (months)	29.5 (14 - 60)	27 (15 - 50)	0.753
Gender (male/female)	51/35	59/56	0.316
Diabetes	37.2%	46.1%	0.249
Hypertension	80.2%	86.8%	0.224
Dyslipidemia	34.9%	42.6%	0.308
Smoke history	34.9%	38.3%	0.659
Previous CV events	37.2%	41.7%	0.562

No statistical differences were found between the two groups about the major cardiovascular risk factors. Results of univariate and multivariate analysis with COX REGRESSION to identify risk factors for reduced event-free survival are described in the following Tables (Table 3 and 4).

Tab. 3: Cox proportional hazards univariate analysis to identify risk factors for reduced event-free survival.

Variables	HR (95% CI)	p-value
sCD40L > 7.8 ng/ml	2.77 (1.45 – 5.29)	0.002*
Age (years)	1.03 (1.01 – 1.06)	0.017*
HD vintage (months)	1.00 (0.99 – 1.00)	0.672
Gender (male/female)	1.42 (0.81 – 2.49)	0.227
Diabetes	1.81 (1.04 – 3.15)	0.036*
Hypertension	2.38 (0.86 – 6.63)	0.096
Dyslipidemia	1.12 (0.64 – 1.96)	0.683
Smoke history	1.04 (0.59 – 1.83)	0.902
Previous CV events	1.65 (0.95 – 2.86)	0.074

Tab. 4: multivariate Cox regression model to identify risk factors for reduced event-free survival

Variables	HR (95% CI)	p-value
sCD40L > 7.8 ng/ml	2.94 (1.53 – 5.66)	0.001*
Age (years)	1.04 (1.01 – 1.06)	0.010*
Diabetes	1.59 (0.91 – 2.77)	0.101

In the univariate Cox proportional hazards regression model, median age, the presence of diabetes mellitus and sCD40L above the median value were associated with a significant increase in the risk of CV morbidity. With the multivariate Cox regression model, we demonstrated that median age and sCD40L concentration are independent risk factors for shortest time to events. Kaplan-Majer curve underlines the significant difference in CV event-free survival between two groups based on sCD40L level (Figure 26).

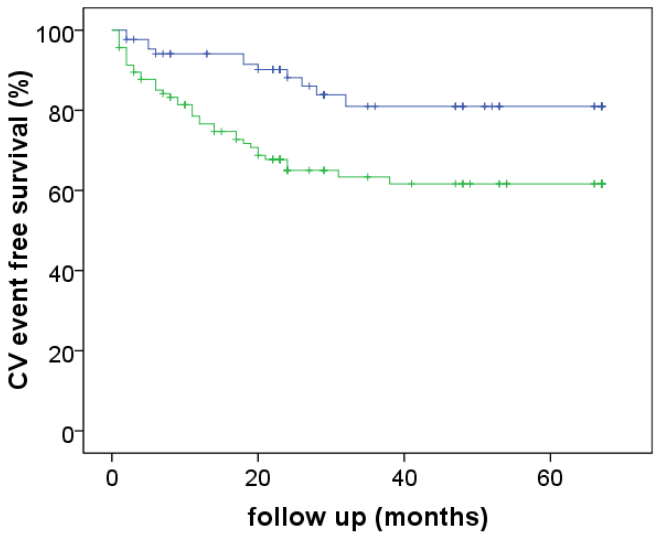

Fig. 26: Kaplan-Majer curve. Green line refers to patients with sCD40L > 7.8 ng/ml;; Blue line refers to patients with sCD40L < 7.8 ng/ml

As described in figure 17, after 25-30 months, event-free survival remains stable in both groups. Therefore, through a logistic regression we analyzed how sCD40L concentration could significantly influence the incidence of cardiovascular events over a period of 24 months. In the univariate regression, age, hypertension and sCD40L level were associated with high cardiovascular risk. The multivariate

regression demonstrated that age and sCD40L concentration are independent risk factors for CV events within two years (Tables 5 and 6).

Tab. 5: Cox proportional hazards univariate analysis to identify risk factors for cardiovascular events over a period of 24 months

Variables	HR (95% CI)	p-value
sCD40L > 7.8 ng/ml	4.44 (1.94 – 10.16)	<0.001*
Age (years)	1.05 (1.01 – 1.08)	0.006*
HD vintage (months)	1.00 (0.99 – 1.01)	0.998
Gender (male/female)	1.26 (0.64 – 2.47)	0.511
Diabetes	1.68 (0.86 – 3.29)	0.131
Hypertension	5.00 (1.15 – 21.82)	0.032*
Dyslipidemia	0.97 (0.49 – 1.92)	0.918
Smoke history	0.86 (0.43 – 1.73)	0.672
Previous CV events	1.52 (0.77 – 2.98)	0.226

Tab. 6: multivariate Cox regression model to identify risk factors for cardiovascular events over a period of 24 months

Variables	HR (95% CI)	p-value
sCD40L > 7.8 ng/ml	4.97 (2.10 – 11.73)	<0.001*
Age (years)	1.05 (1.01 – 1.09)	0.007*
Hypertension	3.28 (0.71 – 15.06)	0.127

6.3. Comparative analysis of the efficacy between PMMA BKF and PS in patients with high cardiovascular risk (double-crossover study)

From this population we enrolled n = 54 patients with increased cardiovascular risk considering values of sCD40L > 7,8 ng/ml cut-off (value very closed to the RISCAVID study). During the study, 6 patients dropped-out because of different causes: 1 death, 4 kidney transplants, 1 transfer to other dialysis center. Two final groups of 24 patients completed the study.

The general characteristics of this cohort are described in Table 7 and in Figure 27: it was composed mainly of females (57.1%), mainly of Caucasian ethnicity (96.4%), with a mean age of 50,2 years. All the cohort patients had been in bicarbonate dialysis replacement therapy for at least 6 months, with an average dialysis vintage of 47.7 months. The mean value of sCD40L was 12.11 ±3.32 ng/ml.

Tab. 7 General features of 48 enrolled patients. Data are presented as mean ± standard deviation and percentage.

Socio-demographic variables	Male	12/28 (42.9%)
	Age (years)	50,29 ± 16,3
	Caucasian	27/28 (96,4%)
General clinical variables	Weight (Kg)	69,3 ± 13,65
	Ipertension	23/28 (82.1%)
	Diabetes	12/28 (42.9%)
	Cardiovascular disease	10/28 (35.7%)
Dialysis clinical variables	Vascular access (FAV)	22/28 (78.6%)
	Dialytic vintage (months)	47,7 ± 20

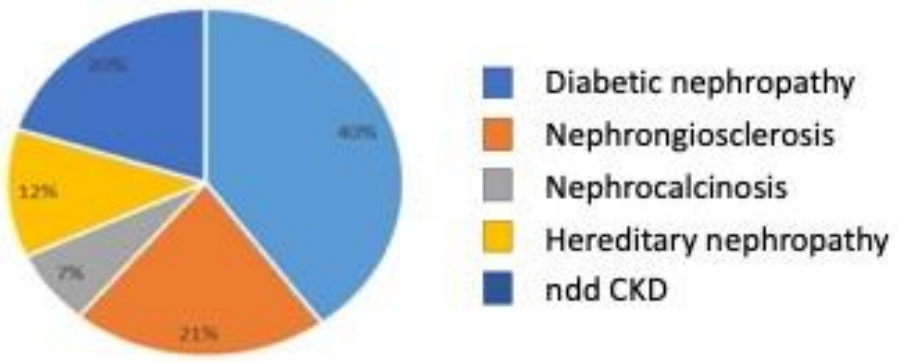

Fig. 27: Prevalence of chronic kidney disease causes in the general study population

The following data are the clinical-laboratory parameters at the T0. The blood chemistry profile of the study court was characterized by inflammatory indices above normal values (CRP 4,90 ± 6,28 mg/L; β2microglobulin 16,87 ± 8,32 mg/L), chronic disorder anemia and erythropoietin resistance anemia (Hb 10,5 ±1,20 g/dl) (Table 8).

Tab. 8 Clinical-laboratory characteristics of the cohort at T0

Clinical-laboratory parameters	Mean ± SD
CRP (mg/L)	4,90 ± 6,28
Fibrinogen (mg/dL)	350,02 ± 109,00
β2microglobulin (mg/L)	16,87 ± 8,32
Ferritin (ng/mL)	270,87 ± 200,08
WBC (/microL)	5541,05 ± 1190,30
Hb (g/dL)	10,5 ± 1,20
PLTs (/microL)	240.093,42 ± 32.000,3
PTH (pg/mL)	378,30 ± 300
Albumin (g/dL)	3,50 ± 0,05
Kt/V	1,18 ± 0,22
sCD40L (ng/mL)	12.11 ± 3.32
Indoxil sulphate (microg/mL)	15,93 ± 16.84

No patient developed local or systemic acute infection, autoimmune or neoplastic pathologies during the follow up.

As a control group for the remaining clinical-laboratory evaluations, the selected cohort represented control of itself, being a double cross-over study.

As a control group for the comparison of in vitro analyses were enlisted n = 15 healthy subjects, corresponding by sex and age.

The selected population was divided into two groups of the same number (n = 24) and as described in detail in "Patients and Methods".

6.3.1. Effects of PMMA BKF and PS on inflammatory molecules (CRP, β2microglobulin)

The evolution of serum levels of CRP and β2microglobulin in the two groups was evaluated at times T0 (zero time), T3 (three months), T6 (six months), T9 (nine months), to assess the effects of the two different dialysis methods on analytes.

The analysis of variance did not show any significant differences among the 2-study group (Tables 9 and 10).

Tab. 9 paired analysis of CRP removal by PMMA vs PS at different time points within two groups. No significant differences found with Friedman Test (p = 0.09 and 0.40, group 1 and 2 respectively)

CRP (mg/dl)		
	Group 1 Median (IQR)	**Group 2 Median (IQR)**
T0	0.91 (0.30 – 4.72)	0.90 (0.21 – 3.25)
T3	0.83 (0.28 – 4.42)	0.60 (0.22 – 4.05)
T6	1.00 (0.48 – 1.54)	0.50 (0.17 – 4.60)
T9	0.57 (0.22 – 1.67)	0.80 (0.25 – 3.00)

Tab. 10 paired analysis of β2microglobulin removal by PMMA vs PS at different time points within two groups. No significant differences found with Friedman Test (p = 0.82 and 0.86, group 1 and 2 respectively)

β2microglobulin (ng/ml)		
	Group 1 Median (IQR)	**Group 2 Median (IQR)**
T0	18.7 (16 – 27.5)	25 (15.7 – 30.6)
T3	20.2 (15.4 – 31)	26.9 (15 – 29.9)
T6	19.7 (11.8 – 29)	26.4 (15.9 – 32.9)
T9	25.4 (11.8 – 31)	20.8 (16.3 – 34.6)

6.3.2. Effects of PMMA BKF and PS on hemoglobin (Hb) and Kt/V

The variations Hb and Kt/V in the two groups were evaluated at different time points (T0-T3-T6-T9), to assess the effects of the two different membranes.

The analysis of variance did not show any significant differences among the 2-study group (Tab. 11 and 12).

Tab. 11 paired analysis of Hb at different time points within two groups. No significant differences found with Friedman Test (p = 0.45 and 0.33, group 1 and 2 respectively)

Hemoglobin (g/dl)		
	Group 1 Median (IQR)	**Group 2 Median (IQR)**
T0	10.80 (9.45 – 11.95)	11.20 (10.95 – 11.60)
T3	11.00 (9.70 – 11.57)	11.10 (9.95 – 11.60)
T6	10.03 (0.48 – 12.23)	11.20 (10.25 – 11.65)
T9	11.25 (10.60 – 11.78)	10.80 (9.80 – 12.05)

Tab. 12 paired analysis of Kt/V changes at different time points within two groups. No significant differences found with Friedman Test (p = 0.40 and 0.29, group 1 and 2 respectively)

Kt/V		
	Group 1 Median (IQR)	**Group 2 Median (IQR)**
T0	1.32 (1.11 – 1.59)	1.36 (1.26 – 1.60)
T3	1.34 (1.19 – 1.59)	1.36 (1.26 – 1.71)
T6	1.30 (1.16 – 1.57)	1.33 (1.16 – 1.58)
T9	1.29 (1.21 – 1.48)	1.40 (1.19 – 1.63)

6.3.3. Effects of PMMA BKF and PS on sCD40L, ICOS and hepcidin

Serum levels of sCD40L, ICOS and hepcidin were evaluated in the two groups at the times T0, T3, T6 and T9 to assess the effect of the two different dialytic membranes.

The variance analysis showed a strong statistically significant difference in both sCD40L and hepcidin levels in the 2-study groups, and the Wilcoxon Signed Ranks Test confirmed that the use of PMMA dialyzer was constantly associated with a significant reduction of sCD40L and hepcidin concentration, which increased again whenever PS was re-started (Table 13-14 and Figure 18-19).

Tab. 13 paired analysis of sCD40L concentrations at different time points within two groups. Statistically significant differences were found in the variance analysis with Friedman Test (p < 0.0001 in both groups) and Wilcoxon Signed Ranks Test

sCD40L (ng/ml)					**p-value**
	T0	**T3**	**T6**	**T9**	**(Wilcoxon test)**
Group 1	10.47 (8.74 – 15.07)	2.93 (1.63 – 4.05)	6.70 (5.38 – 8.53)	2.25 (1.10 – 3.58)	**T3-T0 p <** 0,0001*
					T6-T3 p < 0,0001*
					T9-T6 p < 0,0001*
					T9-T0 p < 0,0001*
Group 2	10.70 (8.86 – 13.30)	11.50 (8.70 – 13.50)	3.10 (1.90 – 4.50)	6.80 (4.40 – 9.60)	**T3-T0 p =** 0,626
					T6-T3 p < 0,0001*
					T9-T6 p < 0,0001*
					T9-T0 p = 0,001*

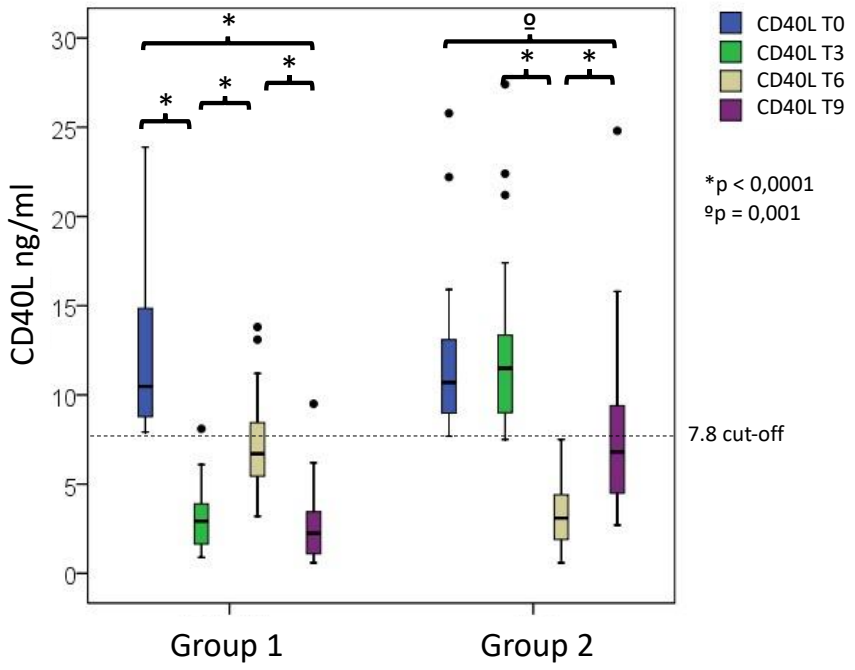

Fig. 28: Box plot (median and IQR) for sCD40L concentrations at different time points within two groups.

Tab. 14 paired analysis of Hepcidin concentrations at different time points within two groups. Statistically significant differences were found in the variance analysis with Friedman Test (p < 0.0001 in both groups) and Wilcoxon Signed Ranks Test

Hepcidin (ng/ml)					**p-value**
	T0	**T3**	**T6**	**T9**	**(Wilcoxon test)**
Group 1	63.1 (43.7 – 86.3)	25.3 (11.3 – 50.1)	38.8 (13.5 – 75.5)	19.4 (4.1 – 51.7)	**T3-T0 p <** 0,0001*
					T6-T3 p = 0,009*
					T9-T6 p = 0,004*
					T9-T0 p = 0,001*
Group 2	60.2 (40.0 – 81.6)	73.3 (48.4 – 92.2)	21.2 (16.4 – 59.9)	59.8 (31.4 – 79.1)	**T3-T0 p =** 0,153
					T6-T3 p < 0,0001*
					T9-T6 p = 0,005*
					T9-T0 p = 0,294

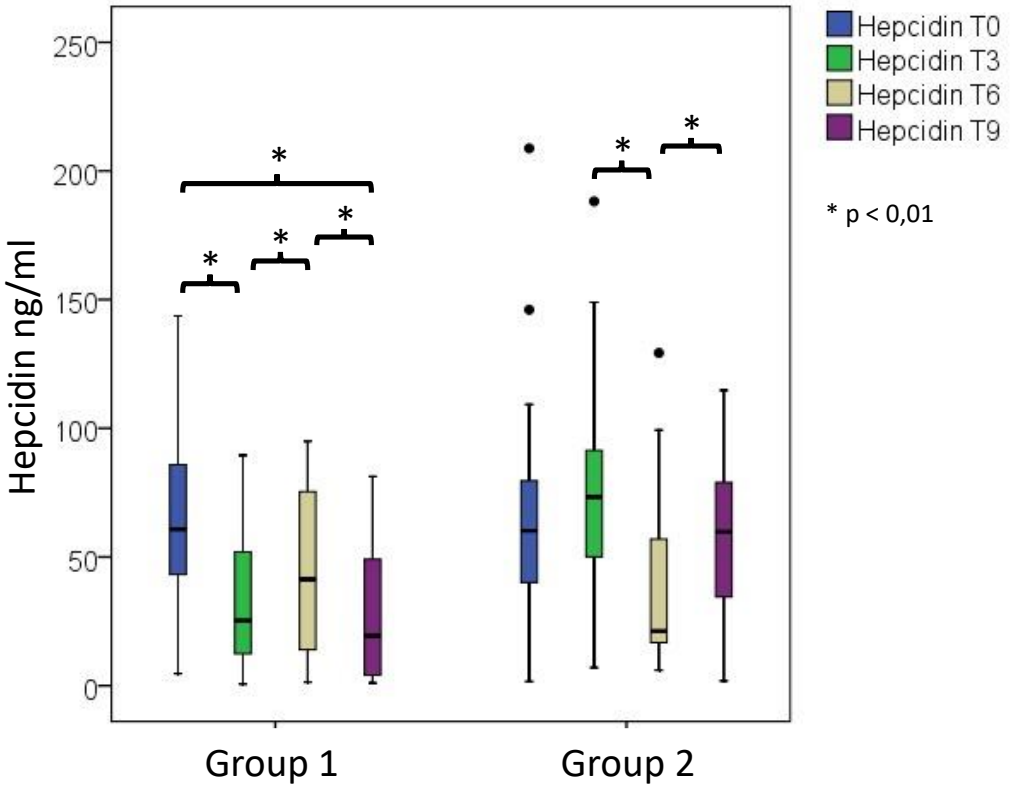

Fig. 29: Box plot (median and IQR) for Hepcidin concentrations at different time points within two groups.

Concerning ICOS concentration, the analysis of the variance did not show any significant differences among the 2-study group (Table 15)

Tab. 15 paired analysis of sICOS concentration changes at different time points within two groups. No significant differences found with Friedman Test (p = 0.93 and 0.15, group 1 and 2 respectively)

sICOS (ng/ml)		
	Group 1 Median (IQR)	**Group 2 Median (IQR)**
T0	1.70 (1.20 – 1.85)	1.60 (1.30 – 1.80)
T3	1.70 (1.30 – 1.70)	1.70 (1.20 – 1.80)
T6	1.50 (1.45 – 1.70)	1.70 (1.30 – 1.80)
T9	1.45 (1.60 – 1.75)	1.50 (1.40 – 1.70)

6.3.4. Effects of PMMA BKF and PS on sCD40L mass removal

To confirm the effect of the dialytic membrane on the reduction of serum levels of sCD40L, the mass removal was calculated in a subgroup of n = 10 patients from Group 2, according to the modalities and timing illustrated in "Patients and Methods".

In patients, when undergoing dialytic treatment with membrane in PS, the calculation of mass removal had highlighted that the amount of sCD40L removed from the plasma respectively after 1, 2, 4 hours was equal to: 10050,30 ± 510,08 ng, 15050,01 ± 506,00 ng and 30105,00 ± 602,20 ng in the first session (Monday) and 9014 ± 794,08 ng, 10100,01 ± 250,09 ng and 29770,09 ± 252,00 ng in the second session (Friday).

In patients, when undergoing dialysis treatment with membrane in PMMA BKF, the calculation of mass removal showed that, respectively after 1, 2, 4 hours, the amount of sCD40L removed from the plasma was equal to: 27000,07 ± 690,05, 39044,05 ± 500,05 and 58976,07 ± 502,01 ng in the first session (Monday), whereas 20100,04 ± 502,00, 40089,00 ± 400,02 and 60040,55 ± 365,02 ng in the second session (Friday) (Table 14, Figure 30). The amount of sCD40L removed by PMMA after the fourth hour was almost three-fold higher than the one removed by PS. All the data obtained were statistically significant ($p<0.05$).

Tab. 14 Comparison of sCD40L mass removal in Group 2, 1-2-4 hours after starting hemodialytic treatment with PS or PMMA BKF, respectively in the following sessions: last Monday and Friday before shift at PMMA BKF, first Monday and Friday treatment with PMMA BKF membrane

Mean mass removal of sCD40L (ng)						
Membrane	**Monday**			**Friday**		
	1° hour	**2° hour**	**4° hour**	**1° hour**	**2° hour**	**4° hour**
PS Mean ± SD	10050,3± 510,1	15050,0 ± 506,0	30105,0 ± 602,2	9014,0 ±794,1	10100,0 ± 250,1	29770,1 ± 252,0
PMMA BKF Mean ± SD	27000,1 ± 690,1	39044,1 ± 500,1	58976,1 ± 502,0	20100,0 ± 502,0	40089,0 ± 400,0	60040,6 ± 365,0

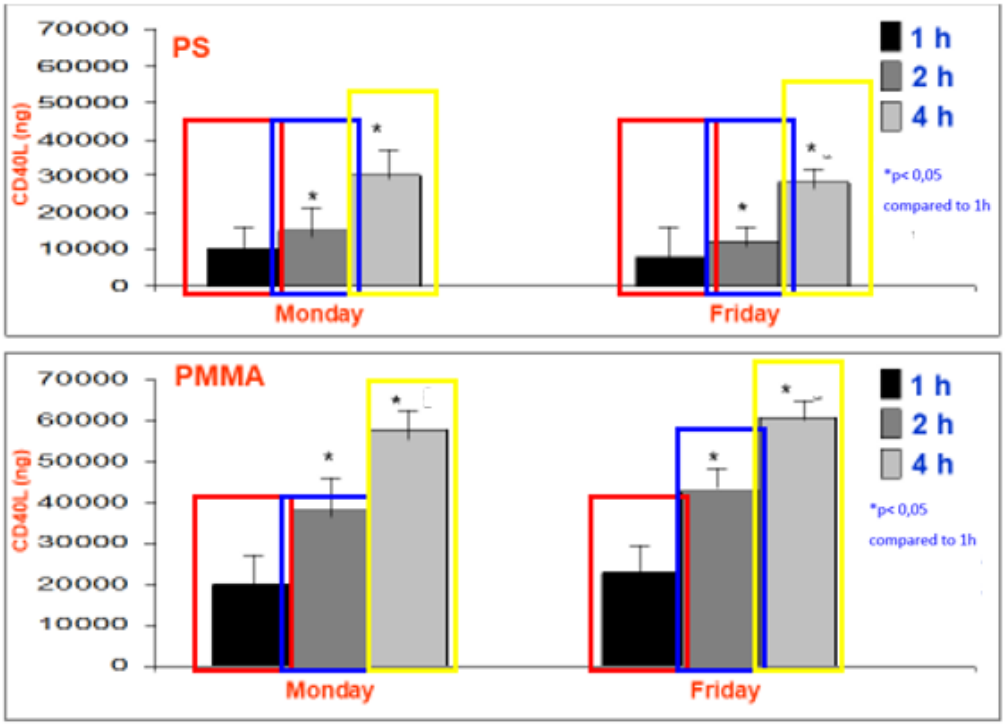

Fig. 30: sCD40L mass removal rate during Monday and Friday HD sessions (PMMA vs. PS): sCD40L serum levels were evaluated after 1-2-4 hours from the start of dialysis

6.3.5. Effects of PMMA BKF and PS on PBUT (Indoxyl sulfate) mass removal

To assess the effect of dialytic membrane on PBUT mass removal, the mass removal of indoxyl sulphate (IS), used as an example toxin of this category, has been calculated in a subgroup of n = 10 patients of Group 2, in accordance with the procedures and timetables described in "Patients and Methods". In patients, the amount of IS removed from plasma respectively after 1, 2, 4 hours of treatment with membrane in PS, was respectively 5000,88 ± 500,08, 15000,11 ± 512,00 and 19005,00 ± 612,20 ng in the first session (Monday), while 4516,00 ± 500,27, 14900,01 ± 470,36 and 22370,00 ± 351,00 ng in the second session (Friday). In patients, the amount of IS removed from plasma respectively after 1, 2, 4 hours of treatment with membrane in PMMA BKF, was equal to: 27000,07 ± 690,05, 39044,05 ± 500,05 and 58976,07 ± 502,01 ng in the first session (Monday), whereas 20100,04 ± 502,00, 40089,00 ± 400,02 and 60040,55 ± 365,02 ng in the second session (Friday) (Table 15, Figure 31). All the data obtained are significant with a p value of 0,05.

Tab. 15 Comparison of IS mass removal in Group 2, 1-2-4 hours after starting hemodialytic treatment with PS or PMMA BKF, respectively in the following sessions: last Monday and Friday before shift at PMMA BKF, first Monday and Friday treatment with PMMA BKF membrane

Mean mass removal of IS (ng)						
Membrane	**Monday**			**Friday**		
	1° hour	**2° hour**	**4° hour**	**1° hour**	**2° hour**	**4° hour**
PS Mean ± SD	5000,9 ± 500,1	15000,1 ± 512,0	19005,0 ± 612,2	4516,0 ± 500,3	14900,0 ± 470,4	22370,0 ± 351,0
PMMA BKF Mean ± SD	27000,1 ± 690,1	39044,1 ± 500,1	58976,1 ± 502,0	20100,0 ± 502,0	40089,0 ± 400,0	60040,6 ± 365,0

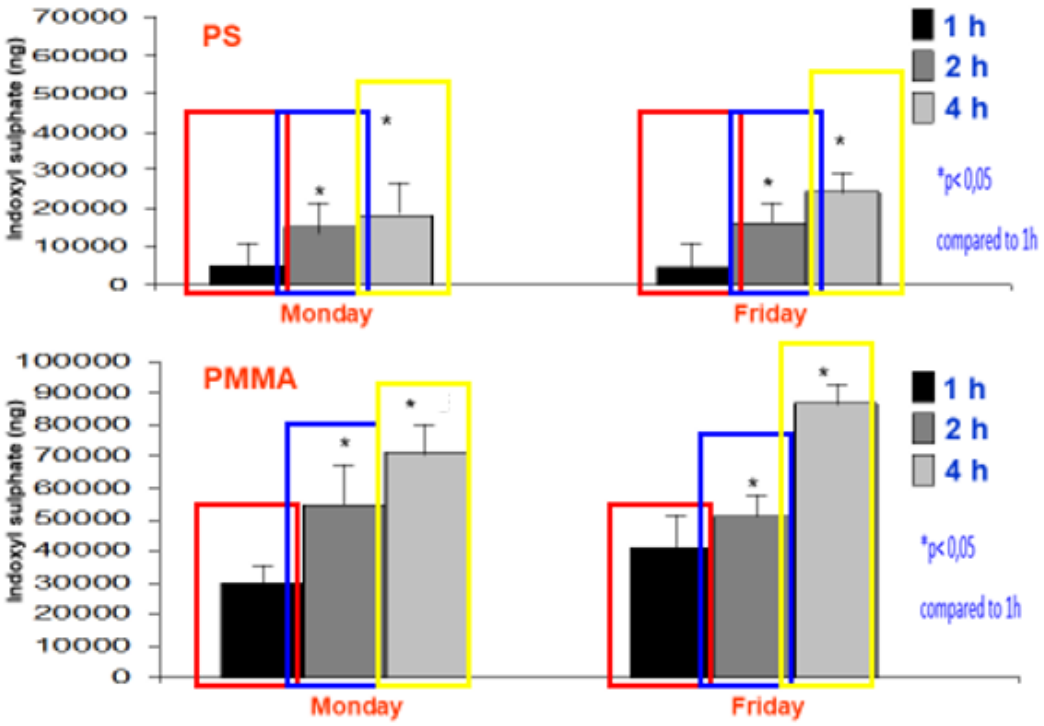

Fig. 31: IS mass removal rate during Monday and Friday HD sessions (PMMA vs. PS): IS levels were evaluated after 1-2-4 hours from the start of dialysis

6.3.6. Relationship between sCD40L and IS levels

A trend to a correlation between serum levels of sCD40L and IS, a PBUT, was found (Figure 32).

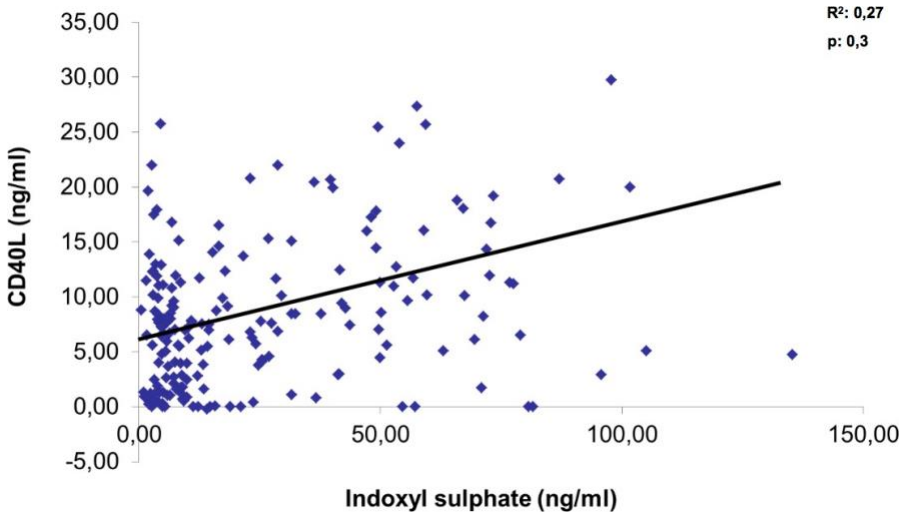

Fig. 32: relationship between sCD40L and IS

6.4. Concentration of sCD40L after platelet stimulation with PBUT in vitro

To further assess the relationship between PBUT and sCD40L, platelet stimulation studies were carried out in vitro.

Five laboratory platelet pools were used, each of which was incubated at increasing levels at a known concentration of indoxyl sulphate (0.1-1-10 microgr/ml), and sCD40L concentrations were measured at 1 hour and 24 hours.

Incubating platelets with increasing doses of PBUT, the levels of sCD40L progressively increased, at the surveys carried out both after 1 hour and after 24 hours, reaching the statistical significance only after stimulation with a concentration of PBUT > 10 microgr/ml, with an associated sCD40L value of 4,9±0,71 ng/ml after 1 hour and 6,8±0,80 ng/ml after 24 hours (Table 16, Figure 33).

Tab. 16 sCD40L concentrations after 1 hour and 24 hours from stimulation of platelet supernatants with increasing doses of IS

	IS (microg/mL)		
	0.1	**1**	**10**
sCD40L a 1h (ng/mL)	2,8 ± 1,30	3,6 ± 0,91	4,9 ± 0,71

sCD40L a 24 h (ng/mL)	4,7 ± 1,27	3,8 ± 0,93	6,8 ± 0,80

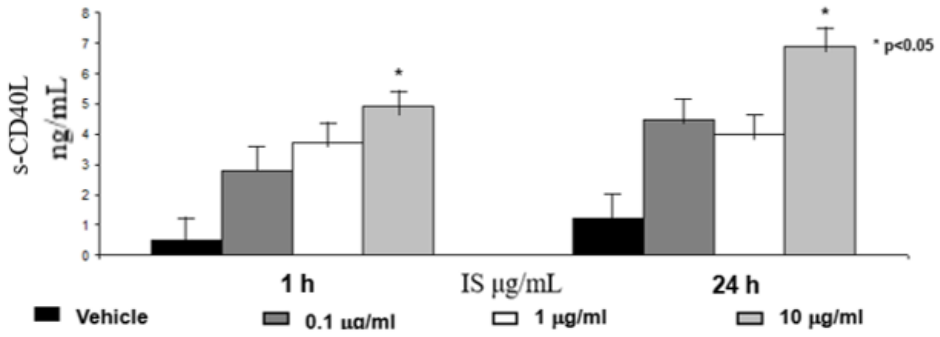

Fig. 33: sCD40L concentrations after incubation of platelet pools with increasing doses of IS, respectively measured after 1 hour and 24 hours of stimulation

6.5. In vitro modulation of endothelial dysfunction and vascular calcifications following RRT with PMMA BKF or PS

In vitro studies were also carried out to assess the association between circulating levels of sCD40L and markers of endothelial dysfunction and vascular calcification, such as free oxygen radicals (ROS), degree of monocyte adhesion and degree of osteoblastic differentiation by smooth vascular muscle cells.

6.6. In vitro assessment of ROS levels in endothelial cells

This evaluation was aimed to identify in Group 1 and 2 the percentage of ROS (Reactive Oxygen Species) produced at T0 and T3 checkpoints. Sera of n = 28 uremic patients were incubated with endothelial cells, to assess the degree of activation and subsequent production of ROS.

In Group 2 the mean ROS expression at T0 was 60,30 ± 5,16 %, with a reduction to 50,40 ± 6,30 % after 90 days (T3) of PS membrane therapy.

In Group 1 the mean ROS expression at T0 was 60 ± 4.12%, with a reduction to 30,21 ± 5,05% after 90 days (T3) of membrane therapy in PMMA BKF (Figure 34). The difference in the latter case was significant, with p-value < 0,05. By comparison, the controls showed mean values of 25,30 ± 5,05 %.

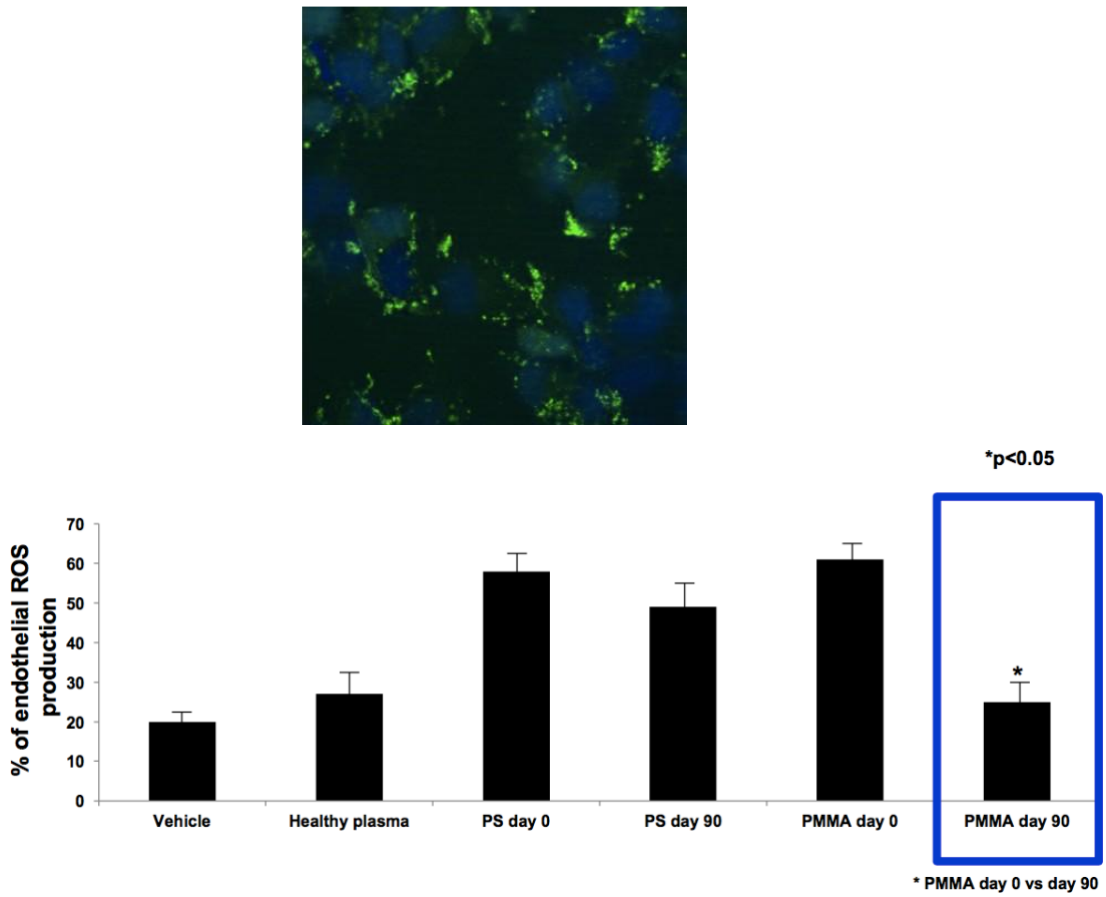

Fig. 34: Mean percentage of oxygen radicals (ROS) produced by endothelial cells incubated with serum of Group 1 and 2 patients, at times T0 (day 0) and T3 (day 90). In the box, an example image of the positive indirect immunofluorescence reaction for the presence of ROS (in green)

6.7. In vitro assessment of the degree of adhesion of monocytes to endothelial cells

Sera of n = 28 uremic patients were incubated with endothelial and monocyte cells, to assess the degree of endothelial activation and monocyte adhesion to endothelial cells.

In Group 2 the number of monocytes adhering to the endothelium activated per field at time T0 was 118 ± 5, with a reduction to 111 ± 8 monocytes adhering after 90 days (T3) of PS membrane therapy.

In Group 1 the number of monocytes adhering to the endothelium activated per field at time T0 was equal to 120 ± 4, with a reduction of up to 17 ± 5 monocytes adhering after 90 days (T3) of membrane therapy in PMMA BKF (Figure 35). In

the latter case, the difference was significant (p-value < 0,05). By comparison, the controls showed mean values of 17 ± 3,5.

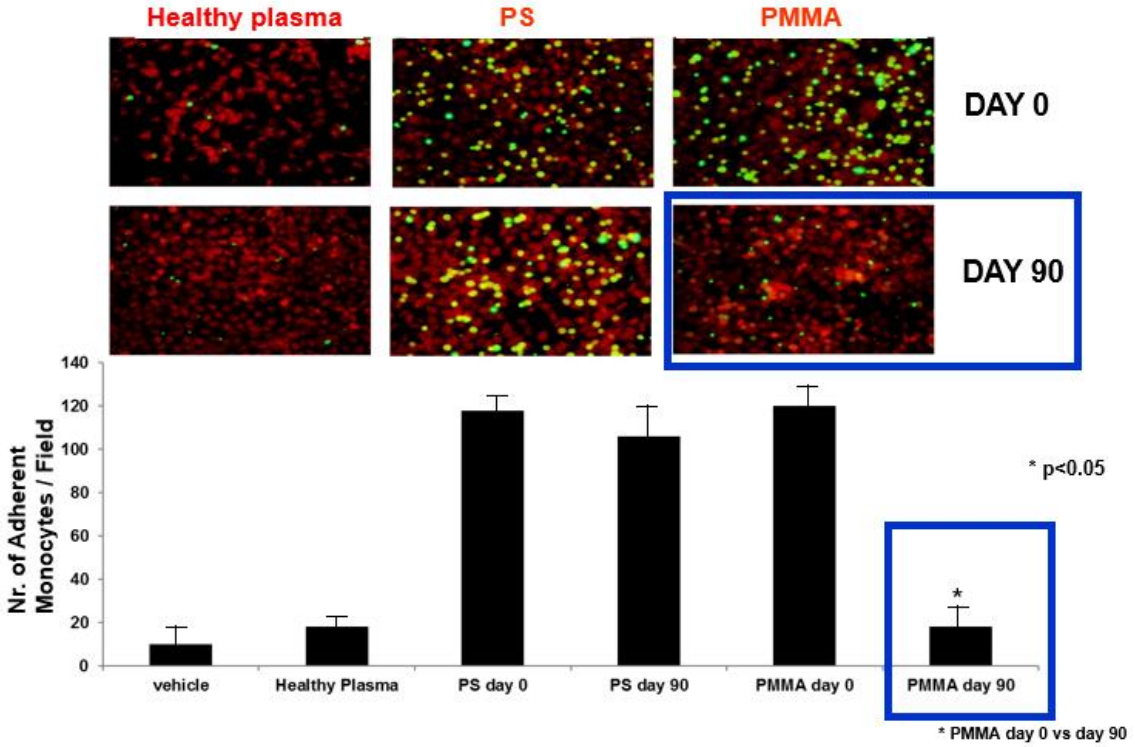

Fig. 35: Mean number of monocytes adhering to endothelial cells after stimulation with sera of Group 1 and 2 patients, at T0 and T3. In the panels, illustrative images that compare the different number of monocytes (green) adhering to the endothelium, stimulated by the sera of patients in RRT with PS or PMMA BKF membrane, at T0 (day 0) and T3 (day 90)

6.8. In vitro assessment of the degree of osteoblastic differentiation of smooth muscle cells

This evaluation was aimed to identify in both groups the reduction of osteoblastic differentiation by smooth muscle cells at T0 and T3.

In Group 2 the number of cells positive to the red alizarin dye at T0 was 93 ± 5, with a reduction to 80 ± 13 after 90 days (T3) of membrane therapy in PS.

In Group 1 the number of cells positive to the red alizarin dye at the time T0 was 90±4, with a reduction of up to 40 ± 5 after 90 days (T3) of membrane therapy in PMMA BKF (Figure 36). The difference was significant with p-value < 0,05.

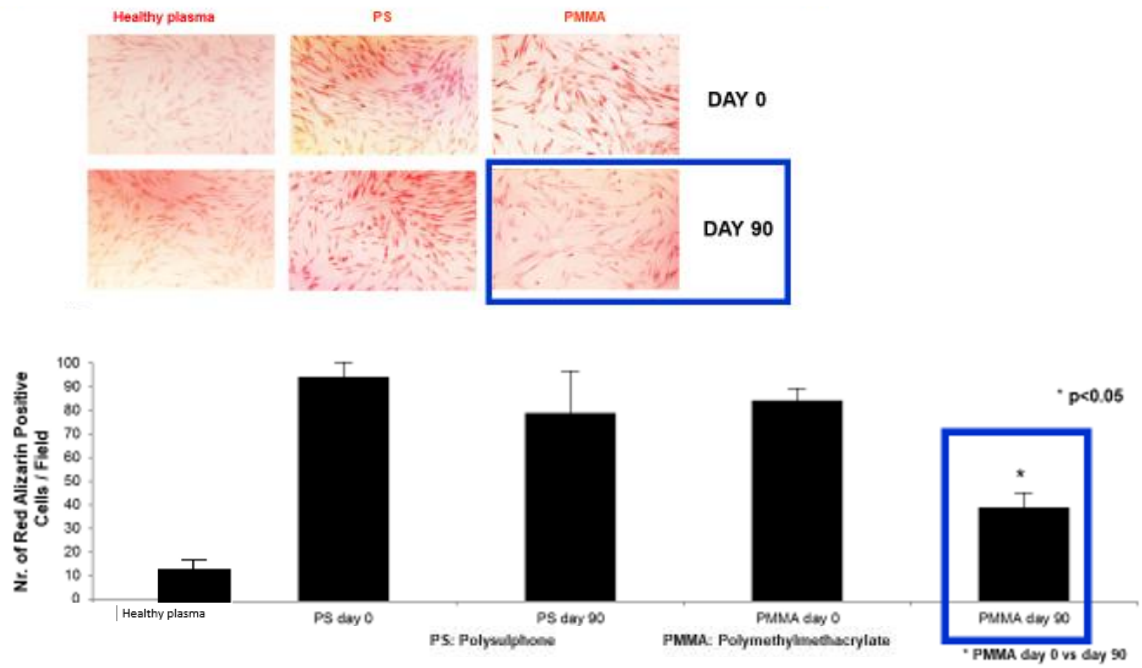

Fig. 36: Comparison of the mean value of smooth muscle cells positive to the Alizarin red dye (osteoblastic differentiation marker) in patients in PS or PMMA BKF filter therapy, at T0 and T3. In the box, the sample images compare the effect on smooth muscle cells determined by the control serum with that taken after RRT procedure with PS and PMMA BKF, in correspondence of T0 (day 0) and T3 (day 90)

Finally, the expression of RUNX-2 was investigated by the smooth muscle cells used in the previous evaluation, incubated with the sera of day 0 (T0) and 90 (T3) of both Group 1 and Group 2.

In Group 2 the percentage of expression of RUNX-2 in smooth muscle cells at the time T0 was 55,50 ± 4,00%, with a reduction to 47,70 ± 4,70 % after 90 days (T3) of membrane therapy in PS.

In Group 1 the percentage of expression of RUNX-2 in smooth muscle cells at T0 was 60,2 ± 5,56 %, with a reduction to 23,35 ± 6,5 % after 90 days (T3) of membrane therapy in PMMA BKF (Figure 37). The difference was significant, with p-value < 0,05.

Increased expression of RUNX-2 was also detected at the gene level via qRT-PCR, as described in the section "Patients and methods" (results not shown)

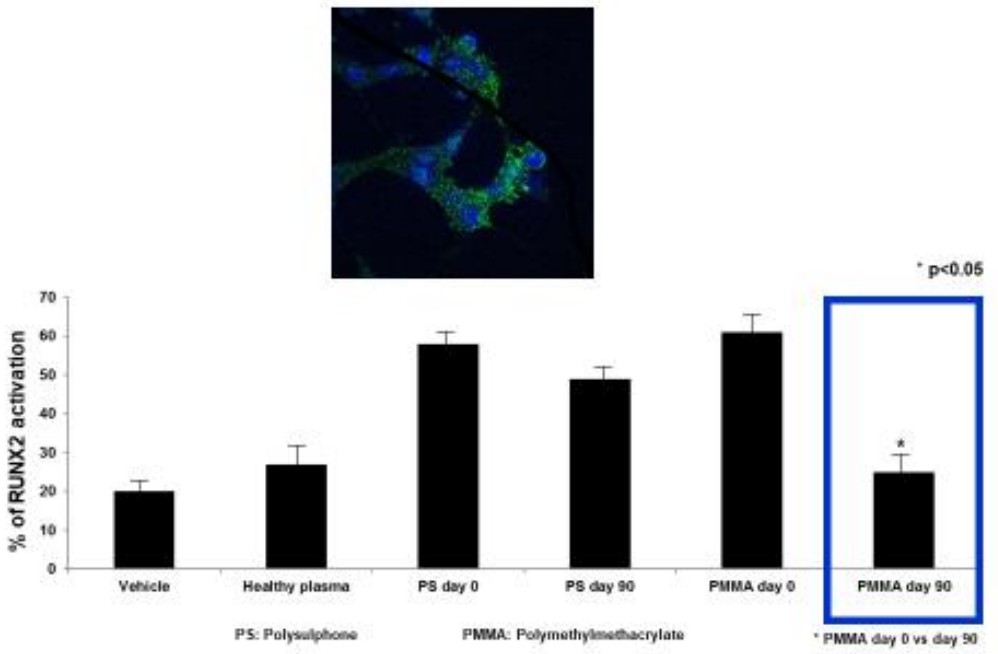

Fig. 37: Mean percentage of activation of RUNX-2 within smooth muscle cells incubated with sera of Group 1 and 2 patients, at T0 (day 0) and T3 (day 90). Above, an example image of the positive indirect immunofluorescence reaction for RUNX-2 (in green)

6.9. EVs isolation and characterization

We performed a first characterization of the EVs present in the plasma of the study cohort at T0, in comparison with healthy subjects.

The results of this analysis showed an increased plasma concentration of EVs in uremic patients ($1,3x10^{12} \pm 1,25x10^{11}$ particles/ml), compared with the healthy controls ($4,8x10^{11} \pm 1,0x10^{11}$ particles/ml). This difference was significant ($p < 0,05$) (Figure 38).

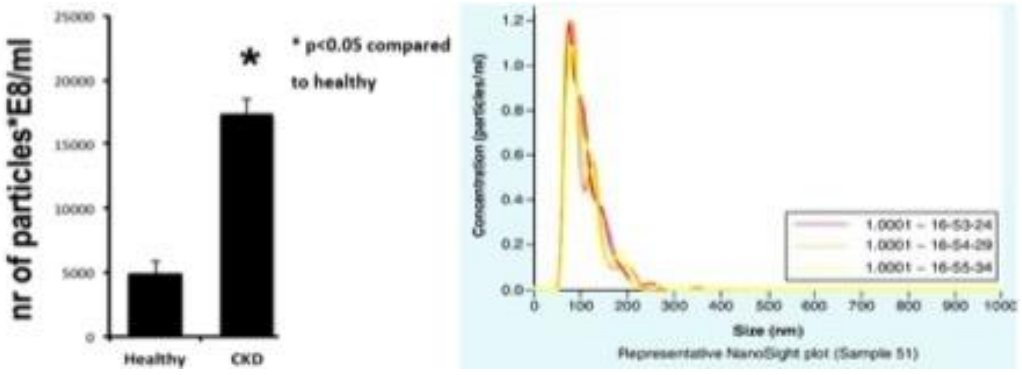

Fig. 38: Concentration of EVs found in patients with chronic kidney disease (CKD) by Nanotrack Analysis (Nanosight). On the right, sample graph of Nanosight analysis that analyzes the dimensions and relative concentrations of Evs (Ex = 10x)

The EVs identified were then characterized using the Nanosight and FACS analysis to assess some of the molecules most expressed on the membrane and thus their cell source.

There is no statistically significant difference in the cell source of CKD-EVs in comparison with healthy controls, except for endothelial EVs ($p<0,05$). (Table 17, Figure 39)

Tab. 17 Mean positivity percentages for specific markers of different cell types in CKD patients in bicarbonate dialysis compared with healthy controls

Specific markers of source cells	% of positivity	
	CKD-EVs	Healthy-EVs
Platelet (CD42b, CD62P, CD41)	50,30±2.50	53,60±5,05
Monocyte (CD14, CD15)	21,30±0,05	24±3,80
T lymphocyte (CD3)	0,13±0	0
B lymphocyte (CD19, CD5, CD40)	1,43±1,03	0.1±0,2
Endothelial cells (CD144, CD31, CD105, CD146)	27,34±2,75	17,04±3

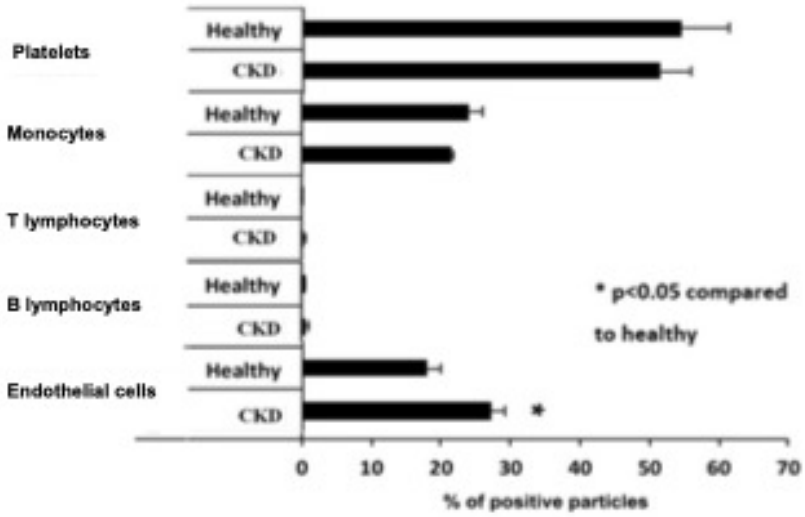

Fig. 39: Origin of EVs obtained from FACS analysis based on the type of membrane cell markers expressed in CKD patients in bicarbonate dialysis in comparison with healthy controls

Subsequently, we evaluated the surface expression of specific markers involved in apoptotic, inflammatory, and pro-coagulatory phenomena.

The CKD-EVs showed on their surface the expression of molecules involved in apoptotic, inflammatory, pro-coagulatory and complement activation phenomena such as Tissue Factor, C5b-9, CD40L, ICOS, FAS-ligand, NGAL, Class I HLA and different types of protein in the selectin and integrin family (Table 18, Figure 40). The statistical significance has always been reached ($p < 0,05$).

Tab. 18 Mean positivity percentages for different apoptotic, inflammatory, and pro-coagulatory markers in CKD patients in bicarbonate dialysis compared with healthy controls

Specific markers	% of positivity	
	CKD-EVs	Healthy-EVs
CD40L	7,50 ± 2,40	2,23 ± 0,01
Tissue Factor	25,44 ± 4,05	25,00 **±** 2,08
C5b-9	10.01 ± 3,00	3,34 ± 3,00
ICOS	11,39 ± 0,03	1,39 ± 1,03
FASL	13,37 ± 4,75	2,73 ± 1,75

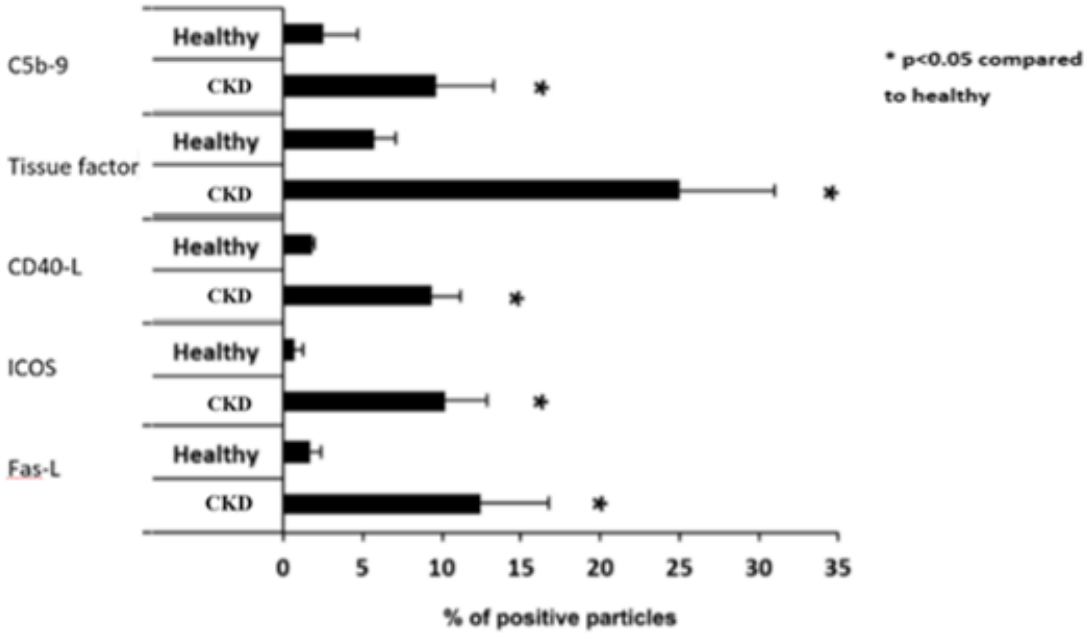

Fig. 40: Expression of surface markers involved in inflammation processes, apoptosis, coagulation and complement activation in CKD patients in bicarbonate dialysis compared with healthy controls

6.10. Characterization of microRNA in CKD-EVs

Through the Protein Quest platform, we identified the 5 most common miRNAs involved in endothelial dysfunction and vascular calcification, with known pro-apoptotic and anti-angiogenic abilities (miR17a-5p, miR92a, miR423-5p, miR451, miR223). Currently, we're performing a relative quantification by RT-PCR of the expression of the 5 miRNA of interest.

6.11. Biological effect of EVs on endothelial cells and VSMC

In order to assess the biological activity of the uremic EVs we evaluated - by immunofluorescence and FACS analysis - the internalization of EVs within endothelial cells and VSMC using a pool of EVs from the surviving samples. As showed in Figure 42, EVs were internalized by EC and VSMC compared to controls.

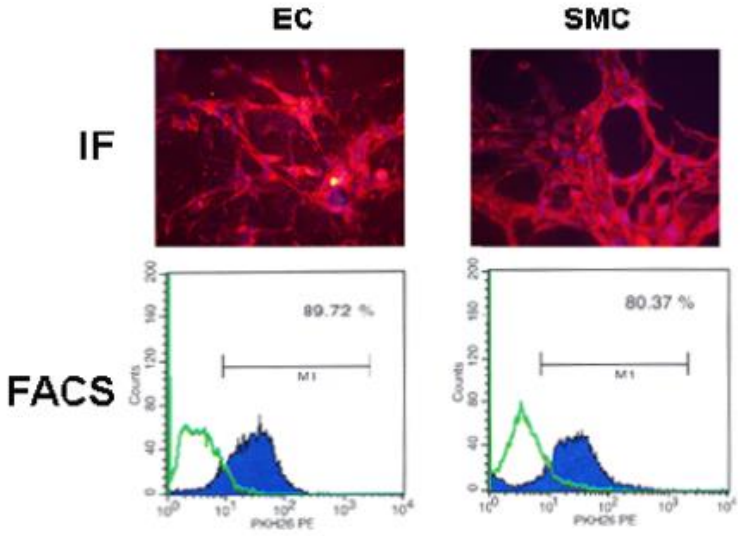

Fig. 42: In the panels, immunofluorescence reaction illustrating the internalization of EVs (in red, PKH26) in EC and VSMC). The cell nuclei were counter-colored with Hoechst (in blue). In the graphs below, FACS analysis related to the internalization of EVs; the cytometric detectors allow to highlight the cell population (EC, VSMC) positive for the internalization of colored EVs in comparison with the control (cells not stimulated by EVs, identified by the green line).

Finally, the degree of osteoblastic differentiation of VSMC incubated with the CKD-EVs pool from the study cohort was assessed.

The different intensity of staining was detected by the absorbance; this parameter in uremic patients compared with healthy controls was statistically significant ($p<0,05$), with an absorbance average of $0,1 \pm 0,005$ in CKD patients and $0,055 \pm 0,001$ in healthy controls (Figure 43).

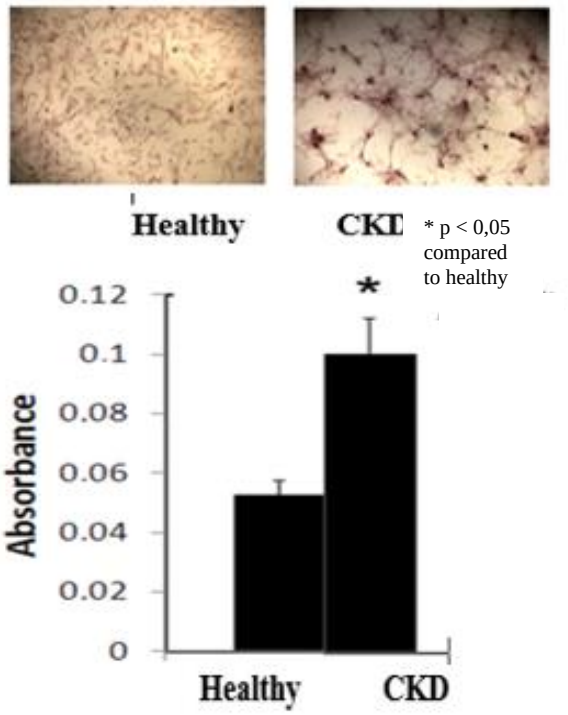

Fig. 43: Absorbance degree associated with intensity quantification for Alizarin red staining in vitro by VSMC incubated with EVs from uremic sera. In the boxes, examples illustrating different degrees of osteoblastic differentiation presented by VSMC

All effects induced by CKD-EVs on the different cell types were enhanced by co-incubation with uremic toxins PBUT (indoxyl sulfate) and were significantly reduced following pre-treatment with RNase, enzyme able to degrade mRNA and miRNA.

7. Discussion

This study has been oriented mainly in two directions: on the one hand the attempt to identify new markers of cardiovascular disease in the uremic patient and on the other to understand what mechanisms may correlate chronic kidney damage with the increased cardiovascular mortality of these patients.

7.1. Effectiveness of dialytic filters with adsorbent properties reducing sCD40L levels, inflammatory processes, and related vascular damage.

Chronic kidney disease, as a model of early senescence and fragility, is characterized by a persistent inflammatory status, which is predominantly mediated by some circulating uremic toxins identified in recent years as medium and large molecules and as PBUT (Protein Bound Uremic Toxins). These molecules seem to be able to modulate vascular damage, directly and indirectly and, in combination with the altered regulation of bone metabolism, are cause of accelerated atherosclerosis of the uremic patient[31].

The CD40/CD40L pathway seems to play a key role in the mechanisms associated with the development of atherosclerosis and vascular calcifications in hemodialysis patients. CD40 is a lymphocytic co-stimulation molecule also present on endothelial, epithelial, and smooth vascular muscle cells, with a pro-inflammatory role that occurs when the molecule is activated by the respective ligand, CD40L, expressed by platelets, smooth vascular muscle cells, endothelial and epithelial cells[37,56].

sCD40L is the soluble form of CD40L and is typically released by platelets because of their activation. This molecule has a complete biological activity and, the ligation with CD40 determines the release of cytokines and the expression of adhesion molecules.

The RISCAVID study[40] was the first to demonstrate the role of sCD40L as a marker of cardiovascular risk, as confirmed by a more recent study of Li et al.[57] and Esposito et al.[58] which defined sCD40L as a predictive marker of cardiovascular morbidity and mortality in hemodialyzed patients. Desideri et al. (RISCAVID study) also found an increase in cardiovascular risk in patients treated

with bicarbonate hemodialysis (BHD) compared to those treated with hemodiafiltration online (OL-HDF), suggesting a possible relationship between type of dialytic method (diffusive versus convective-diffusive mixed) and circulating levels of sCD40L.

In addition, recent evidence from Japanese studies suggests that the adoption of filters based on the physical principle of adsorption, such as PMMA, can provide better purification of uremic toxins than PS. In one of the latest published papers, Abe et al.[53], based on a cohort of 136,676 hemodialysis patients, showed that PMMA is associated with better outcomes in terms of mortality and general morbidity. In this work, therefore, a standard hemodialysis replacement therapy such as dialysis bicarbonate was evaluated but using adsorbent dialytic filters. The adsorbent membrane in PMMA helps to remove medium-high molecular weight molecules with a reduction of inflammatory mediators[55]. There are different subtypes of filters, and the PMMA BKF series is particularly effective in eliminating molecules of high medium-weight difficult to remove because they are linked to plasma proteins, such as sCD40L or PBUT[54].

On this basis, our group has therefore launched some translational research studies, with the aim on the one hand to assess the effectiveness of HDF-OL and absorptive membranes (PMMA filters and Theranova), and on the other hand to evaluate new potential diagnostic and therapeutic damage markers, such as lymphocytic co-stimulation molecules and EVs.

In the first part of this study, ROC analysis confirmed the biological role of sCD40L, finding a strikingly similar threshold value to RISCAVID study as predictor of MACE (RISCAVID median values 7.6 ng/ml vs Our ROC value 7.8 ng/ml). This slight difference between the two cut-off values could be explained by the general characteristics of the two populations. In particular, the percentage of hypertensive and diabetic patients is greater in our cohort than RISCAVID therefore this figure could explain a higher cut-off in our population. Moreover, this predictive effect is the strongest and independent risk factor (OR 4.97) compared to the traditional risk factors such as diabetes, arterial hypertension, and age. sCD40L level and patient's age are the only independent factors confirmed at

multivariate analysis. Therefore, any dialyzer which is proven to reduce sCD40L levels could be expected to have a positive impact on cardiovascular risk, which represents the first cause of death in dialysis patients. Furthermore, we analyzed the efficacy of PMMA BKF in the removal of sCD40L, as well as the role of sCD40L in cardiovascular damage. The results, although on a small sample size, showed a significant and rapid reduction of the levels of sCD40L, following the start of RRT with PMMA BKF filter and at switch from PS to PMMA BKF; consistently, the mass removal of sCD40L was higher by adopting the membrane in PMMA BKF. In addition to the reduction of sCD40L levels, the PMMA BKF filter seems to have a higher impact in the reduction of hepcidin, since it supports the biological plausibility of a protective effect on the inflammatory anemia, the accelerated atherosclerotic process, and the vascular disease of CKD.

Of particular interest are the data concerning the removal of PBUT, uremic toxins with medium-high molecular weight (e.g., indoxyl-sulfate). Also in this context, the adsorbent filter has proven more efficient, reducing PBUT levels by removing more mass than PS.

In vitro studies also demonstrated the pro-atherogenic and inflammatory role of sCD40L and, for the first time, the existence of a correlation between platelet activation status and PBUT levels (resulting in an increase in sCD40L concentration). In fact, in the serums of patients treated with the adsorbent membrane were detected: 1) a reduced amount of ROS (Reactive Oxygen Species) produced by endothelial cells, 2) a reduced adhesion of monocytes at endothelial cell level (expression of reduced endothelial activation) and 3) a reduced osteoblastic differentiation by smooth vascular muscle cells, all essential aspects of the ongoing vasculopathy of uremia. Being the peculiarity of this filter to eliminate more effectively sCD40L through adsorption, it is biologically plausible to correlate the lower concentration of sCD40L with the anti-inflammatory and vascular-protective effects previously mentioned (lower production of ROS, lower degree of osteoblastic differentiation and monocyte adhesion).

Therefore, the reduction of endothelial dysfunction and calcification of smooth muscle cells is probably at least partly due to the reduction of the levels of sCD40L, which is achieved not only through direct adsorption of PMMA, but also thanks to the adsorption of PBUT stimulating the release of the mediator. It could therefore be assumed a double protective effect determined by the membrane in PMMA, consisting of a direct effect linked to the adsorbent properties of the same and an indirect effect, linked to the removal of PBUT and the resulting reduction in platelet release of sCD40L.
This second "indirect" protective mechanism of PMMA filters has never been reported to our knowledge and is therefore a peculiarity of our study.

7.2. Role of extracellular vesicles (EVs) in endothelial dysfunction and vascular calcifications in the uremia.

EVs are newly discovered structures released by multiple cell types and implicated in intercellular communication[59]. EVs appear to be increased in CKD patients, with a predominantly endothelial and platelet origin; in addition, their levels would correlate directly with an increased cardiovascular risk[46,49(p142)]. In the second part of this study, we first confirmed that the EV concentration was increased in CKD patients compared to healthy controls. In addition, the analysis of the expression of different membrane antigens allowed to highlight the increase of endothelial EVs in uremic patients compared to controls. The finding of a positivity for markers related to inflammation, endothelial dysfunction, and vascular calcification, allowed to hypothesize that the EVs are involved in these phenomena. In particular, CD40L and ICOS lymphocytic co-stimulation molecules positivity on EV surface makes the hypothesis of an involvement of EVs in the development of pro-atherogenic and pro-inflammatory phenomena more plausible.

The progression of cardiovascular damage as a result of the action of EVs appears confirmed in some studies described in the Literature, such as those carried out by Stenvinkel et al., which described the alterations induced by the EVs in uremia on muscle relaxation mediated by nitric oxide (NO), exploiting "ex vivo" models of isolated vessel[11,32]. In addition, Lee et al.[60] described the release of EVs from patients with IMA and the subsequent inoculation in experimental rats

favoring vasomotor dysfunction and formation of local clots. In addition, EVs of monocytic and lymphocytic origin have been identified in atherosclerotic plaques, with higher concentration than those of platelet origin. Boulanger et al.[45] have shown that EVs are present in atherosclerotic plaque and derived from leucocyte and smooth muscle cells. Finally, EVs isolated from atherosclerotic plaques can transfer molecules such as ICAM-1 to endothelial cells, thus facilitating the adhesion and transmigration of leukocytes in such locations.

In our study, the pathological effects of EVs appear to be mediated not only by the action of membrane proteins, but also by the presence of miRNA carried by EVs (e.g., the most important seems to be miR-223). This genetic material seems to act on endothelial cells and smooth vascular muscles, following the internalization of EVs, as observed in FACS and microscopic analyses performed in vitro. A pro-calcific role associated with the internalization of the EVs was noted, presumably associated with miR-223 action. These results confirm the data present in Literature[61] and therefore suggest that the EVs not only play a role of biomarkers, but also are effective damage mediators, as real uremic toxins. According to this interpretation, all previous effects induced by EVs on different cell types were enhanced by co-incubation with uremic PBUT toxins (p-cresyl sulfate or indoxyl sulfate) and significantly reduced by pre-incubation RNase treatment, an enzyme that can destroy miRNA.

Useful insights for the correlation of these laboratory data with clinical data of cardiovascular damage could be represented by: 1) detection of aPWV (Pulse Wave Velocity), an indirect measure of aortic wall stiffness, and 2) detection of the thickness of the intimate of the carotid artery (cIMT), a systemic atherosclerotic disease index[62]. Moreover, a study of patients with CKD in stage IV-V analyzed the relationship between circulating endothelial EVs and endothelial dysfunction, showing that the concentration of CD144+ EVs (caderine of vascular endothelium) was correlated with the vessel's capacity to dilate in response to increased blood flow, accompanied by evidence of increased vascular rigidity measured by aPWV[62].

7.3. Strengths and limitations of the study

This study has some strengths and some limitations. Among the strengths, the main is the analysis and characterization of the EVs, which represent a new frontier, and which will likely provide much information on the mechanisms of the disease and many potential biomarkers, not only within the CKD, but also for other diseases. In fact, the EVs are involved in different pathological processes and could also be exploited, as well as biomarkers, also as a new therapeutic tool of negative modulation of different pathological processes (see "Future Perspectives").

An important strength lies in the fact that the study is part of a project dedicated to the identification of the most effective dialysis methods for treatment, and to the prevention of the development of cardiovascular damage in patients with CKD, main factor of mortality and morbidity in this cohort. As previously noted, the identification of "non-traditional" risk factors, associated with the high increase in cardiovascular risk associated with CKD patients, has been the subject of study for many years because of the relevant clinical implications. The results of our study provide new evidence in this area, configuring the EVs and the co-stimulation molecule sCD40L as possible new actors in the pathogenesis of vascular damage in the uremia, and suggesting that certain RRT may be effective in inhibiting these processes. Among the limitations of the study, the reduced size of the enlisted population should be noted.

8. Conclusions

Our study provides new insights into the cardiovascular protective effect of PMMA, as compared with PS, supporting the hypothesis that this dialyzer is more efficient in removal of sCD40L due to its adsorptive properties. Not only PMMA BKF is associated with a lower degree of inflammation, but also with an improvement of endothelial dysfunction and vascular calcification processes, mediated by the reduction of sCD40L and hepcidin levels. In fact, the in vitro study of sera treated with PMMA BKF, characterized by reduced levels of sCD40L, showed 1) a reduced stimulus to the production of ROS (Reactive Oxygen Species) by endothelium, 2) a reduction of endothelial activation (expressed by reduced monocytic adhesion) and finally 3) the degree of osteoblastic differentiation of smooth vascular muscle cells. The results highlight the impact of the removal of this soluble molecule on several aspects related to chronic micro-inflammation of the uremia. At the same time, we assessed the PMMA BKF ability to adsorb PBUTs - such as indoxyl sulfate (IS) - which are able to determine the exposure of CD40L on the platelet membrane and the consequent cleavage, with release of sCD40L. This represents an unprecedented mechanism of modulation of CD40L levels because the PMMA dialyzer, can effectively break down both sCD40L and PBUT levels, inhibiting the platelet release of sCD40L.

Moreover, we found that EVs concentration is significantly increased in CKD patients with a predominantly platelet and endothelial origin. The expression of the CD40L and other molecules potentially implicated in inflammatory, pro-apoptotic and pro-coagulant processes (ICOS, C5b-9, TF, FAS-L) has been demonstrated on the surface of the EVs suggesting that these can contribute to the development of functional alterations of endothelial and smooth muscle cells in the uremic patients. Furthermore, the EV effects are also attributable to the transfer of gene material including some specific miRNA. To confirm this hypothesis, we observed in vitro that the biological activity of EVs significantly modulated the degree of osteoblastic differentiation of smooth muscle cells. In particular, in CKD patients mir-223 expression was higher than healthy controls and CKD EVs therefore appear to act synergically with the uremic toxins in the development of endothelial and smooth muscle cell damage, through the action of membrane proteins and horizontal transfer of miRNA. In addition, all EVs effects were enhanced by co-

incubation with uremic PBUT toxins and were significantly reduced following pre-treatment with RNase.

In conclusion, sCD40L does not appear exclusively a marker of cardiovascular damage in the uremic patient, but also a mediator of the CV progression. The reduction of sCD40L levels using adsorbent filters (PMMA BKF) could therefore have an impact on the reduction of cardiovascular risk in the CKD patient. In addition, our work allows us to outline a role of potential biomarker for the development risk of MACE, providing new evidence about the mechanisms of damage. Similarly, EVs are biomarkers and main players of cardiovascular damage in uremia. The EVs internalization and the transfer of specific miRNA, could play a key role towards inflammation, endothelial dysfunction, vascular calcification, and development of cardiovascular disease in the uremic patient. The EVs would therefore constitute real uremic toxins. Further studies should be carried out to understand through which mechanisms the genetic material contained within EVs, and the proteins expressed on their surface interact with the surrounding environment modulating molecular pathways that can contribute to damage progression.

8.1. Milestones and deliverables

The results of this study will be presented at national and international scientific meetings and **are currently submitted to a peer-reviewed scientific journal.**

9. Future perspective

One of the main perspectives is the begin of a prospective study on a larger population, with a duration of at least 5 years, in order to verify the correlation between the use of different dialytic filters (PMMA/BHD), serum levels of sCD40L and MACE. The correlation between sCD40L and cardiovascular events would in fact represent an important relapse of our work from the clinical point of view and would confirm the initial evidence of the Literature on this topic. If the role of sCD40L will be confirmed, the determination of its levels could be used to stratify the cardiovascular risk of CKD patients, thus assuming a new role as biomarker and therapeutic target.

Another possible development could be a further study to evaluate the role of CD40L through genetic silencing of CD40L (for example through siRNA - small interfering RNA) in the endothelial cell and smooth muscle cell, to verify the abrogation of the effects associated with sCD40L in our study.

Of interest, the interactions between CD40/CD40L and other co-stimulation molecules, such as the ICOS/ICOSL system, could represent an additional field of study, considering that these molecules were expressed on the surface of EVs in our results. Moreover, there are numerous data in the Literature supporting a role in the regulation and modulation of cardiovascular damage by the ICOS/ICOSL pathway, in particular in relation to atherosclerosis[37,38].

In addition to T-cell co-stimulatory pathways, the role of EVs in uremia should be considered in depth. The results of our study suggest that the EVs do not have a simple role of biomarkers but can be active mediators in the development of vascular damage typical of uremia. Their function as "carriers" of pro-atherogenic and anti-angiogenic genetic material makes them ideal candidates to study the mechanisms of damage of uremia and therefore, in perspective, to identify miRNA that can be used both as biomarkers (for example, mirna-223) and as therapeutic targets. The development of monoclonal antibodies able to inhibit the internalization of EVs, or interfering RNA or specific miRNA with inhibitory activity against pathogenic miRNA, are possible developments with modern biotechnology. Furthermore, it could be hypothesized a removal of EVs through the use of absorptive membrane (e.g. PMMA BKF).

Finally, the elimination of both PBUT and sCD40L by dialyzers with PMMA BKF will be of great interest in the future. According to the Literature, the treatment of high volume convective hemodialytic infusion (HDF) would determine the best clinical outcomes, being associated with a more effective removal of medium-large toxic molecules. It could therefore be assumed that the combined use of absorptive membranes (e.g. PMMA, Theranova) and HDF-OL could be the most effective elimination modality of traditional and "non-traditional" uremic toxins with an optimization of the positive effects on the slowing of the progression of cardiovascular damage.

9.1. Other research projects related to the main study

Based on the results obtained in the main study and literature data, we carried out - during the three-years of PhD program - 2 other research project to investigate the potential efficacy of other hemodialytic strategies:

- **Theranova study**: a multicenter, prospective, one-arm, clinical study, lasting 6 months. In this study were enrolled 60 patients with CKD stage V according to K/DOQI in chronic bicarbonate hemodialytic treatment and at the beginning of the study they switched to a hemodialytic treatment with a new absorption membrane, called Theranova, for 6 months. At the beginning of the study (T0) and therefore every month all patients underwent to blood sampling for evaluation of inflammation markers and uremic toxins. The results of this study showed the ability of the Theranova membrane to reduce blood concentrations of certain uremic toxins (medium molecules) such as β2-microglobulin (Table 19 and Figure 44), free light chains (Tables 20-21 and Figure 45-46) and myoglobin (Table 22 and Figure 47), compared to PS.

Tab. 19 β2-microglobulin concentrations (median and IQR) at different time points. Statistically significant differences were found in the variance analysis with Friedman Test (p < 0.0001) and Wilcoxon Signed Ranks Test

Theranova study	T0	T3	T6	p-value (Wilcoxon test)
β2-microglobulin (ng/ml)	29.10 (23.72 – 33.36)	26.53 (22.65 – 29.48)	24.70 (21.40 – 31.20)	**T3-T0 p =** 0,001*
				T6-T0 p < 0,0001*
				T6-T3 p = 0,105

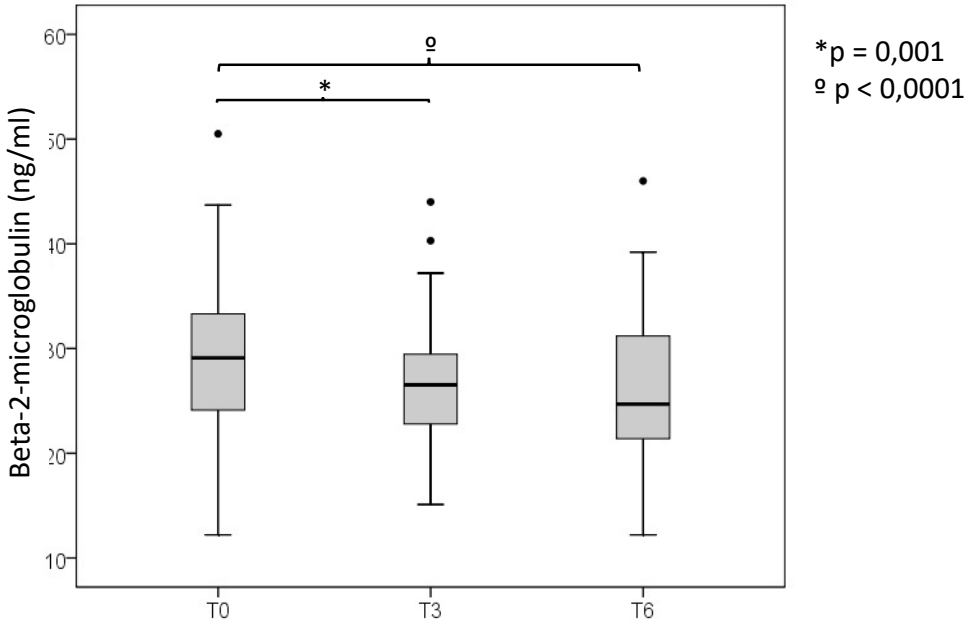

Fig. 44: Box plot (median and IQR) for β2-microglobulin concentrations at different time points within two groups.

Tab. 20 Light chain Lambda concentrations (median and IQR) at different time points. Statistically significant differences were found in the variance analysis with Friedman Test (p < 0.0001) and Wilcoxon Signed Ranks Test

Theranova study	T0	T3	T6	p-value (Wilcoxon test)
Light chain Lambda (mg/dl)	16 (10.8 – 22)	12 (9.3 – 17.9)	10,5 (6.9 – 17)	**T3-T0 p <** 0,0001*
				T6-T0 p < 0,0001*
				T6-T3 p < 0,0001*

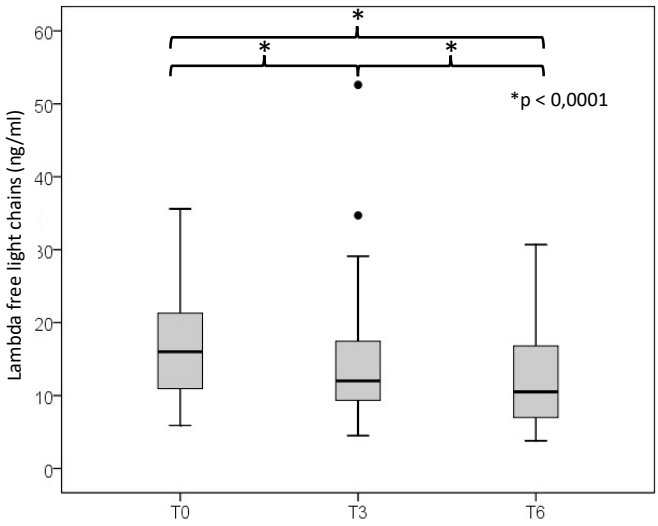

Fig. 45: Box plot (median and IQR) for light chain Lambda concentrations at different time points within two groups.

Tab. 21 Light chain Kappa concentrations (median and IQR) at different time points. Statistically significant differences were found in the variance analysis with Friedman Test (p < 0.0001) and Wilcoxon Signed Ranks Test

Theranova study	T0	T3	T6	p-value (Wilcoxon test)
Light chain Kappa (mg/dl)	16.5 (13.3 – 20.2)	12.2 (8.8 – 18)	11.9 (4.4 – 19.2)	**T3-T0 p <** 0,0001*
				T6-T0 p < 0,0001*
				T6-T3 p < 0,0001*

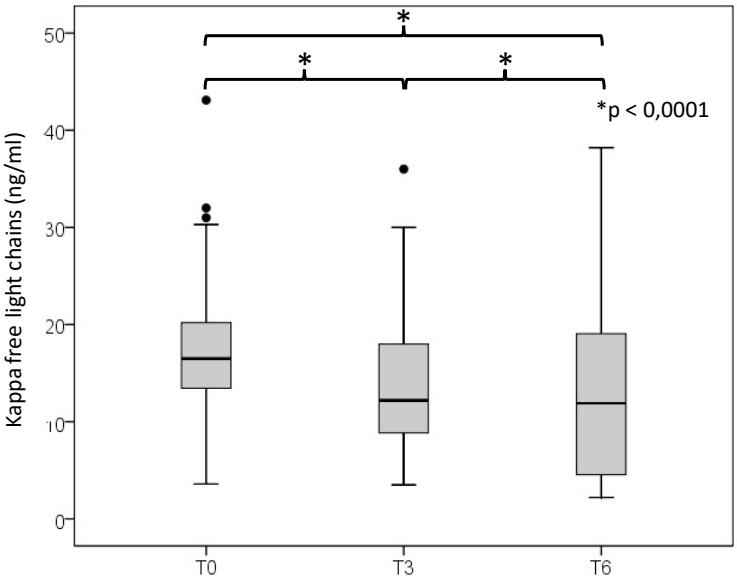

Fig. 46: Box plot (median and IQR) for light chain Kappa concentrations at different time points within two groups.

Tab. 22 Myoglobin concentrations (median and IQR) at different time points. Statistically significant differences were found in the variance analysis with Friedman Test (p = 0.031) and Wilcoxon Signed Ranks Test

Theranova study	T0	T3	T6	p-value (Wilcoxon test)
Myoglobin (ng/ml)	186 (124 – 282)	182 (151 – 256)	179 (129 – 248)	**T3-T0 p =** 0,375
				T6-T0 p = 0,121
				T6-T3 p = 0,015*

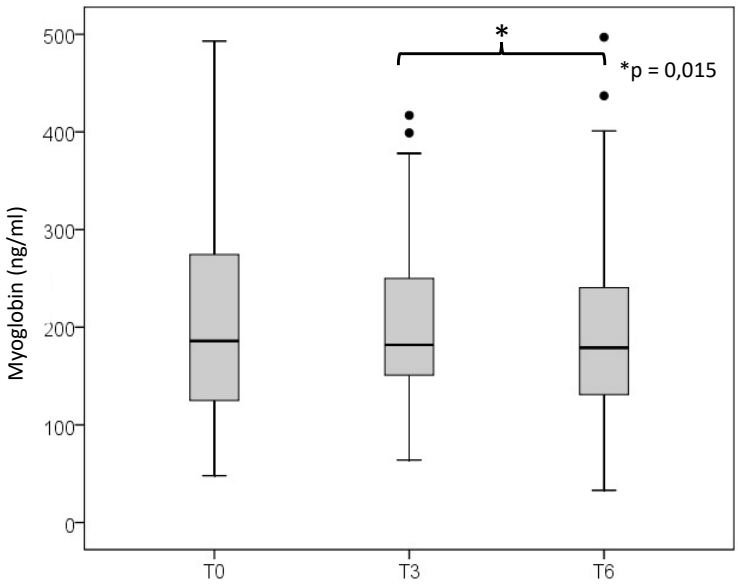

Fig. 47: Box plot (median and IQR) for myoglobin concentrations at different time points within two groups.

This study confirms the dialytic efficacy of Theranova membrane in eliminating molecules of medium weight compared to PS. **The results of this study are currently submitted to a peer-reviewed scientific journal**

- **CRC-CARIPLO study**: a multicenter, prospective, three-period, randomized, crossover clinical study, lasting 18 months. In this study were enrolled 47 patients with CKD stage V according to K/DOQI in chronic hemodialytic treatment. The inclusion criteria were: 1) Age between 18 and 80 years, 2) Hemodialysis treatment with BHD for at least 1 month, three-weekly rhythm, 12 hours/week; 3) diuresis <500 ml/ day; 4) Qb > 250 ml/min and 5) mean Kt/V >1.2. We excluded patients with local or systemic acute infectious processes, active malign neoplasm (excluding skin tumors other than

melanoma), patients with kidney transplantation in place but no longer functioning, patients with autoimmune diseases or active vasculitis. The patients were randomized in three arms to continue BHD or switch to mOL-HDF or absorption membrane (PMMA or Theranova) and every 6-months they will switch to a different dialytic treatment. At the beginning of the study (T0) and therefore every 3 months all patients underwent to blood sampling for quantification and characterization of plasma MVs and miRNA content and evaluation of inflammation markers and uremic toxins (Figure 48). Moreover, at the time of modification of the dialysis therapy every 6 months all patients evaluated arterial stiffness by PWV, thickness of the carotid wall using ecoDoppler and diastolic dysfunction by echocardiogram. We also performed in vitro studies on EC and VSMC to evaluate the pathogenic role of EV isolated from CKD plasma and Ex vivo studies on isolated human arteries to assess the effect of uremic EV on the mechanics of contraction and relaxation of the vessel. The ex vivo experiments will be performed in collaboration with Prof. Peter Stenvinkel, Karolinska Institutet (Stockholm, Sweden).

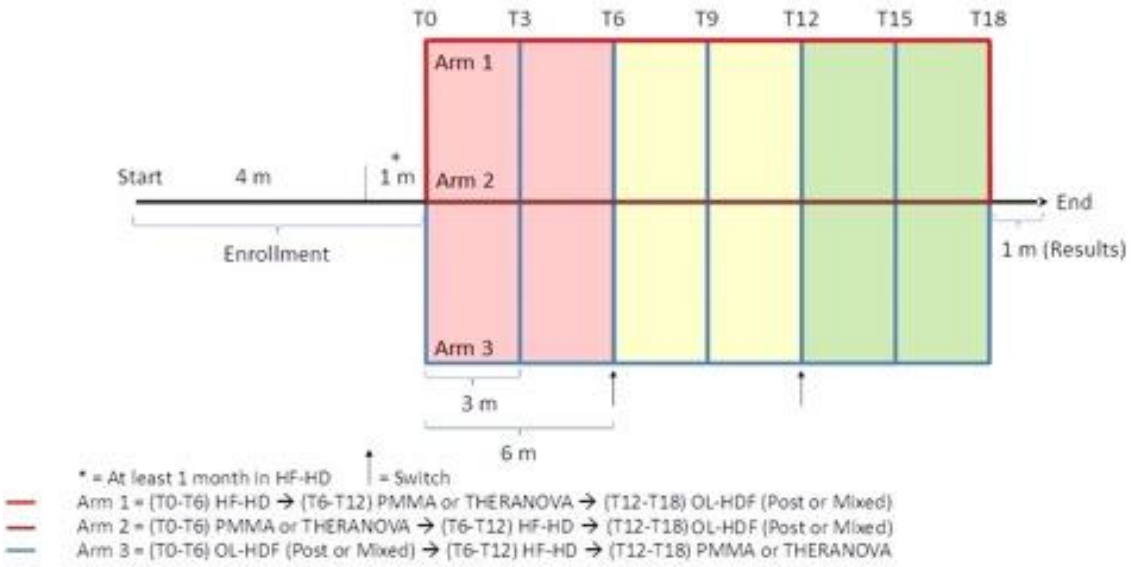

Fig. 48: CRC-Cariplo study protocol

Up to now, **the study is over, and we are concluding the experiments and the statistical analysis.** We performed in vitro study using plasma EVs isolated from healthy subject, BHD and mOL-HDF patients at T0 and T6.

EVs isolated from plasma of T0 HD patients measured around 162 nm and were meanly concentrated at $2x10^{11}$ particles/ml (Figure 49).

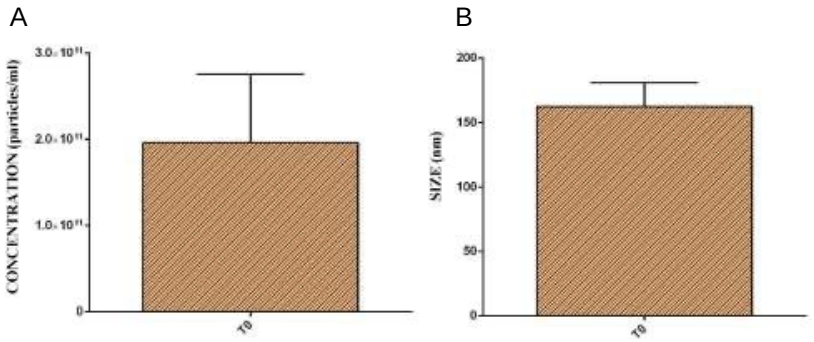

Fig. 49: Average concentration (particle/ml) and size (nm) of EVs from T0 samples

Concerning the surface protein expression, the most expressed markers are typical of T cells, in particular activated T cells and the cytotoxic subpopulation, B cells, macrophages, antigen presenting cells, platelets, and endothelial cells. Interestingly, there are difference between T0 and T6 samples. Results suggested that in T6 samples compared to T0 samples, there was a decrease of EVs deriving from general T cell population (Figure 50), immature B cell population, macrophages, platelets (Figure 51), antigen, presenting cells (Figure 52), exosomes. The decrease in markers expression may mean a reduction of the EVs themselves after the hemodialysis.

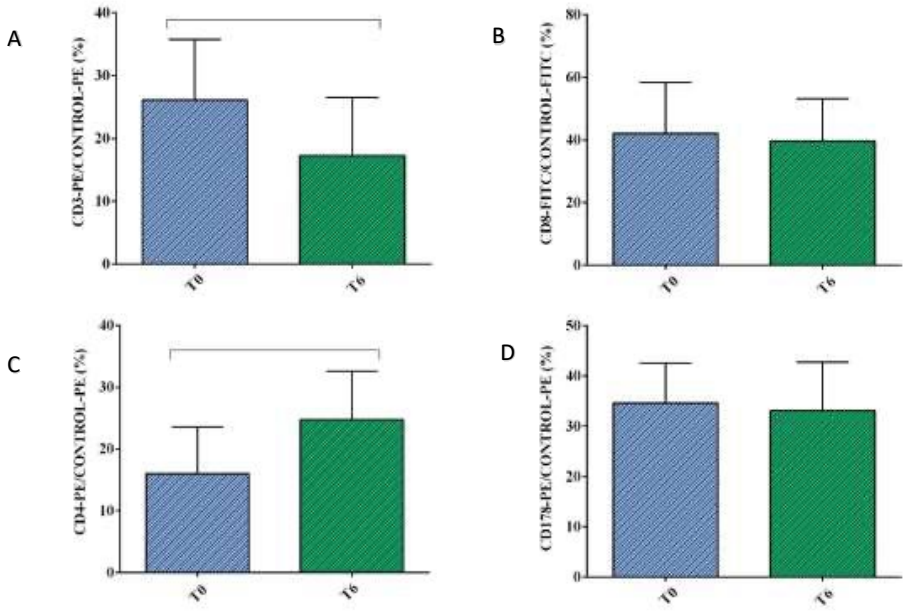

Fig. 50: Percentage of expression of T cell surface markers. In A, CD3 marked PE; in B, CD8 marked FITC; in C, CD4 marked PE; in D, CD178 marked PE. The data are expressed as percentage of positive cells, relative to the isotype control. Reported data are means ± SD of five independent experiments. Short square brackets indicate significance between groups (P<0.05).

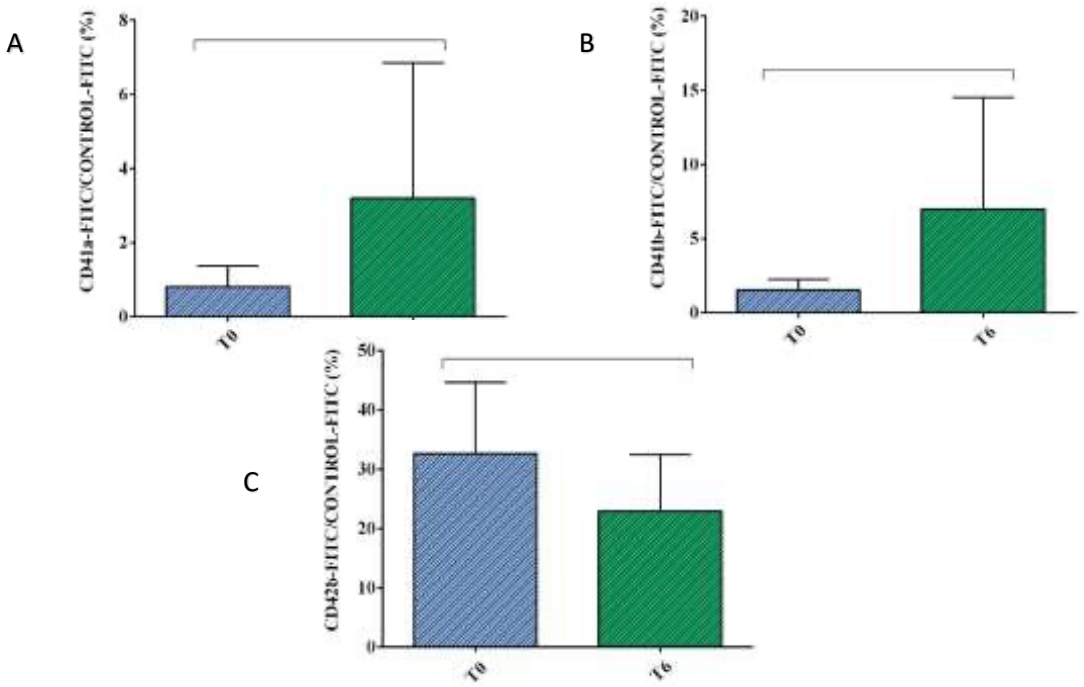

Fig. 51: Percentage of expression of platelet surface markers. In A, CD41a marked FITC; in B, CD41b marked FITC; in C, CD42b marked FITC. The data are expressed as percentage of positive cells, relative to the isotype control. Reported data are means ± SD of five independent experiments. Short square brackets indicate significance between groups (P<0.05).

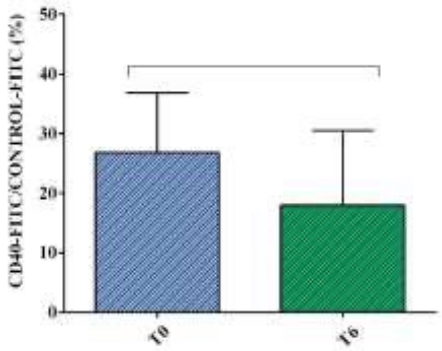

Fig. 52: Percentage of expression of antigen presenting cell surface markers. CD40 marked FITC. The data are expressed as percentage of positive cells, relative to the isotype control. Reported data are means ± SD of five independent experiments. Short square brackets indicate significance between groups (P<0.05).

Different results were obtained as regarding EVs deriving from ECs. Hence, we observed a fall of the percentage in T6 samples of EVs marked with CD81, which however is not specific for ECs, being also present on leukocytes.

Instead, we found an increase of markers for activated ECs, such as CD62e and CD146 from T0 to T6 samples (Figure 53).

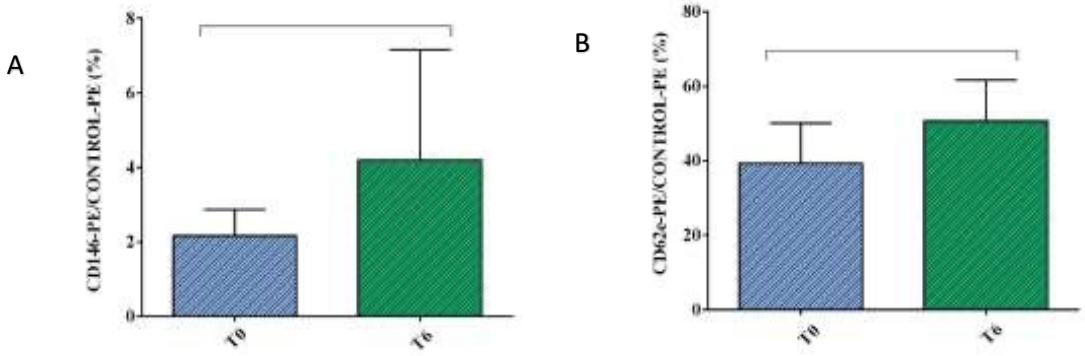

Fig. 53: Percentage of expression of endothelial cell surface markers. In A, CD146 marked PE; in B, CD62e marked PE. The data are expressed as percentage of positive cells, relative to the isotype control. Reported data are means ± SD of five independent experiments. Short square brackets indicate significance between groups (P<0.05).

Results on endothelial cell markers might suggest that, even if the dialysis membrane is more efficient in capturing the EVs, the mechanical stress of the process itself may cause endothelial stress, leading to its activation and EVs release. The same concept might be further attributed to EVs characterized with the marker (CD11b) that is involved in many adhesion-related associations between leukocytes, which was found to be increased from T0 to T6 samples. Also, some markers related to mature B cells, helper T cells, and platelets increased their expression on EVs during time. In the case of the rise in mature B cells and helper T cells derivation, a possible explanation can be addressed to the inflammatory reaction triggered by the dialysate content or the dialysis membrane, which stimulates helper T cells to activate mature B cells in order to produce antibodies against not-self molecules. Concerning the time- course elevation in time of EVs deriving from platelets (CD41a and CD41b markers), that finding was in contrast with finding about another platelets surface marker (CD42b), which decreased in T6 samples. In this case, it is also important to check the percentage of expression of these markers, in fact the CD42b marker is much more expressed in both T0 and T6 samples compared to CD41a and CD41b markers. Thus, it would be more reliable to take in account the trend of the CD42b marker when talking about EVs deriving from platelets, stating that they decrease from T0 to T6 samples. Furthermore, EVs deriving

from cytotoxic T cells and activated T cells did not change in percentage from T0 to T6 samples, which could be due to the release of pro- inflammatory mediators and cell-mediated cytotoxicity caused by the dialysis procedure.
Moving to the in vitro experiments, results show that after the stimulation with EVs, endothelial cells are notably less viable, as confirmed through the mitochondrial membrane potential test, and produce more oxidants in form of ROS and NO (Figure 54).

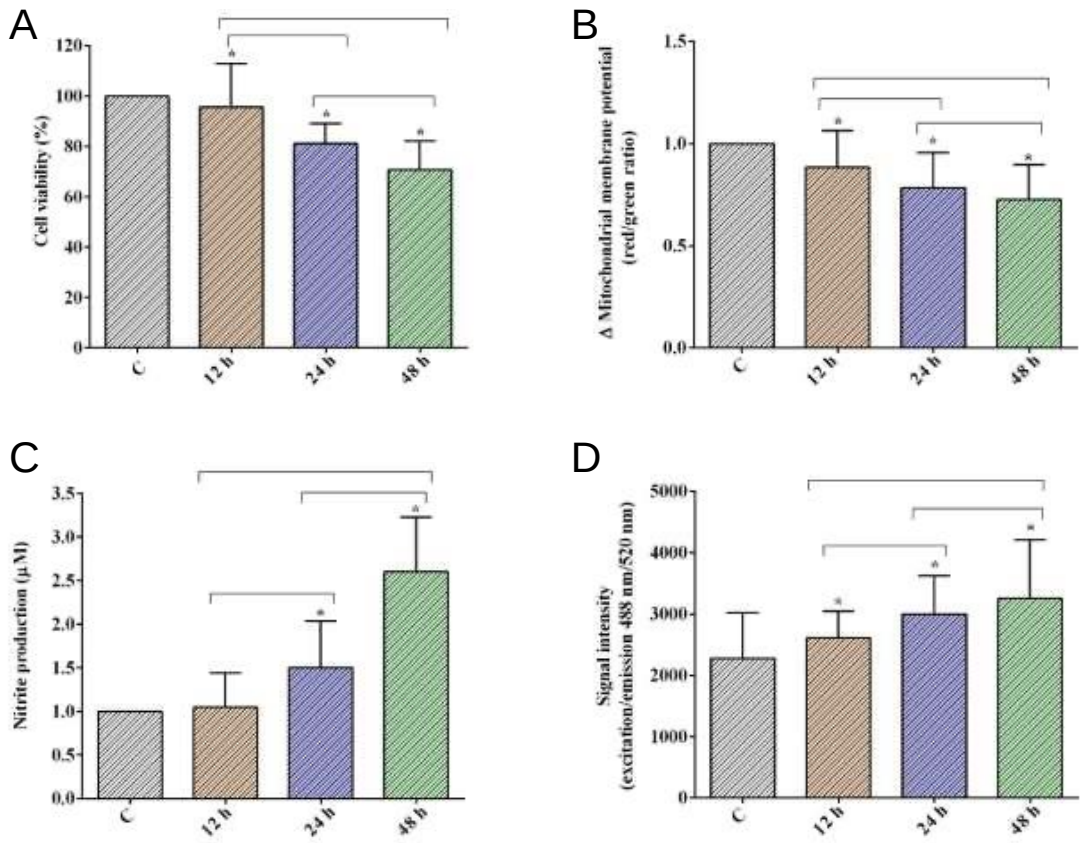

Fig. 54: Time-course effects of EVs from T0 samples on (A) cell viability, (B) mitochondrial membrane potential, (C) NO release and (D) ROS release in ECs. The data are normalized versus control value. Reported data are means ± SD of five independent experiments. Significance between groups: *P<0.05 vs C. Short square brackets indicate significance between groups (P<0.05).

All of these results are time dependent that means that the more EVs are on ECs, the highest is cell damage that they cause. Therefore, taken altogether, these results demonstrate the role of the EVs on triggering the renal endothelial cells damage. On the other hand, in vitro experiments on VSMCs suggest that in the presence of EVs, they activate themselves as demonstrated

by the increase in cell viability and mitochondrial membrane potential, and the increased [Ca2+] in cytoplasm. In fact, it is possible to hypothesize that EVs may influence the movement of calcium from the extracellular environment, since in the presence of EGTA (calcium-chelanting agent) EVs did not have any effect in the increase of [Ca2+]c. Moreover, EVs in the presence of ATP, were able to reduce the effects of ATP alone on [Ca2+]c. Taken altogether, results on VSMCs indicate that when they are stimulated with EVs from T0 samples, they turn into activated cells, increase their calcium content which could be used for their contraction (Figure 55).

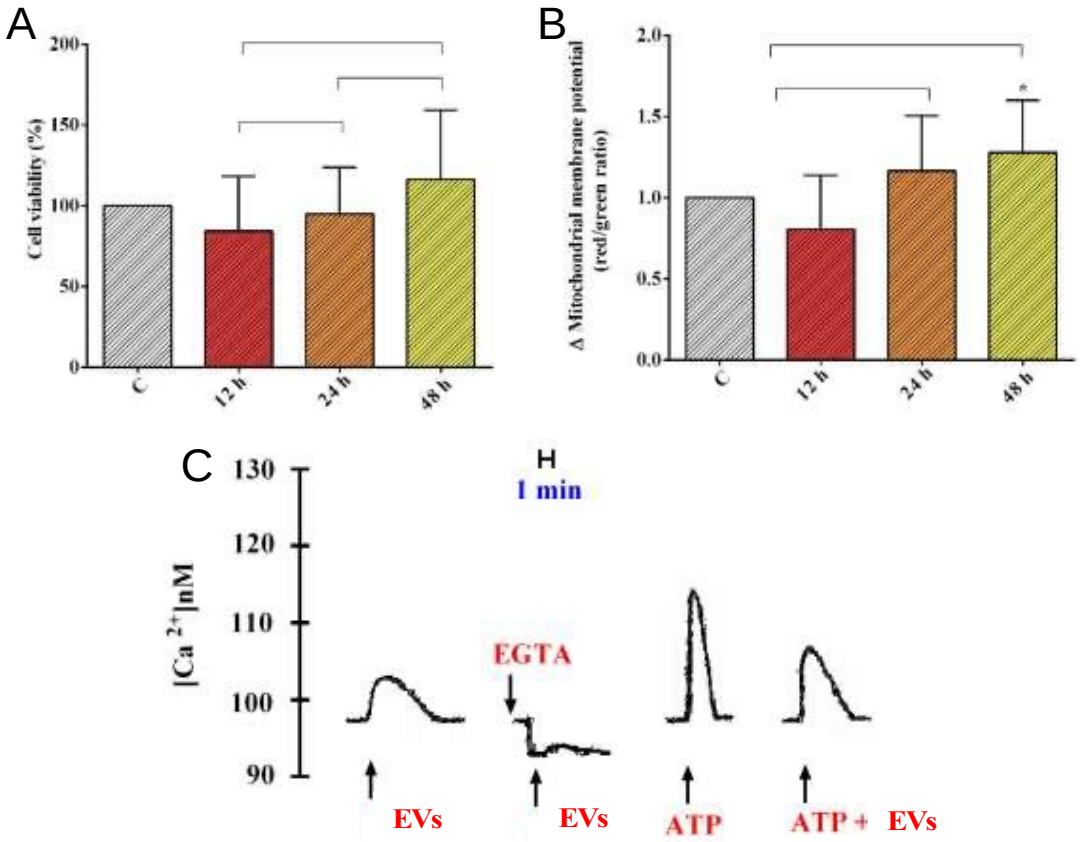

Fig. 55: Time-course effects of EVs from T0 samples on (A) cell viability and (B) mitochondrial membrane potential in VSMCs. The data are normalized versus control value. Reported data are means ± SD of five independent experiments. Short square brackets indicate significance between groups (P<0.05). (C) Analysis of intracellular Ca2+ pool mobilized by EVs of T0 samples in VSMCs. EGTA (50 mM), ATP (10 μM). The results are the mean ± SD of 5 experiments for each experimental protocol

It is notable that this event is at the basis of vasoconstriction and hypertension, which is a typical feature of end-stage CKD patients. Further, an increase of

cytosolic calcium could be followed by the activation of oxidative stress mechanisms at the basis of apoptosis.

The expected results of this project could lead to the identification of new therapeutic targets with a translational approach that put together in vitro studies on endothelial and smooth muscle cells, ex vivo studies on isolated human arteries and clinical evaluation of cardiovascular damage through analysis of arterial stiffness, carotid thickness and diastolic dysfunction. Furthermore, the identification of the pathogenic role of plasma EV may lead to the identification of new pathways, thus allowing to block the progression toward ESRD as well as the cardiovascular damage. As a future approach, the identification of EV surface molecules essential for their internalization into target cells, could also lead to the development of therapeutic monoclonal antibodies able to inhibit this internalization. Evaluation of mRNA and particularly microRNA involved in these mechanisms of damage will be more interesting for the potential development of therapeutic strategies based on the administration of small interfering RNA (siRNA) or specific inhibitors of microRNAs (antagomiRs). Finally, the identification of the pathogenic role of circulating plasma EV in the inflammatory environment could also find application in disease other than CKD and CVD and characterized by patients' frailty such as sepsis and cancer, diseases more prevalent in the older population. The development of extracorporeal therapies and specific inhibition of mRNA and microRNA present in circulating EV as assumed in this research project could be applied, therefore, also in these pathologies with additional beneficial impact on the regional and national health care systems.

10. Other research activities during PhD program

During the PhD program, further studies were carried out in other fields of research such as kidney transplantation starting national collaborations, as follow:

- We collaborated with Virology and Urology Units of our University to evaluate the role of BK polyomavirus (BKPyV) reactivation in the development of kidney and urothelial cancer in kidney transplant recipients (KTRs). In a retrospective single center cohort of KTRs (n = 1307), 10 clear cell renal cell carcinomas and 5 urinary bladder carcinomas were analyzed from 15 KTRs for the presence of

BKPyV infection through immunohistochemistry and fluorescent in situ hybridization (FISH). Three of these patients had already exhibited biopsy-proven polyomavirus-associated nephropathies (PyVAN). Although the presence of BKPyV large-T antigen was evident in the urothelium from a kidney removed soon after PyVAN diagnosis, it was undetectable in all the formalin-fixed and paraffin-embedded (FFPE) blocks obtained from the 10 kidney tumors. By contrast, large-T antigen (LT) labeling of tumor cells was detected in two out of five bladder carcinomas. Lastly, the proportion of BKPyV DNA-FISH-positive bladder carcinoma nuclei was much lower than that of LT-positive cells. Taken together, our findings further strengthen the association between BKPyV reactivation and cancer development in KTRs, especially bladder carcinoma. **The results of this study were published in a peer-reviewed journal** (Borgogna C, Albertini S, Martuscelli L, Poletti F, Volpe A, **Merlotti G**, Cantaluppi V, Boldorini R, Gariglio M. "*Evidence of BK Polyomavirus Infection in Urothelial but not Renal Tumors from a Single Center Cohort of Kidney Transplant Recipients*". *Viruses*. **2021**; 13(1):56. doi:10.3390/v13010056)

- We collaborated with Nephrology and Transplant Unit of University of Bari to assess the role of the extracellular vesicles in endothelial-to-mesenchymal transition and tubular senescence in renal antibody-mediated rejection. **This collaboration leaded to 4 accepted abstracts in international congresses and publicized in peer-reviewed journal** (Franzin R, Divella C, Stasi A, Sallustio F, Curci C, **Merlotti G**, Quaglia M, Cantaluppi V, Gesualdo L, Castellano G "*Extracellular Vesicles can mediate tubular inflammaging in Antibody-Mediated Rejection via Cyclin-Dependent Kinase Inhibitors*", Nephrology Dialysis Transplantation, June 2019 - Vol. 34, (Issue suppl 1); - Cantaluppi V, **Merlotti G**, Quaglia M, Rosso G, Clemente N, Cappellano G, Chiocchetti A, Castellano G, Dianzani U, Camussi G. "*Activation of the ICOS/ICOS-Ligand Pathway in Antibody-Mediated Kidney Graft Rejection*" [abstract]. Am J Transplant. 2020; 20 (suppl 3); - Castellano G, Franzin R, Stasi A, Divella C, **Merlotti G**, Quaglia M, Sallustio F, Stallone G, Cantaluppi V, Gesualdo L. "*Extracellular Vesicles Mediate Endothelial to Mesenchymal Transition and Tubular Senescence in Renal Antibody- Mediated Rejection by Inducing Complement Activation*" [abstract]. Am J Transplant. 2020; 20 (suppl 3).; - Franzin R, Stasi A, Sallustio F, Divella C,

Merlotti G, Quaglia M, Curci C, Stallone G, Cantaluppi V, Gesualdo L, Castellano G, "*Plasma extracellular vesicles mediate endothelial to mesenchymal transition and tubular senescence in renal antibody mediated rejection by complement activation*" Nephrology Dialysis Transplantation, June 2020 - Vol. 35. (Issue suppl 3), gfaa141.doi:10.1093/ndt/gfaa141.TO007)

In addition, these two collaborations have allowed the realization of **3 reviews published in peer-reviewed journals** on the following topics:

- New biomarkers of kidney graft dysfunction: (1) Quaglia M, **Merlotti G**, Guglielmetti G, Castellano G, Cantaluppi V. "*Recent Advances on Biomarkers of Early and Late Kidney Graft Dysfunction*". *Int. J. Mol. Sci.* **2020**, *21*, 5404. doi:10.3390/ijms21155404; (2) Quaglia M, Dellepiane S, Guglielmetti G, **Merlotti G**, Castellano G, Cantaluppi V. "*Extracellular Vesicles as Mediators of Cellular Crosstalk Between Immune System and Kidney Graft*". *Front Immunol*. 2020;11:74. doi:10.3389/fimmu.2020.00074
- Systemic Lupus Erythematosus and viral infection (Quaglia M, **Merlotti G**, De Andrea M, Borgogna C, Cantaluppi V, "*Viral Infections and Systemic Lupus Erythematosus: New Players in an Old Story*" *Viruses* **2021**, 13, 277. doi:10.3390/v13020277)

11. References

1. Chapter 1: Definition and classification of CKD. *Kidney Int Suppl (2011)*. 2013;3(1):19-62. doi:10.1038/kisup.2012.64

2. Jha V, Garcia-Garcia G, Iseki K, et al. Chronic kidney disease: global dimension and perspectives. *Lancet*. 2013;382(9888):260-272. doi:10.1016/S0140-6736(13)60687-X

3. Couser WG, Remuzzi G, Mendis S, Tonelli M. The contribution of chronic kidney disease to the global burden of major noncommunicable diseases. *Kidney Int*. 2011;80(12):1258-1270. doi:10.1038/ki.2011.368

4. Beaglehole R, Bonita R, Horton R, et al. Priority actions for the non-communicable disease crisis. *Lancet*. 2011;377(9775):1438-1447. doi:10.1016/S0140-6736(11)60393-0

5. National Kidney Foundation. K/DOQI clinical practice guidelines for chronic kidney disease: evaluation, classification, and stratification. *Am J Kidney Dis*. 2002;39(2 Suppl 1):S1-266.

6. Coresh J, Selvin E, Stevens LA, et al. Prevalence of chronic kidney disease in the United States. *JAMA*. 2007;298(17):2038-2047. doi:10.1001/jama.298.17.2038

7. De Nicola L, Donfrancesco C, Minutolo R, et al. [Epidemiology of chronic kidney disease in Italy: current state and contribution of the CARHES study]. *G Ital Nefrol*. 2011;28(4):401-407.

8. Keith DS, Nichols GA, Gullion CM, Brown JB, Smith DH. Longitudinal follow-up and outcomes among a population with chronic kidney disease in a large managed care organization. *Arch Intern Med*. 2004;164(6):659-663. doi:10.1001/archinte.164.6.659

9. Subbiah AK, Chhabra YK, Mahajan S. Cardiovascular disease in patients with chronic kidney disease: a neglected subgroup. *Heart Asia*. 2016;8(2):56-61. doi:10.1136/heartasia-2016-010809

10. Stenvinkel P, Larsson TE. Chronic kidney disease: a clinical model of premature aging. *Am J Kidney Dis*. 2013;62(2):339-351. doi:10.1053/j.ajkd.2012.11.051

11. Alexander MR, Owens GK. Epigenetic control of smooth muscle cell differentiation and phenotypic switching in vascular development and disease.

Annu Rev Physiol. 2012;74:13-40. doi:10.1146/annurev-physiol-012110-142315

12. Torres N, Guevara-Cruz M, Velázquez-Villegas LA, Tovar AR. Nutrition and Atherosclerosis. *Arch Med Res*. 2015;46(5):408-426. doi:10.1016/j.arcmed.2015.05.010

13. White WE, Yaqoob MM, Harwood SM. Aging and uremia: Is there cellular and molecular crossover? *World J Nephrol*. 2015;4(1):19-30. doi:10.5527/wjn.v4.i1.19

14. Lacolley P, Regnault V, Segers P, Laurent S. Vascular Smooth Muscle Cells and Arterial Stiffening: Relevance in Development, Aging, and Disease. *Physiol Rev*. 2017;97(4):1555-1617. doi:10.1152/physrev.00003.2017

15. Kuro-o M, Matsumura Y, Aizawa H, et al. Mutation of the mouse klotho gene leads to a syndrome resembling ageing. *Nature*. 1997;390(6655):45-51. doi:10.1038/36285

16. Barker SL, Pastor J, Carranza D, et al. The demonstration of αKlotho deficiency in human chronic kidney disease with a novel synthetic antibody. *Nephrol Dial Transplant*. 2015;30(2):223-233. doi:10.1093/ndt/gfu291

17. Kuro-O M. The Klotho proteins in health and disease. *Nat Rev Nephrol*. 2019;15(1):27-44. doi:10.1038/s41581-018-0078-3

18. Nitta K, Nagano N, Tsuchiya K. Fibroblast growth factor 23/klotho axis in chronic kidney disease. *Nephron Clin Pract*. 2014;128(1-2):1-10. doi:10.1159/000365787

19. Huang X-Z, Wen D, Zhang M, et al. Sirt1 activation ameliorates renal fibrosis by inhibiting the TGF-β/Smad3 pathway. *J Cell Biochem*. 2014;115(5):996-1005. doi:10.1002/jcb.24748

20. Lee S-H, Lee J-H, Lee H-Y, Min K-J. Sirtuin signaling in cellular senescence and aging. *BMB Rep*. 2019;52(1):24-34.

21. Fry JL, Shiraishi Y, Turcotte R, et al. Vascular Smooth Muscle Sirtuin-1 Protects Against Aortic Dissection During Angiotensin II-Induced Hypertension. *J Am Heart Assoc*. 2015;4(9):e002384. doi:10.1161/JAHA.115.002384

22. Li H, Xia N, Hasselwander S, Daiber A. Resveratrol and Vascular Function. *Int J Mol Sci*. 2019;20(9). doi:10.3390/ijms20092155

23. Herzog CA, Asinger RW, Berger AK, et al. Cardiovascular disease in chronic kidney disease. A clinical update from Kidney Disease: Improving Global Outcomes (KDIGO). *Kidney Int*. 2011;80(6):572-586. doi:10.1038/ki.2011.223

24. Babitt JL, Lin HY. Mechanisms of anemia in CKD. *J Am Soc Nephrol*. 2012;23(10):1631-1634. doi:10.1681/ASN.2011111078

25. Misra M. The basics of hemodialysis equipment. *Hemodial Int*. 2005;9(1):30-36. doi:10.1111/j.1492-7535.2005.01115.x

26. Okada R, Wakai K, Naito M, et al. Pro-/anti-inflammatory cytokine gene polymorphisms and chronic kidney disease: a cross-sectional study. *BMC Nephrol*. 2012;13:2. doi:10.1186/1471-2369-13-2

27. Himmelfarb J, Ikizler TA. Hemodialysis. *N Engl J Med*. 2010;363(19):1833-1845. doi:10.1056/NEJMra0902710

28. Price AM, Edwards NC, Hayer MK, et al. Chronic kidney disease as a cardiovascular risk factor: lessons from kidney donors. *J Am Soc Hypertens*. 2018;12(7):497-505.e4. doi:10.1016/j.jash.2018.04.010

29. Gupta J, Mitra N, Kanetsky PA, et al. Association between albuminuria, kidney function, and inflammatory biomarker profile in CKD in CRIC. *Clin J Am Soc Nephrol*. 2012;7(12):1938-1946. doi:10.2215/CJN.03500412

30. Lisowska-Myjak B. Uremic toxins and their effects on multiple organ systems. *Nephron Clin Pract*. 2014;128(3-4):303-311. doi:10.1159/000369817

31. Akchurin OM, Kaskel F. Update on inflammation in chronic kidney disease. *Blood Purif*. 2015;39(1-3):84-92. doi:10.1159/000368940

32. Luksha N, Luksha L, Carrero JJ, Hammarqvist F, Stenvinkel P, Kublickiene K. Impaired resistance artery function in patients with end-stage renal disease. *Clin Sci (Lond)*. 2011;120(12):525-536. doi:10.1042/CS20100277

33. Sage AP, Lu J, Tintut Y, Demer LL. Hyperphosphatemia-induced nanocrystals upregulate the expression of bone morphogenetic protein-2 and osteopontin genes in mouse smooth muscle cells in vitro. *Kidney Int*. 2011;79(4):414-422. doi:10.1038/ki.2010.390

34. Lu X, Hu MC. Klotho/FGF23 Axis in Chronic Kidney Disease and Cardiovascular Disease. *Kidney Dis (Basel)*. 2017;3(1):15-23. doi:10.1159/000452880

35. Fujii H, Goto S, Fukagawa M. Role of Uremic Toxins for Kidney, Cardiovascular, and Bone Dysfunction. *Toxins (Basel)*. 2018;10(5). doi:10.3390/toxins10050202

36. Kneis C, Beck W, Boenisch O, et al. Elimination of middle-sized uremic

solutes with high-flux and high-cut-off membranes: a randomized in vivo study. *Blood Purif*. 2013;36(3-4):287-294. doi:10.1159/000356224

37. Gerdes N, Zirlik A. Co-stimulatory molecules in and beyond co-stimulation - tipping the balance in atherosclerosis? *Thromb Haemost*. 2011;106(5):804-813. doi:10.1160/TH11-09-0605

38. Wikenheiser DJ, Stumhofer JS. ICOS Co-Stimulation: Friend or Foe? *Front Immunol*. 2016;7:304. doi:10.3389/fimmu.2016.00304

39. Wang J-H, Zhang Y-W, Zhang P, et al. CD40 ligand as a potential biomarker for atherosclerotic instability. *Neurol Res*. 2013;35(7):693-700. doi:10.1179/1743132813Y.0000000190

40. Desideri G, Panichi V, Paoletti S, et al. Soluble CD40 ligand is predictive of combined cardiovascular morbidity and mortality in patients on haemodialysis at a relatively short-term follow-up. *Nephrol Dial Transplant*. 2011;26(9):2983-2988. doi:10.1093/ndt/gfq823

41. Yáñez-Mó M, Siljander PR-M, Andreu Z, et al. Biological properties of extracellular vesicles and their physiological functions. *J Extracell Vesicles*. 2015;4:27066. doi:10.3402/jev.v4.27066

42. Raposo G, Stoorvogel W. Extracellular vesicles: exosomes, microvesicles, and friends. *J Cell Biol*. 2013;200(4):373-383. doi:10.1083/jcb.201211138

43. Massy ZA, Metzinger-Le Meuth V, Metzinger L. MicroRNAs Are Associated with Uremic Toxicity, Cardiovascular Calcification, and Disease. *Contrib Nephrol*. 2017;189:160-168. doi:10.1159/000450774

44. Cantaluppi V, Biancone L, Figliolini F, et al. Microvesicles derived from endothelial progenitor cells enhance neoangiogenesis of human pancreatic islets. *Cell Transplant*. 2012;21(6):1305-1320. doi:10.3727/096368911X627534

45. Boulanger CM, Loyer X, Rautou P-E, Amabile N. Extracellular vesicles in coronary artery disease. *Nat Rev Cardiol*. 2017;14(5):259-272. doi:10.1038/nrcardio.2017.7

46. Nicoll R, Henein M. Arterial calcification: A new perspective? *Int J Cardiol*. 2017;228:11-22. doi:10.1016/j.ijcard.2016.11.099

47. Cianciolo G, Capelli I, Cappuccilli M, Schillaci R, Cozzolino M, La Manna G. Calcifying circulating cells: an uncharted area in the setting of vascular calcification in CKD patients. *Clin Kidney J*. 2016;9(2):280-286. doi:10.1093/ckj/sfv145

48. Edelstein LC. The role of platelet microvesicles in intercellular communication. *Platelets*. 2017;28(3):222-227. doi:10.1080/09537104.2016.1257114
49. Chiva-Blanch G, Crespo J, Suades R, et al. CD142+/CD61+, CD146+ and CD45+ microparticles predict cardiovascular events in high risk patients following a Mediterranean diet supplemented with nuts. *Thromb Haemost*. 2016;116(1):103-114. doi:10.1160/TH16-02-0130
50. Kapustin AN, Chatrou MLL, Drozdov I, et al. Vascular smooth muscle cell calcification is mediated by regulated exosome secretion. *Circ Res*. 2015;116(8):1312-1323. doi:10.1161/CIRCRESAHA.116.305012
51. Poppelaars F, Gaya da Costa M, Faria B, et al. Intradialytic Complement Activation Precedes the Development of Cardiovascular Events in Hemodialysis Patients. *Front Immunol*. 2018;9:2070. doi:10.3389/fimmu.2018.02070
52. Poppelaars F, Gaya da Costa M, Berger SP, et al. Strong predictive value of mannose-binding lectin levels for cardiovascular risk of hemodialysis patients. *J Transl Med*. 2016;14(1):236. doi:10.1186/s12967-016-0995-5
53. Abe M, Hamano T, Wada A, Nakai S, Masakane I. High-Performance Membrane Dialyzers and Mortality in Hemodialysis Patients: A 2-Year Cohort Study from the Annual Survey of the Japanese Renal Data Registry. *Am J Nephrol*. 2017;46(1):82-92. doi:10.1159/000478032
54. Contin-Bordes C, Lacraz A, de Précigout V. Potential role of the soluble form of CD40 in deficient immunological function of dialysis patients: new findings of its amelioration using polymethylmethacrylate (PMMA) membrane. *NDT Plus*. 2010;3(Suppl 1):i20-i27. doi:10.1093/ndtplus/sfq033
55. Aucella F, Gesuete A, Vigilante M, Prencipe M. Adsorption dialysis: from physical principles to clinical applications. *Blood Purif*. 2013;35 Suppl 2:42-47. doi:10.1159/000350847
56. Chatzigeorgiou A, Lyberi M, Chatzilymperis G, Nezos A, Kamper E. CD40/CD40L signaling and its implication in health and disease. *Biofactors*. 2009;35(6):474-483. doi:10.1002/biof.62
57. Li J, Wang Y, Lin J, et al. Soluble CD40L Is a Useful Marker to Predict Future Strokes in Patients With Minor Stroke and Transient Ischemic Attack. *Stroke*. 2015;46(7):1990-1992. doi:10.1161/STROKEAHA.115.008685
58. Esposito P, Dal Canton A. CD40/CD40L and cardiovascular risk in patients on

haemodialysis: a role for soluble CD40? *Nephrol Dial Transplant*. 2011;26(7):2414-2415; author reply 2415-2416. doi:10.1093/ndt/gfr227

59. Camussi G, Deregibus MC, Cantaluppi V. Role of stem-cell-derived microvesicles in the paracrine action of stem cells. *Biochem Soc Trans*. 2013;41(1):283-287. doi:10.1042/BST20120192

60. Lee H, Zhang D, Zhu Z, Dela Cruz CS, Jin Y. Epithelial cell-derived microvesicles activate macrophages and promote inflammation via microvesicle-containing microRNAs. *Sci Rep*. 2016;6:35250. doi:10.1038/srep35250

61. Tedla YG, Yano Y, Carnethon M, Greenland P. Association Between Long-Term Blood Pressure Variability and 10-Year Progression in Arterial Stiffness: The Multiethnic Study of Atherosclerosis. *Hypertension*. 2017;69(1):118-127. doi:10.1161/HYPERTENSIONAHA.116.08427

62. Agarwal R. Arterial stiffness and its relationship to clinic and ambulatory blood pressure: a longitudinal study in non-dialysis chronic kidney disease. *Nephrol Dial Transplant*. 2017;32(11):1850-1856. doi:10.1093/ndt/gfw281

12. Acknowledgments

Grazie a mia moglie Francesca e alla mia piccola pulcina Alessia…perché siete il mio "Tutto"

Grazie alla mia famiglia che mi è sempre vicina e rappresenta un punto di confronto e sostegno nelle decisioni importanti

Grazie al Professore Vincenzo Cantaluppi per avermi fatto appassionare al mondo della ricerca e per la fiducia che mi dimostra quotidianamente

Grazie alla Dottoressa Marita Marengo e a tutto il personale medico-infermieristico dell'Unità Operativa Nefrologia e Dialisi di Savigliano per avermi accolto e aiutato nella realizzazione del progetto di ricerca.

Grazie alla Dottoressa Caterina Canavese e al Professor Piero Stratta per i preziosi insegnamenti e per avermi fatto innamorare della Nefrologia

Grazie ai miei colleghi di "corsia" e a tutto il personale medico-infermieristico della SCDU Nefrologia e Trapianto Renale di Novara per i momenti vissuti insieme che mi aiutano a crescere sia come medico che come uomo

Vincere non è importante, è l'unica cosa che conta (G. Boniperti)